Long-term effects of immunostimulation on synaptic plasticity and neurodegeneration

Von der Fakultät für Lebenswissenschaften

der Technischen Universität Carolo-Wilhelmina zu Braunschweig

zur Erlangung des Grades

einer Doktorin der Naturwissenschaften

(Dr. rer. nat.)

genehmigte

D i s s e r t a t i o n

von Marianna Martha Simona Beyer

aus Braunschweig

1. Referent	Professor Dr. Martin Korte
2. Referent	Professor Dr. Reinhard Köster
3. Referent	Professor Dr. Michael Heneka
eingereicht am:	30.11.2015
mündliche Prüfung (Disputation) am:	19.04.2016

Druckjahr 2016

Vorveröffentlichungen der Dissertation

Teilergebnisse aus dieser Arbeit wurden mit Genehmigung der Fakultät für Lebenswissenschaften, vertreten durch den Mentor der Arbeit, in den folgenden Beiträgen vorab veröffentlicht:

Publikationen

Parlog, A., Harsan, L.A., Zagrebelsky, M., **Weller, M.***, von Elverfeldt, D., Mawrin, C., Korte, M., Dunay, I.R.: Chronic murine toxoplasmosis is defined by subtle changes in neuronal connectivity, *Disease Models & Mechanisms 2014 Apr; 7(4): 459–469.*

Tagungsbeiträge

Weller, M.*, Heneka, M.T., Korte, M.: Long-term Effects of Immunostimulation on Neuronal Morphology, *First N-RENNT Symposium on Neuroinfectiology, Hannover (2014)*

Weller, M.*, Heneka, M.T., Korte, M.: Long-term effects of an immunostimulation on neuronal function and morphology, *9th FENS Forum of Neuroscience, Mailand (2014)*

Young investigator oral: Beyer, M., Heneka, M.T., Korte, M.: Long-term influences of an immune stimulation on neuronal structure and plasticity, *11th Göttingen Meeting of the German Neuroscience Society, Göttingen (2015)*

Beyer, M., Heneka, M.T., Korte, M.: Long-term influences of an immune stimulation on neuronal structure and plasticity, *Second N-RENNT **Symposium on** Neuroinfectiology, Hannover (2015)*

Best Poster Prize: Beyer, M., Heneka, M.T., Korte, M.: Enduring changes in neuronal structure and function upon acute and systemic administration of LPS, *4th Venusberg Meeting on Neuroinflammation, Bonn (2015)*

Posterbeiträge

Weller, M.* Dunay, R.I., Zagrebelsky, M., Korte, M.: Changes in neuronal architecture upon *Toxoplasma gondii* infection in mice, *4th Public Retreat of the HZI Graduate School, Hahnenklee (2013)*

Weller, M.*, Heneka, M.T., Korte, M.: Long-term Effects of Immunostimulation on Neuronal Morphology, *6th International phD Symposium of the HZI Graduate School, Braunschweig, (2013)*

Beyer, M., Heneka, M.T., Korte, M.: Long-term Effects of an Immune Stimulation on Synaptic Plasticity, *7th International phD Symposium, Braunschweig, (2014)*

Beyer, M., Heneka, M.T., Korte, M.: Enduring changes in neuronal structure and function upon acute and systemic administration of LPS, *6th Public Retreat of the HZI Graduate School, Braunschweig (2015)*

***** Marianna Beyer, geb. Weller

Nothing in this world that´s worth having comes easy.

Dr. Robert Kelso

Für Martin, Martin, Margit, Moritz und Maximilian

Table of Contents

ZUSAMMENFASSUNG

Die angeborene Immunantwort vermittelt die schnelle Abwehr einwandernder Pathogene und die Beseitigung von Pathogen-assoziiertem sowie wirtseigenem Material. Die Aktivierung von Makrophagen und dendritischen Zellen bestimmt die Immunantwort im Körper, während Mikroglia und Astrozyten durch die Produktion pro-inflammatorischer Zytokine entzündliche Prozesse im Gehirn induzieren, welche als Neuroinflammation bezeichnet werden. Neuroinflammation ist ein pathologisches Merkmal neurodegenerativer Erkrankungen und exzessive sowie anhaltende Immunaktivierung wurden als Risikofaktoren für die Alzheimer-Krankheit identifiziert.

In dieser Arbeit habe ich langanhaltende Effekte einer systemischen Immunaktivierung mit verschiedenen endotoxischen Komponenten aus Bakterien auf neuronale Architektur, elektrophysiologische Funktionalität und räumliches Lernen von Mäusen untersucht. Auch der Einfluss des natürlichen Alterns wurde dabei analysiert. Zusätzlich wurden Veränderungen der Neurodegeneration im APP/PS1 Mausmodel für die Alzheimer-Krankheit erforscht.

Die Daten im ersten und zweiten Teil dieser Arbeit präsentieren eine altersabhängige Sensitivität gegenüber einer Immunaktivierung mit Lipopolysaccharid (LPS) aus *Salmonella enterica serovar typhimurium* (*S.typhimurium*) und mit Peptidoglycan (PGN) zusammen mit Lipoteichonsäure (LTA) aus *Staphylococcus aureus*. Alte Mäuse zeigen eine Reduktion der dendritischen Komplexität und der Dichte dendritischer *spines* hippokampaler und kortikaler Neurone. Zusätzlich wurden Beeinträchtigungen im räumlichen Lernen und der Langzeitpotenzierung (LTP), welche als zelluläre Grundlage von Lernen und Gedächtnis betrachtet wird, in alten Mäusen entdeckt. Des Weiteren weisen die gealterten Tiere eine erhöhte Mikroglia Aktivierung auf, welche durch die LPS Stimulation noch verstärkt wird. Die Behandlung mit LPS aus *Escherichia coli* zeigt diese negativen Auswirkungen nicht. Jedoch zeigen alte APP/PS1 Mäuse Einbußen der dendritischen Komplexität und dendritischer *spines* mit beiden LPS Sorten. Die LTP ist sowohl nach LPS als auch nach PGN/LTA Stimulation reduziert. Interessanterweise zeigen die jungen APP/PS1 Mäuse ebenfalls negative Auswirkungen der systemischen Immunaktivierung. Ferner konnte ich zeigen, dass das NLRP3 Inflammasom, welches die Reifung der proinflammatorischen Zytokine IL-1β and IL-18 vermittelt, essentiell für die Minderung neuronaler Komplexität und der LTP nach LPS *S.typhimurium* Aktivierung ist.

Der letzte Teil der Dissertation verdeutlicht die Auswirkungen einer chronischen Infektion mit *Toxoplasma gondii* (*T.gondii*) auf neuronale Strukturen. Bereits junge Mäuse reagieren sensitiv auf eine Infektion des Zentralen Nervensystems mit *T.gondii*. Hier ist eine generalisierte Reduktion der dendritischen Komplexität in verschiedenen Zelltypen zu sehen ist.

ABSTRACT

The innate immunity provides rapid and important protection against invading pathogens and obtains clearance of pathogen-associated as well as host-derived danger-associated material. The activation of macrophages and dendritic cells orchestrates the inflammatory response in the body, while microglia and astrocytes induce an inflammatory response by production of pro-inflammatory cytokines in the brain, termed neuroinflammation. Neuroinflammation is part of the pathogenesis of neurodegenerative diseases and excessive or prolonged innate immune activation has been identified as risk factor for Alzheimer´s disease.

In this thesis, I investigated the long-term effects of a systemic immune activation on neuronal architecture, function and learning behavior of mice. Different inflammatory components as well as the influence of age were examined. Additionally the APP/PS1 mouse model of Alzheimer´s disease was taken to determine changes in neurodegeneration upon peripheral immune stimulation.

In the first and second part of the thesis the presented data provide evidence for an age-dependent vulnerability towards an immune stimulation with lipopolysaccharide (LPS) of *Salmonella enterica* serovar *typhimurium (S.typhimurium)* as well as with peptidoglycan (PGN) and lipoteichoic acid (LTA) of *Staphylococcus aureus*. Aged mice exhibit decreased dendritic complexity and spine density of hippocampal and cortical excitatory neurons. Moreover, the long-term potentiation (LTP) as enduring enhanced synaptic transmission reflecting the cellular correlate of learning, and the formation of spatial memory, was impaired in aged wildtype mice. Moreover, aged mice showed a higher microglia activation under basal conditions and further activation upon LPS stimulation which was not detectable in adult mice. The treatment with LPS of *Escherichia coli (E.coli)* did not show these deleterious effects. However, in aged APP/PS1 mice, both *E.coli* and *S.typhimurium* LPS resulted in reduction of dendritic branches and spine density of hippocampal and cortical excitatory neurons. Moreover, synaptic plasticity was inhibited with both kinds of LPS and upon PGN/LTA treatment. Interestingly, also adult APP/PS1 mice exhibited detrimental effects on neuronal morphology upon systemic immune activation. In addition, I could demonstrate that the impairment in neuronal structure and LTP after LPS *S.typhimurium* treatment can be rescued with genetic ablation of the NLRP3 inflammasome which is required for the maturation of the proinflammatory cytokines IL-1β and IL-18.

The last part of this thesis demonstrates the impact of chronic *Toxoplasma gondii (T.gondii)* infection on neuronal architecture. I could provide evidence that even young adult mice are sensible towards a CNS infection with *T.gondii* as they show a generalized reduction in dendritic complexity in various different brain areas and cell types.

1. INTRODUCTION

The modern human has come a long and successful way since its genesis about 200,000 years ago in Africa. With rise of civilization and – much later – technology, humans conquered many problems, survived many crises. And still, microbes of about 1 µm and even smaller particles only 10 nm in size deprived of any kind of metabolism can serve as tremendous threat to the human being. It was thought that with the discovery of penicillin by Alexander Fleming in 1928 the battle against bacteria was won, but today infections are still among the leading causes of death worldwide. The overuse of antibiotics in agriculture and medicine, excessive hygiene and exorbitant travel going along with globalization are only some of the man-made factors helping microbes to everlasting world supremacy. And even when infections are overcome they can promote distinct types of cancer, heart failure, allergies and possibly also neurodegeneration. In an ever older growing society, neurodegenerative disease represents a major threat to the human well-being. The term neurodegeneration covers all conditions characterized by a progressive loss of neuronal function associated with neuronal death. Neurodegeneration can be caused by accumulation of small particles seen in prion diseases or misfolded proteins such as α-synuclein in Parkinson´s disease and huntingtin in Huntington´s disease. Also in Alzheimer´s disease as the most eminent neurodegenerative disease and the leading cause of dementia amongst the elderly, protein aggregation plays a crucial role. Even though genetic factors have been discovered accounting for a small subset of cases, answers are still missing to why the prevalence for Alzheimer´s disease doubles every 5 years once people reached an age of 65 (Qiu et al. 2009).

The underlying mechanisms causing neurodegenerative diseases are not well understood yet, but the fact that diseases featuring inflammatory conditions as type 2 diabetes and obesity (Luchsinger and Gustafson 2009), systemic infection (Perry et al. 2007), sepsis (Holmes et al. 2009) and periodontitis (Cerajewska et al. 2015) are identified as environmental risk factors for Alzheimer´s disease, opens a whole new, interesting field of research into the origin and progression of neurodegenerative disease. And possibly, a fight against infectious diseases and immune activation within the body might serve as double strike against other human health threats.

1.1. Innate immunity

Although all individuals, humans and animals, are surrounded by numerous potentially harmful microorganisms, these organisms do rarely cause diseases. Physical as well as chemical barriers like epidermal or mucosal tissues provide protection against invasion of

bacteria, viruses or protozoa. But even when the attachment and invasion of a pathogen is successful, the majority of invaders are eliminated within minutes or hours by the host's defense mechanisms underlying epithelial surfaces.

Together with the adaptive or acquired immunity (only present in vertebrates), the innate immune response is part of the mammalian immune system. While the adaptive immunity plays a role in the late phase of infection and the formation of an immune memory, the innate immunity is the first and rapid response to invading pathogens or host-derived danger signals. Thereby pathogen associated molecular patterns (PAMPs) as well as danger associated molecular patterns (DAMPs) are recognized by germline-encoded pattern recognition receptors (PRRs). The different PRRs include membrane bound and cytoplasmic receptors. Membrane bound receptors are Toll like receptors (TLRs) and C-type lectin receptors, cytoplasmic receptors are NOD like receptors (NLRs) and RIG-I- like receptors. The motives recognized by PRRs are usually highly conserved molecules within microbes which are essential for survival or pathogenicity and therefore unlikely to undergo mutation (Akira et al. 2006, Mogensen 2009).

PRRs are constitutively expressed on various cell types like macrophages and dendritic cells but also on non-immune cells. The expression of PRRs is upregulated by the presence of pathogens. Dependent on the receptor and bound PAMP or DAMP, different signaling cascades are initiated which mediate the initiation, propagation and subsequent elimination of inflammation. Inflammation ensures the delivery of effector molecules, the killing of the infectious agent by phagocytes, mainly macrophages and polymorphonuclear neutrophilic leukocytes, the prevention of pathogen spreading and the subsequent tissue repair. Primary proinflammatory cytokines like IL-1β, IL-6 and TNF-α orchestrate those functions via various pathways comprising the mitogen activated protein kinases ERK, Jak/p54 and p38, and promote local and systemic reactions (Dinarello 1991).

1.2. Lipopolysaccharide and peptidoglycan-mediated innate immune activation

Different PRRs as mediators of the innate immunity show distinct expression patterns, they can recognize different pathogen associated ligands and activate specific as well as overlapping intracellular cascades. The binding of PAMPs or DAMPs via different Toll like receptors for example leads to activation of the same cytoplasmic domains like MyD88, interleukin 1 receptor (IL-1R) -associated protein kinase and tumor necrosis factor receptor-activated factor 6 (TRAF6), which overlap with the signaling of the IL-1 receptor (Bowie and O´Neill 2000). Toll, as the namesake and founding member of the TLR family,

was discovered in *Drosophila melanogaster* as a factor of embryonic dorsal-ventral polarity (Anderson and Nüsslein-Volhard 1986, Hashimoto et al. 1988). To date, 9 different TLRs are known in insects, 13 in mammals of which 11 are expressed in humans (reviewed in Takeda et al. 2003). The Toll like receptors are type I integral membrane glycoproteins containing an extracellular domain comprised of varying numbers of leucine-rich-repeat (LRR) motifs and the Toll/IL-1R homology (TIR) cytoplasmic signaling domain which shows homology to the IL-1R intracellular domain (Bowie and O'Neill, 2000). The usage of different TIR domain-containing adaptors like the mentioned MyD88, TIRAP (TIR domain-containing adapter protein or Mal = MyD88-adaptor like), TRIF and TRAM mediate the specificity of the TLR signaling. TLR 1, 2, 4, 5 and 6 are trafficked to the cell membrane, whereas TLR 3, 7, 8 and 9 are expressed on intracellular compartments. Therefore, the recognition of internalized viral dsRNA, ssRNA and prokaryotic DNA is mediated by the later group of TLRs.

While some TLRs perceive only one group or a small number of ligands, others are able to recognize several microbial molecules. For example, TLR 5 only binds bacterial flagellin, TLR 1 recognizes soluble factors and triacylic lipopeptides of bacteria and mycobacteria. TLR 2 and TLR 4 can bind several molecules of different origin like bacteria, viruses, fungi and also host material. TLR 4 (as well as TLR 2 to some extend) recognizes bacterial lipopolysaccharide (LPS) as a very strong immune activator.

LPS is a complex glycolipid of the outer membrane of Gram negative bacteria. The polysaccharide of the LPS contains a core region and the O-antigen. The O-antigen generates the high structural diversity of the LPS. Here, the composition and linkage of monosaccharides raises this high variation. The lipid A comprises the hydrophobic membrane anchor of the LPS and is connected to the inner core region via an unusual 2-keto-3-deoxyoctonoic acid, L-glycero-D-manno-heptose, often together with phosphate or sulfate groups and ethanolamine. The lipid A fraction gives rise to the endotoxic function of the molecule. The recognition of LPS is realized via binding to the serum-protein LBP (LPS binding protein, Schumann et al. 1990), which subsequently binds to the membrane bound or soluble CD14 (Hailman et al. 1994). This ternary complex is able to activate the receptor complex of TLR 4 and MD-2.

TLR 2 shows response to PAMPs like lipoteichoic acid, di- and triacylated cysteine-containing lipopeptides and peptidoglycan. Lipoteichoic acid (LTA) is a component of Gram positive bacteria which is anchored to the up to 80 nm thick peptidoglycan (PGN) layer mounting the bacterial cell membrane. LTAs mediate the adhesion to host cells, autolysis and like LPS they also induce fever and septic shock in the host during a severe infection. The signaling of TLR 2 requires heterodimerization with TLR 1 or TLR 6 (Ozinsky et al. 2000). In both cases, downstream of the MyD88-dependent signaling of

TLR 2 and TLR 4 lays the activation of different transcription factors like nuclear factor κB (NF-κB) or cyclic AMP-responsive element-binding protein (CREB) (Figure 1).

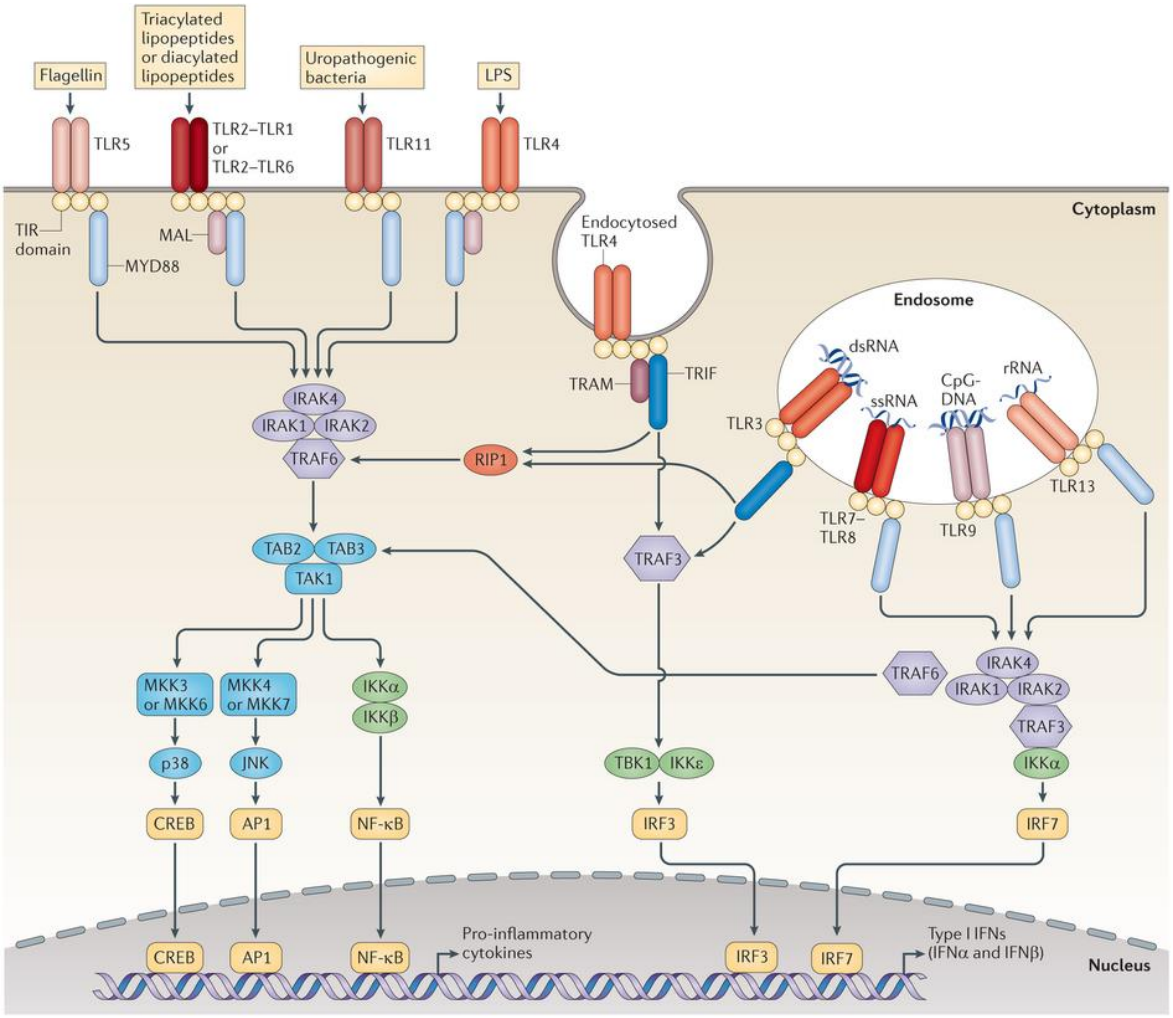

Figure 1.1 | Mammalian TLR signaling pathways (O´Neill et al. 2013). While Toll like receptor (TLR) 5, TLR 11, TLR 4 and the heterodimers of TLR 1–TLR 2 and TLR2–TLR6 are localized on the cell surface, TLR 3, the heterodimer TLR 7–TLR 8, TLR 9 and TLR 13 bind their ligands at endosomes. There, they recognize microbial and host-derived nucleic acids. TLR 4 is found plasma membrane and endosome associated. Upon ligand binding, the receptors form dimers; which induces linking to the Toll/IL-1-resistence (TIR) domains of the TLRs to TIR domain-containing adaptor proteins. These are either myeloid differentiation primary-response protein 88 (MyD88) and MyD88-adaptor-like protein (MAL) or TIR domain-containing adaptor protein inducing IFN-β (TRIF) and TRIF-related adaptor molecule (TRAM). The downstream signaling cascade involves binding of IL-1R-associated kinases (IRAKs) and the adaptor molecules TNF receptor-associated factors (TRAFs), which leads to activation of the mitogen-activated protein kinases (MAPKs), JUN N-terminal kinase (JNK) and p38 driving nuclear factor-κB (NF-κB) and the interferon-regulatory factors (IRFs) mediated transcription. But also cyclic AMP-responsive element-binding protein (CREB) and activator protein 1 (AP1) are important transcription factors. As major consequence sensing of extracellular ligands induces production of pro-inflammatory cytokines, while endosomal associated signaling drives Type I interferon transcription. dsRNA, double-stranded RNA; IKK, inhibitor of NF-κB kinase; LPS, lipopolysaccharide; MKK, MAP kinase kinase; RIP1, receptor-interacting protein 1; rRNA, ribosomal RNA; ssRNA, single-stranded RNA; TAB, TAK1-binding protein; TAK, TGFβ-activated kinase; TBK1, TANK-binding kinase 1.

The activation of these transcription factors leads to the expression of a series of genes of pro-inflammatory cytokines such as IL-6, IL-18, IL-1β and TNF-α orchestrating the inflammation. These immediate and strong reactions to DAMPs or PAMPs are unspecific and eliminate most of the invading pathogens. However, when this first step of defense is overcome by an invading pathogen the presentation of antigens by dendritic cells and tissue macrophages associated with MHC class I or II (major histocompatibility complex) molecules leads to activation of further lymphocytes such as B cells and T cells as part of the adaptive immunity. Eventually after pathogen clearance, tissue repair and anti-inflammatory signaling represses the pro-inflammatory activation of the mobilized immune cells.

1.2.1 Lipopolysaccharide as model for sepsis and systemic immune activation

Sepsis and septic shock as systemic inflammatory response to infection with bacteria, viruses or fungi exhibit a high lethality and are among the leading causes of death in intensive care units worldwide (Bone et al. 1992, Angus et al. 2001). It is believed that many features of such a severe bacterial infection with symptoms like fever, hypotension, sepsis induced brain dysfunction, multiple organ failure or even death are due to the activation of macrophages and the secretion of pro-inflammatory cytokines like IL-18, IL-6, IL-1β and TNF-α (reviewed in Blackwell and Christman 1996). Subsequently, however also an extensive production of anti-inflammatory cytokines like IL-10 and TGF-β occurs and can lead to immune paralysis and an overwhelming pathogen load due to immune inactivation (Bogdan et al. 1993, Astiz et al. 1996). So it seems that sepsis and septic shock are likely caused by an imbalance of pro- and anti-inflammatory signaling. As a consequence of a severe bacteraemia also brain functions can be affected. Symptoms like impairment in attention and memory, delirium and coma can occur and are summarized as septic or sepsis-induced encephalopathy (Pine et al. 1983, Sprung et al. 1990, Wilson and Young 2003).

In rodents, the intraperitoneal administration of lipopolysaccharide (LPS) is widely used to mimic severe bacterial infections and sepsis as it was shown that the application of this endotoxic Gram negative bacterial cell wall component is sufficient to induce high production of IL-1β and TNF-α (Michie et al. 1988, Cannon et al. 1990). In this model, not only the level of blood or liver cytokines was increased only hours after LPS administration, but also the cytokine production in the brain parenchyma was increased (Qin et al. 2007, Semmler et al. 2008). Already more than one decade ago, studies revealed impairment in synaptic plasticity upon peripheral immune stimulation only hours after application. Most studies used intraperitoneal administration of different *E.coli* LPS

types and showed the acute influences of a systemic immune stimulation. The acute consequences of the peripheral LPS administration range from impairment in long-term potentiation (Commins et al. 2001, Jo et al. 2001, Hennigan et al. 2007, Strehl et al. 2014) to deficits in learning and memory (Arai et al. 2001, Shaw et al. 2001, Sparkman et al. 2005). In the Morris water maze task, mice injected intraperitoneally with *E.coli* LPS took longer to find the hidden platform after 6 hours of incubation. Also the number of correct choices in the Y-maze was significantly reduced (Arai et al. 2001). This demonstrates that reference as well as working memory function is impaired. It was also suggested, that these changes in learning performance are not transient but more stable and linger even when the initial illness is overcome (Valero et al. 2014).

However, long-term influences of a peripheral immune activation have not been satisfyingly addressed so far. In addition to this, also factors like age and the innate immune activation as facilitator of neurodegenerative disease have probably not been adequately taken into account.

1.2.2. Sepsis induced by Gram positive bacteria

Until the 1990s, sepsis was considered to be specific for Gram negative bacteria (Parrillo et al. 1990). Today most cases of sepsis are actually caused by Gram positive bacteria with the most prominent representatives *Staphylococcus aureus*, *Streptococcus pyogenes*, *Pseudomonas aeruginosa* and *Klebsiella* spp. (Martin et al. 2003).

Sepsis in its different aspects is a complex inflammatory immune response of the host's immune system to virulence factors like endotoxins. The two major components of the Gram positive cell wall are peptidoglycan (PGN) and lipoteichoic acid (LTA). Both, in synergy, are able to severely activate the innate immune system. At LTA recognition, the immune activation is mediated by TLR 2, LBP, and CD14, whereas TLR 4 and MD-2 are not involved (Schröder et al. 2003). PGN recognition also uses TLR 2. In contrast to LPS, as it seems PGN or LTA does not cause lethality or multi organ failure alone. These two components in synergy however cause septic shock and organ toxicity only 6 hours after intravenous application in rats at doses of 10 µg/g and 3 µg/g, respectively (De Kimpe et al. 1995). Nevertheless, the magnitude of the inflammatory reaction towards Gram positive bacteria seems to be smaller (Abe et al. 2010). And therefore still most immune stimulatory experiments in rodents are performed with LPS and research about appropriate doses for a long-term study with PGN/LTA stimulation and consequences for neuronal architecture, synaptic plasticity and spatial learning is missing.

1.3. Chronic central nervous system infection with *Toxoplasma gondii*

Toxoplasma gondii (*T.*gondii) is a protozoan parasite of the family of apicomplexa which can infect a great variety of mammals and birds. The three different routes for humans to get infected by this obligate intracellular pathogen are the food-born, zoonotic and mother-to-child transmission. Humans and rodents only serve as intermediate or secondary hosts and sexual reproduction of *T.gondii* occurs only in members of the felidae (Dubey et al. 1970). Most frequently, humans get infected via contaminated uncooked meat and therefore at first the pathogen crosses the gastrointestinal barrier as rapidly dividing tachyzoites (Frenkel et al. 1973). From the submucosal tissue, the pathogen disseminates throughout the body and eventually reaches immune protected sites like the brain, retina or fetus (Hunter and Remington 1994, Pavesio and Lightman 1996, Montoya and Remington 2008). *T.gondii* is most likely able to enter the brain via the “Trojan horse” mechanism, hijacking and activating immune cells such as macrophages, which subsequently squeeze through the blood endothelial cells of the blood brain barrier (Lachenmaier et al. 2011). After the acute phase of the infection which lasts about two weeks and can be asymptomatic or can feature symptoms typical for a common cold, *T.gondii* evades the host´s immune system and remains within the host over its whole lifespan via formation of intracellular cysts. Even though, this protozoan is able to infect and form intracellular cysts within astrocytes, microglia and neurons *in vitro* (Fischer et al. 1997), *in vivo* the majority of cysts are found in the axon, cell body or dendrites or neurons (Ferguson and Hutchison 1987). The persistent form of the protozoan within these cysts is the slowly dividing bradyzoite (Frenkel 1973). The conversion of tachyzoites into bradyzoites is mediated by factors of the immune system such as a heat shock during fever, nitric oxide, high or low pH and IFN-γ production (Lyons et al. 2002). Encysted in neurons, bradyzoites remain undetected by invading immune cells such as T cells due to a lack of MHC class I normally mediating the $CD8^+$ T cell executed death of infected cells. On the other hand, the silent bradyzoite stage can be reversed to the active tachyzoite form in the absence of IFN-γ, TNF-α, IL-12, NO and T cell response (Lyons et al. 2002). While a latent *Toxoplasma* infection remains unnoticed in most people, it can cause severe complications in immunocompromised patients, where a transition back to the tachyzoites can have a lethal course (Montoya and Liesenfeld 2004). Nowadays, we know that *Toxoplasma gondii* causes way more subtle symptoms in immune competent people promoting mental disorders including depression and schizophrenia (Flegr 2007). However, these studies are based on the seroprevalence of patients as brain cysts can only be detected post-mortem. In rodents, infection with *T.gondii* leads to a more curios and active behavior (Hay et al. 1985, Webster et al. 1994) and infected animals lose their innate fear of feline odors (Berdoy et al. 2000) which most likely serves to increase

pathogen transmission. Even though some studies already suggested a contribution of low-level inflammation (Hermes et al. 2008), neurotransmitter imbalance (Gatkowska et al. 2012) or dopamine overproduction (Prandovszky et al. 2011) most likely more than a single factor is involved in the complex manipulation of neuronal networks. Further studies on the mouse model of chronic *T.gondii* CNS infection are necessary to gain a complete picture of the underlying mechanisms.

1.4. Immune cells of the central nervous system

For a very long time, it was believed that the central nervous system, separated from the peripheral organs by the blood brain barrier, exhibit an immune-privileged status with no communication to or interaction with the peripheral immune system. Indeed, the blood brain barrier which is build via tight junctions between the brain blood capillary epithelial cells prevents pathogens and immune cells in larger quantity from entering the CNS. Nevertheless, even in the absence of an infection, there is communication between the immune system and the central nervous system and brain specific as well as peripheral immune cells occupy the brain (for a review see Ousman and Kubes 2012).

Part of the CNS innate immunity are the brain resident astrocytes and microglia cells. These two types of glia cells were first described as glue-like connective tissue between neurons and introduced in 1846 by Rudolf Virchow. However, the differentiation between astroglia, microglia and oligodendrocytes was established by Pio del Rio Hortaga, a student of Santiago Ramón y Cajal, in 1932 (del Rio Hortaga 1920, 1932). Del Rio Hortaga already postulated that microglia are cells with amoeboid morphology of mesodermal origin invading the brain during early development. There, they evenly disperse and transform into a branched, ramified morphological phenotype in the more mature brain each cell occupying a defined territory. After a pathological event, these cells acquire amoeboid morphology similar to the one observed early in development. And these cells have the capacity to migrate, proliferate and phagocytose. Correctly pointed out by H. Kettenmann and colleagues, all these statements are still valid today (Kettenmann et al. 2011). Microglia are the specialized CNS macrophages and – depending on the brain area – make up 5 – 20% of the glial cell population (Lawson et al. 1990, Perry & Gordon 1991). They express several macrophage-associated markers like CD11b, CD14 and F4/80 (also known as EGF-like module-containing mucin-like hormone receptor-like 1 (EMR1), but they also differ from peripheral macrophages in the following aspects: The primary role of microglia is the support and maintenance of tissue function. Under non-activated conditions or as resting microglia with their highly branched and motile processes, they constantly contact neurons, astrocytes and blood-vessels sensing

even subtle changes in their microenvironment (Nimmerjahn et al. 2005). This status is promoted by neurons which down regulate the microglia activation via cell-cell-contact and soluble factors like neuronal CX_3CL1, CD47, CD200 and CD22. These factors bind to the receptors CX_3CR1, CD172, CD200R and CD45 on the microglia cell surface, respectively (Ransohoff and Cardona 2010). Also the expression of TREM-2 (triggering receptor expressed on myeloid cells 2) induced via IL-4 signaling attenuates microglia and macrophage activation (Turnbull et al. 2006).

As house-keeping function microglia in this “steady-state” participate in synapse maintenance via direct contact to astrocytic processes, dendritic spines and synaptic clefts (Murabe and Sano 1982, Wake et al. 2009, Paolicelli et al. 2011, Tremblay et al. 2011). They also provide support of neuronal development and function by expression of the neurotrophins NT-3 (neurotrophin-3) and BDNF (brain-derived neurotrophic factor). The microglia themselves also react to neurotrophins and they enhance proliferation and phagocytic activity *in vitro* (Elkabes et al. 1996). Almost any manipulation or insult of the brain homeostasis can lead to microglia activation causing rapid changes in morphology and upregulation or *de novo* synthesis of cell surface receptors (Kreutzberg 1996, Perry et al. 2010). Microglia display a huge diversity of activation phenotypes with a linear activation progression from partial to full activation (Perry et al. 2010). However, this diversity is most likely not detectable by changes in morphology and expression of a limited number of surface markers. Therefore, it is widely accepted that microglia as well as peripheral macrophages appear in two major activation variants: M1 or classical activation via TLR and interferon signaling and M2 or alternative activation mediated by IL-4 and IL-13 (Martinez et al. 2008). The M1 activation is associated with pro-inflammatory signaling and production of TNF-α, IL-1β, superoxide, nitric oxide (NO), reactive oxygen species (ROS), and different proteases (reviewed by Block et al. 2007). Besides the signaling via TLRs and IFNs, also necrotic neurons and amyloid-β aggregates lead to classical activation of microglia (Figure 1.2). The M1 state of activation was coined for peripheral macrophages and underlines the close relationship between T cells and macrophages. Thereby, the interaction with Th1 cells leads to M1 activation of macrophages. In the brain, not only T cells produce the M1 triggering cytokines, but also astrocytes and microglia themselves are reported to do so (Kawanokuchi et al. 2006). In return, microglia enhance the differentiation of naïve T cells via the expression of MHC class II (O´Keefe et al. 2002).

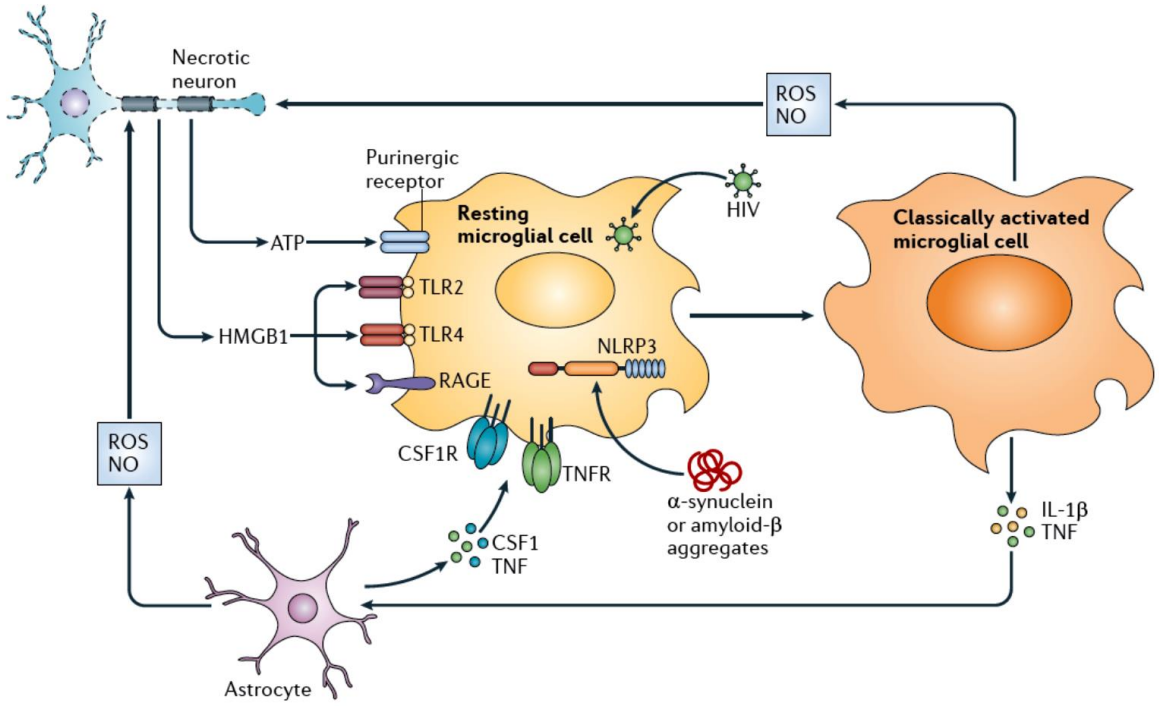

Figure 1.2 | Classically activated microglia in the context of neurodegenerative disease (Saijo and Glass 2011). The M1 or classical activation of microglia is triggered via signaling through pattern-recognition and purinergic receptors. Factors like infections with HIV, damage-associated molecular patterns (DAMPs) like HMGB1, histones and ATP, as well as protein aggregates typical for certain neurodegenerative diseases like Alzheimer´s (amyloid-β) and Parkinson´s disease (α-synuclein) lead to production of pro-inflammatory mediators. Communication between microglia and astrocytes via pro-inflammatory cytokines such as CSF1 amplifies the reaction and contribute to pathology of neurodegenerative disease. IL-1β, interleukin-1β; HMGB1, high-mobility group box 1 protein; NLRP3, NOD-, LRR- and pyrin domain-containing 3; NO, nitric oxide; RAGE, receptor for advanced glycation end-products; ROS, reactive oxygen species; TLR, Toll-like receptor.

On the other hand, the M2 activation is characterized by an anti-inflammatory phenotype of microglia with its function in immune suppression, cell debris clearance and tissue repair. The concept of alternative activation was adapted from peripheral macrophages as well, which showed mannose receptor (CD206) expression upon IL-4 binding, a phenotype not seen so far and therefore termed “alternative” (Stein et al. 1992).

In the M2 state, microglia and peripheral macrophages produce anti-inflammatory mediators like IL-10, extracellular matrix protecting proteins, ornithine and polyamines for wound repair (synthesized by argniase 1 as counterpart of iNOS, both using arginine as substrate) and receptors associated with phagocytosis, such as scavenger receptors (reviewed by Saijo and Glass 2012). Under normal conditions, an infection or injury is a self-limited process characterized by the down regulation of inflammation after the pathogen or danger associated molecules are cleared and tissue repair is fulfilled. However, it is not clear so far whether microglia return to a resting state with the same phenotype as before the insult or whether they hold some kind of memory function (Saijo and Glass 2012). Under certain conditions however, microglia can maintain their M1 state

and drive ongoing production of pro-inflammatory factors. Such conditions are found in chronic inflammatory disease like type 2 diabetes or arteriosclerosis (reviewed by Olefsky and Glass 2010, Hansson and Hermansson 2011). Here, a low-grade of inflammation contributes to the disease pathology.

Moreover, there is evidence that markers of classical microglia activation are upregulated in mice and also humans as a consequence of normal aging: The expression of TLRs (Letiembre et al. 2007), major histocompatibility complex (MHC) class II and complement receptor 3 (CD11b) (Morgan et al. 1999; Nicolle et al. 2001, Godbout et al. 2005) is enhanced in aged rodents. Also here this "priming state" of microglia leads to a stronger and prolonged production of the pro-inflammatory cytokines such as IL-1β and IL-6 after a peripheral immune stimulus (Godbout et al., 2005; Barrientos et al., 2009a). And, even more interesting the hyper reactive inflammatory response of the microglia was shown to be restricted to the brain (Godbout et al., 2005; Barrientos et al., 2009a, 2015a).

Also astrocytes are involved in the CNS innate immunity. Astrocytes are the most abundant cell population in the brain and long believed to solely support nervous tissue structure. Today it is known that there is a huge morphological, biochemical and functional heterogeneity amongst astrocytes. Roughly, the astrocytic population is divided into the protoplasmic astrocytes with various fine branched processes found in the gray matter and the fibrous astrocytes of the white matter exhibiting many long fiber-like processes. Protoplasmic astrocytes contact neurons via enwrapping of synapses. In this so called tripartite synapse, bidirectional communication takes place between the pre- and postsynaptic neuron and an astrocyte (for a review see e.g. Clarke et al. 2013). Here, they actively regulate neuronal and synaptic transmission by responding to neuronal signaling with changes in their intracellular Ca^{2+} levels mediated via neurotransmitter binding (reviewed by Perea et al. 2009). Moreover, astrocytes release several neuroactive molecules like ATP, D-serine, GABA, glutamate, NO and TNF-α and they also take up excessive neurotransmitter and various ions such as chloride, hydrogen, potassium and sodium contributing to ion homeostasis (Simard and Nedergaard 2004, Ota et al. 2013).

In association with brain microvessels, astrocytes support neurons within "neurovascular units". With their specialized perivascular end feed they contact blood vessels and contribute to the physical, metabolic and transport barrier features of the blood brain barrier (BBB) and ion and water homeostasis (Abbott et al. 2006). Besides their physiological role, modulation of the BBB phenotype and integrity is probably the most important factor also for the brains immunity. Furthermore, in case of brain injury a strong astrogliosis and astroglial scar formation shutting off degenerative and infected tissue is often detectable by upregulation of the GFAP-signal. Of note, immunohistochemical identification of astrocytes via GFAP expression seems not to be accurate for non-reactive astrocytes in a healthy brain (Sofroniew and Vinters 2010). Astrocytes also contribute to

neuroinflammation via secretion of pro-inflammatory cytokines such as IL-1, IL-6, IL-3, and TNF-α in response to IFN-γ, IL-1 signaling or LPS (Chung and Benveniste 1990). Like microglia, they are able to detect pathogens via a subset of TLRs and sense an inflammatory environment via expression of IL-1RI, TNF-αR and IFN-γR. But the inflammatory signaling of astrocytes is strikingly slower than in microglia.

Surprisingly, also the third type of glia cells, the oligodendrocytes express immune modulatory receptors such as TLR 2 and 3 (Bsibsi et al. 2012) and receptors for TNF-α, IL-4, IL-6, IL-7, IL-10, IL-11, IL-12 and IL-18 (reviewed by Peferoen et al. 2014). And to a minor extent oligodendrocytes also secrete cytokines and chemokines, which either activate and attract (CCL2, IL-6 and IL-8) or inactivate (CD47, CD200) other immune cells like microglia (Amor et al. 2014, Peferoen et al. 2014). However, the main function of astrocytes and oligodendrocytes in contrast to microglia are clearly found in normal brain function and only secondary in disease. Although it was long believed that no appreciable immune functions are present in the brain, glia cells represent a very potent but unique subset of the innate immunity.

1.5 Learning and memory

The brain gives rise to our consciousness and is the base of thinking, feeling, curiosity, learning and memory. While learning describes the acquisition of new information and skills, memory comprises the storage and application of this information. Of course memory can be further classified according to the duration of storage and the type of information. Memories are available for seconds to minutes within the short-term memory which gives convenient access to information but bears limitation in its duration and storage capacity. After memories gained admission to the long-term memory, they can be recalled over hours, months and even a whole life time. The hippocampus as part of the limbic system is of crucial interest in the interface of short- and long-term memory (Alvarez et al. 1994). It was also identified to play a major role in the formation of episodic, contextual memory and formation of spatial maps (Kinsbourne and Wood 1975, O'Keefe and Nadel 1979). Humans and many other vertebrates possess two hippocampi under the neocortex which are linked via dorsal and ventral commissures. The hippocampus is named after its resemblance to a seahorse and is also compared to the ram´s horn of the Egyptian god *Ammon*. Hence, part of the hippocampus formation is the *cornu ammonis* (CA) or Ammon´s horn with its subregions CA1, CA2, CA3 and CA4 area. In the basic circuit of the hippocampus formation, signals from the entorhinal cortex as major gate way of sensory information gain entry to the hippocampus via the perforant path to the dentate gyrus, CA3 and CA1 area (figure 1.3). From the dentate, the information flow goes further

via the mossy fiber pathway to CA3. Subsequently, the major connection between the CA3 and CA1 are the axons of the Schaffer collateral pathway. From CA1, signals are transferred back to the entorhinal cortex which itself is connected to several other cortex areas.

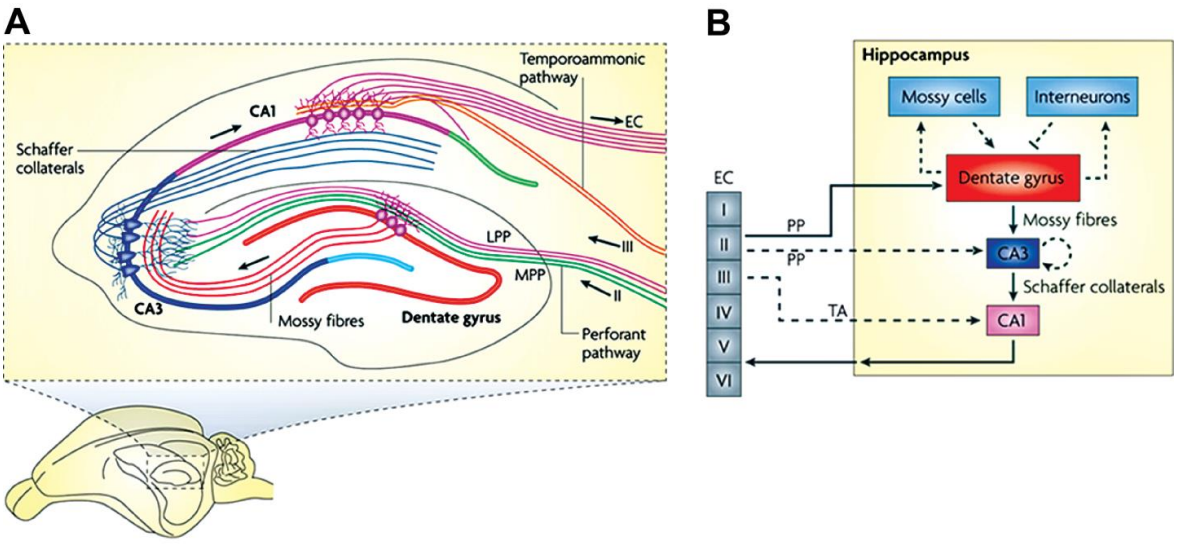

Figure 1.3 | Schematic illustration of the information flow through a transversal section of the mouse hippocampus and related cortical regions (Deng et al. 2010). (A) Signals from layer II and III of the entorhinal cortex along the medial and lateral perforant path into the dentate gyrus are further transmitted via the mossy fibers to CA3. Signals are further transferred from CA3 to CA1 via the Schaffer collaterals and back to the entorhinal cortex. **(B)** Simplified scheme of the information flow of the different layers of the entorhinal cortex into and within the hippocampus. EC entorhinal cortex; PP perforant path; LPP lateral PP; MPP medial PP; TA Temporoammonic pathway.

In contrast to these different cortex areas, the connections within the hippocampus are mostly unidirectional. The excitatory neurons of the hippocampus are organized into several sublayers of the pyramidal neurons of the CA and granule neurons of the dentate. The cell bodies of the CA regions form the *stratum pyramidale*. The basal dendrites are localized within the *stratum oriens*, while the *stratum radiatum* and *stratum lacunosum-moleculare* contains the proximal and distal apical dendrites of the CA pyramidal neurons, respectively. Even though information is not stored within single neurons or synapses within the hippocampus it plays an essential role in the processing of information, which was shown in studies of patients and animals with hippocampal damage or lesions (Scoville and Milner 1957, Eichenbaum 2004). Therefore, the interaction of the hippocampus with neocortical areas and other brain regions promotes strengthening and reorganization of neuronal connections as well as information consolidation. Molecular and cellular mechanisms enabling memory consolidation are based on the so called activity dependent synaptic plasticity.

1.6. Functional and structural synaptic plasticity of hippocampal neurons

Synaptic plasticity provides the basis of learning and memory processes. In neuroscience, the term synaptic plasticity indicates the activity-dependent alterations of connections between neurons and their ability to adapt to a diversity of stimuli. It thereby combines functional and structural modifications as growth and retraction of neuronal protrusions and synapses as well as the changes in synaptic efficacy. These changes can result in strengthening or weakening of synapses and are therefore bidirectional. Moreover, plastic changes can be short- or long-lived alterations and are called short-term and long-term plasticity, respectively. On the one hand parts of short-term plasticity are alterations lasting only seconds or minutes such as the neuronal facilitation, augmentation or post tetanic potentiation (Zucker and Regehr 2002). On the other hand, enduring changes in synaptic transmission can last hours to days. The long-term potentiation (LTP) as long-lasting enhancement of synaptic efficacy was discovered in 1973 by Terje Lømo and Timothy Bliss (Bliss and Lømo 1973) in the rat hippocampus. The opponent mechanism is the long-term depression as activity-dependent reduction of synaptic efficacy (Dudek and Bear 1992). Further, LTP and LTD are divided into an early and a late phase. The early phase of LTP (E-LTP) can be experimentally induced in the hippocampus via a single tetanic stimulation and lasts only a few hours. Processes of E-LTP comprise post-translational modifications of various post-synaptic proteins but are independent of protein synthesis and therefore quickly decaying. The late phase LTP (L-LTP) lasts several hours *in vitro* and even weeks or months *in vivo* (Frey et al. 1988, Bliss and Gardner-Medwin 1973, Abraham 2003). Both forms of LTP and also LTD require the influx of Ca^{2+} into the postsynaptic compartment, the activation of Ca^{2+}/calmodulin-dependent protein kinase II (CamKII) and protein kinase C (PKC) and trafficking of AMPA (α-amino-3-hydroxy-5-methyl-4-isoxazolepropionic acid) receptors in or out of the postsynaptic membrane (Collingridge et al. 2004, Malenka and Bear 2004). LTP at the Schaffer collateral pathway from CA3 to CA1 neurons is also dependent on activation of N-methyl-D-aspartate (NMDA) receptors and protein kinase A (PKA). NMDA receptors are so called “coincidence detectors“ as their activation depends on binding of the pre-synaptically released neurotransmitter glutamate and the depolarization of the postsynaptic membrane above – 50 mV (Collingridge 2003).

NMDAR-dependent LTP is characterized by input-specificity, associativity and cooperation (Bliss and Collingridge 1993, Bear and Malenka 1994, Malenka and Nicoll 1999). Therefore, upon successful induction of LTP only stimulated synapses are strengthened allowing participation of single synapses in separate circuits. Furthermore, a strong stimulation of adjacent synapses can lead to expression of LTP in weakly

stimulated synapses of the same cell. Lastly, two distinct afferent systems can “cooperate” and the summation of EPSPs leads to induction of LTP in a postsynaptic cell.

LTP and LTD as processes of synaptic plasticity are associated with changes within the structure of the postsynaptic compartments, termed structural plasticity. Besides the remodeling of dendritic and axonal arbors, shrinkage, growth, elimination and *de novo* formation of dendritic spines and axonal boutons promote the strengthening, weakening or rewiring of synaptic connections (Holtmaat and Svoboda, 2009). Dendritic spines are small protrusions on dendritic branches forming the postsynaptic site of a synapse. Only two years after the discovery of LTP, an enlargement of dendritic spines within the stimulated vs. non-stimulated pathways was discovered by electron microscopy (Harreveld and Fifkova 1975). Spines form biochemical compartments allowing changes in Ca^{2+} concentration at single synapses and therefore mediate input specificity (Hayashi and Majewska 2005). The architecture of dendritic spines is very divers, but they are usually classified as stubby, thin, mushroom and filopodia. While thin spines and filopodia lack an appreciable head and represent an immature “learning spine” phenotype. Mushroom spines posses a well defined neck and prominent spine head, and due to their strong stability they are also referred to as “memory spines” (Bourne and Harris 2007). Mushroom spines exhibit the most mature spine phenotype as head volume correlates with synaptic strength, area of the postsynaptic density and the number of inserted AMPA receptors (Harris and Stevens 1989, Takumi et al. 1999). Especially thin spines and filopodia are very dynamic structures and form or disappear rapidly in response to changes in synaptic transmission. These rapid morphological changes are mediated by changes in the actin cytoskeleton which is highly enriched in dendritic spines. Upon LTP, a transient depolymerization of F-actin in the stimulated spines allows transport of plasticity related proteins and polyribosomes mediating the long-lasting alterations in synaptic efficacy on the level of single spines (Ouyang et al. 2005). Subsequent increase in F-actin ratio however facilitates spine growth and stabilization (Lin et al. 2005). Changes in G-actin to F-actin ratio are mediated by the activity of small GTPases and their regulators, through the action of actin-binding proteins such as profilin and cofilin. As the actin cytoskeleton serves as regulator of protein trafficking and structural framework of dendritic spines a tight control of these proteins is always required. Together, functional as well as structural alterations on the level of single spines in response to specific stimuli are necessary to allow adaptation during learning and memory events.

1.7 Crosstalk between the immune and central nervous system

The first evidence that the brain is quite different from the rest of the body in respect to immune functions was gained in 1921 when an experiment showed that rat sarcoma cells proliferate intensely in the brain parenchyma but do not after subcutaneous or intramuscular transplantation (Shirai 1921). The perception that indeed the brain - along with the eyes and testis - is an immune-privileged site was persistently locked in peoples´ brains for almost 90 years. The isolation from the peripheral circuitries by the BBB, the lack of lymphatic vessels, low constitutive levels of MHC class I and II and the supposed immunoincompetence of microglia (Carson et al. 2006) were further points supporting this hypothesis. Research in the last decades shifted the view of the immune-privileged brain: "It has become increasingly clear that the central nervous system is *immune-different* rather than *immune-privileged*" (Josep Dalmau, University of Pennsylvania).

Indeed, the brain and the immune system communicate via shared messengers namely neurotransmitters, cytokines or hormones, which have overlapping functions in both systems. The brain regulates the production of immune modulators via the hypothalamic-pituitary-adrenal (HPA) axis. Here, the hypothalamus and the pituitary gland stimulate the production of these mediators in the adrenal gland. In return products generated by the immune system influence the neuroendocrine axis activity. Cytokines as major immune modulators are not only transported into the brain across the BBB but also expressed by brain cells. Astrocytes, microglia and neurons express pro-inflammatory cytokines such as IL-1β, IL-6 and TNF-α (Vitkovic et al. 2000) during tissue insult as well as normal brain function, e.g. after induction of LTP (Schneider et al. 1998) or for normal sleep regulation (Krueger et al. 1998). Of note, impaired IL-1β signaling as well as an increased IL-1β concentration leads to deficits in hippocampal LTP and learning and memory processes (Avital et al. 2003, Hein et al. 2010, Tong et al. 2012). Today we know that the production of cytokines especially by microglia but also by astrocytes is only one important function shared with peripheral immune cells (see chapter 1.4.). Furthermore, also the tightly controlled access of peripheral immune cells must occur to maintain brain homeostasis. Peripheral immune cells can fulfill different tasks in the brain and are part of complex signaling cascades to protect the brain from health threats, but they also seem to participate in normal brain function. Indeed, immune cells from the periphery can enter the cerebrospinal fluid (CSF) via the choroid plexus and the leptomeningeal vessels with the help of selectins and integrins controlling cell-adhesion, rolling and endothelial passage (Engelhardt and Ransohoff 2012). It was further revealed, that also the blood brain barrier, the perivascular space and the basement membranes of endothelial cells and astrocytes can be crossed by different leukocytes, which is called diapedesis. The underlying mechanism is best described for the α4-integrins mediated crossing of CD4+ T cells into

the brain parenchyma during multiple sclerosis (Engelhardt 2006). Here and in other diseases, the integrity of the BBB can be reduced by dysregulation of tight junction proteins. In addition to their role during disease, CNS-specific T cells seem important for spatial learning and neurogenesis (Ziv et al. 2006). T cells also migrate into the meninges and acquire Th2 activation upon learning tasks (Marin and Kipnis 2013). T cells, B cells and blood monocytes are also able to secrete the brain-derived neurotrophic factor (BDNF) and respond to the nerve growth factor (NGF) (Kerschensteiner et al. 1999, Prencipe 2014), which can activate microglia and promote anti-inflammatory processes despite their classical role as neurotrophic factors (Jiang et al. 2010, Tong et al. 2012). However, numerous questions about the functions of immune cells and immune modulators during normal brain functions are yet to be answered.

1.8 Alzheimer´s disease

Alzheimer´s disease (AD) was first described by Dr. Alois Alzheimer in 1906, when he reported progressive cognitive impairment, focal symptoms, hallucinations, delusions, and psychosocial incompetence in his patients Auguste Deter. Today, according to the Alzheimer´s association about 44 million people suffer from Alzheimer´s disease which makes it the most common cause of dementia in the elderly. Already in the early 20th century Dr. Alzheimer described the pathological hallmarks of the disease: First, the extracellular amyloid-β or senile plaques (he called these miliary foci, Alzheimer et al. 1907, translated into English in 1995) identified as an accumulation of a 4.2 kDa peptide primarily of 40 – 42 amino acids of length (Glenner and Wong 1984). The amyloid-β peptide as major component of senile plaques is a byproduct of the amyloidogenic cleavage of the amyloid precursor protein (APP) by β- and γ-secretases. And second, the abnormal intracellular aggregates he named neurofibrillary tangles. Today we know that these tangles are composed of hyperphosphorylated forms of the microtubule-associated and stabilizing protein tau (Mandelkow and Mandelkow 1998). The tau protein loses its ability to promote microtubule assembly in neurons upon phosphorylation, which is due to an imbalance in kinase and phosphatase activity (Gong and Iqbal 2008). However, it is most likely the gain of a neurotoxic function which causes tau associated neurodegeneration as other microtubule associated proteins could substitute for tau function (Gong and Iqbal 2008). While the incidences of amyloid plaques cannot be correlated with severity of cognitive decline during AD progression, the aggregation of intraneuronal phopho-tau and the extraneuronal “ghost tangles” which appear after death of tau bearing neurons parallel neuronal and synaptic loss (Braak and Braak 1991). During the disease progression, the death of single neurons as well as the early loss of

single synapses is strongly correlated with the cognitive impairments. Only after a long preclinical phase of at least 10 – 20 years and a very slow progression in the early stage of AD cognitive symptoms appear (Price and Morris 1999). Early stage AD symptoms include impairment in short-term memory, slight temporal or spatial disorientation (Tarawneh and Holtzmann 2012) and even subtle changes in personality such as depression (Zubenko et al. 2003). While there is a marked progressive decline in cognitive functions and behavioral symptoms such as aggression, anxiety, and aimless or restless activities during the moderate stage of disease (Devanand et al. 1997), in the severe stage of AD patients are usually bedridden due to impairment in basic motor functions and they often die of complications with aspiration or infection (Tarawneh and Holtzmann 2012). While there are cases of early onset AD which are mediated by mutations in either the APP or the catalytic subunits presenilin 1 or 2 (PS1 or PS2) of the γ-secretase leading to increased Aβ production (Bertram and Tanzi 2008), most cases are of sporadic nature with age as the most important risk factor. Besides the two AD specific hallmarks neuroinflammation, astrogliosis and microglia activation are associated with neurodegeneration during disease progression (Beach et al. 1989, Itagaki et al. 1989). The idea that neuroinflammation may be an early event in AD pathogenesis was proposed in the same breath as the disease discovery (Fischer 1907, Eikelenboom 2010). In fact, elevated levels of cytokines, chemokines and their receptors were found in post-mortem AD brain tissue (Cartier et al. 2005) and microglia surrounding Aβ plaques are positive for activation markers and pro-inflammatory mediators such as MHC class II, Cox-2, MCP-1, TNF-α, IL-1β, and IL-6 (Akiyama et al. 2000, Glass et al. 2010). However, it is quite challenging to study and understand the sources and patterns of this multi-factorial disease and the involvement of inflammatory processes solely in human post-mortem tissue. Not to mention that early stages of the pathology and healthy controls are difficult to identify. Therefore, several mouse models have been developed reflecting one or more pathological hallmarks of the disease even with young age. These mouse models are based on mutations within the human APP, PS or tau gene of familial AD cases. A variety of these different transgenic mouse models have been developed during the last 20 years. Some mice are transgenic for the APP such as APP23 (Sturchler-Pierrat et al. 2009), APP-Au (Van Broeck et al. 2008), PD-APP (Games et al. 1995), Tg2576 (Hsiao et al. 1996), or tg APP_ArcSwe (Lord et al. 2006). Others carry two mutations with either a stronger amyloid-plaque phenotype like APPswe/PSEN1dE9 (Borchelt et al. 1997) APP/PS1 (Blanchard et al. 2003) and PS2APP (Richards et al. 2003) or reflect the APP and tau pathology such as APP/tau (Ribé et al. 2005), 3xTg (Oddo et al. 2003) or TauPS2APP (Grueninger 2009). Even though, these mouse models have been proven to be very valuable tools in AD research, none of them combines all features of the disease.

One of the widely-used and best characterized mouse models is the APPswe/PSEN1dE9 (in the following APP/PS1) mouse, first described in the late 1990s (Borchelt et al. 1997, Jankowsky et al. 2001). This mouse model reflects the amyloid-portion of the pathology as a chimeric mouse/human APP with the Swedish mutation K595N/M596L found in early onset AD and the relevant γ-secretase presenilin1 which facilitates the amyloidogenic cleavage of the APP are overexpressed in the murine brain. The APP/PS1 mouse model for AD is characterized by an increasing Aβ plaque load starting with about 6 months of age resulting in a substantial plaque load in the hippocampus and cortex by 9 months (Jankowski et al. 2004) and a peak in plaque formation until 12 months of age (Garcia-Alloza et al. 2006). This leads to neurodegenerative phenotype with neuronal death, synapse loss and learning and memory deficits. Various studies show decreased numbers and altered morphology of synapses in the hippocampus of APP/PS1 mice (Moolmann et al. 2004, Grutzendler et al. 2007, Kummer et al. 2011, Alonso-Nanclares et al. 2013, Heneka et al. 2013, Šišková et al. 2014). Also synaptic plasticity was investigated in this and other AD models and studies showed that an elevation in aggregated Aβ causes impairment in LTP (Nalbantoglu et al. 1997, Chapman et al. 1999, Kummer et al. 2011, Heneka et al. 2013). Deficits in learning and memory start as early as 6 months of age and extent over the whole lifespan of the animals (Cao et al. 2007, Ding et al. 2008).

1.9 Alzheimer´s disease and innate immune response

During the last decade, cumulative evidence points to a connection between inflammatory conditions in the brain or the body and Alzheimer´s disease progression. For example as microglia cells, the resident brain macrophages, are the main cell type to clear Aβ deposits a pro- or anti-inflammatory environment could likely influence phagocytosis of senile plaques. In AD mouse models as well as post mortem tissue of AD patients, there is an elevation of activated microglia, astrogliosis and pro-inflammatory mediators (reviewed by Wyss-Coray 2006, Heneka and O´Banion 2007).

In AD brains microglia convert from their ramified inactive to an amoeboid state and express several activation markers and the production of all important pro-inflammatory cytokines and chemokines is up regulated (Akiyama et al. 2000, Cartier et al. 2005). Even if the neurotoxic properties of Aβ deposits alone might be sufficient to induce neuronal death and cognitive decline, this activation of microglia and astrocytes via TLR-, NLR- and RAGE-pathways further amplifies these reactions. But not only local inflammatory reactions might drive disease pathogenesis, but also the activation of the systemic innate immune system enhances or at least modifies AD progression. Infection as cause of peripheral immune activation may be involved in the early stages of AD pathogenesis

(Perry et al., 2007). Also traumatic brain injury can increase the risk to develop AD. Activated microglia can persist for months or even years after injury highlighting the secondary neuroinflammatory reaction as pathophysiologically even more relevant than the initial insult (Heneka et al. 2015). But also less obvious immune activities associated with obesity and type 2 diabetes act as risk factors for AD (Granic et al. 2009, Jones et al. 2009). Here, activated macrophages in the white fat tissue constantly secrete pro-inflammatory cytokines. Type 2 diabetes and AD both are associated with desensitization of insulin receptors in the brain and might involve changes in BBB integrity. Therefore, both conditions lack neuroprotective properties of insulin independent of glucose utilization and feature alterations in BBB protection.

Research on AD mouse models provides some hints for the involvement of immune activation in disease onset and progression. In the context of an additional activation of the innate immune system, some studies suggest a worsening of Aβ accumulation, tau pathology and even cognitive function in AD models upon peripheral immune stimulation with LPS (Qiao et al. 2001, Sheng et al. 2003, Lee et al. 2010, Valero et al. 2014). But also an enhanced clearance of Aβ plaques and improved AD pathology under pro-inflammatory conditions were reported (DiCarlo et al. 2001, Michaud et al. 2012). Interestingly, the production of nitric oxide as inflammatory response was found to enhance Aβ aggregation. NO mediates post-translational nitrosylation of Aβ filaments promoting their aggregation (Kummer et al. 2011). Even more interesting, the genetic ablation of the NLRP3 inflammasome rescues the AD phenotype (Heneka et al. 2013). IL-1β and IL-18 both are expressed as inactive pre-cursor forms pro-IL-1β and pro-IL-18 respectively which require cleavage by the protease caspase-1 for activation and secretion as mature cytokines. The caspase-1 protein itself gets activated via cleavage by cytosolic multiprotein complexes called inflammasomes. The most prominent inflammasome is the NOD-like receptor family, pyrin domain containing 3 (NLRP3) in macrophages and microglia. NLRP3 expression is activated in parallel to pro-IL-1β and pro-IL-18 expression usually by PAMPs like LPS, but a second stimulus is necessary to promote NLRP3 oligomerization with the adaptor protein ASC (apoptosis-associated-speck-like protein) which leads to autocatalytic cleavage of caspase-1 protease. Not only PAMPs but also amyloid-β aggregates are able to activate the NLRP3 inflammasome (Halle et al. 2008). It was shown that NLRP3 or ASC deficiency can indeed prevent AD related pathology in the APP/PS1 model (Heneka et al. 2013).

As currently no cure or preventive method is available for AD, the observation that exposure to nonsteroidal anti-inflammatory drugs (NSAIDs) decreases the risk to develop AD provided new hope. Most NSAIDs exhibit pain-killing, fever-reducing and anti-inflammatory properties due to the inhibition of cyclooxygenase-1 (COX-1) and -2 (COX-2) and synthesis of prostaglandins and thromboxanes. Several clinical trials with different

NSAIDs identified the respective component, duration of treatment and the age of patients as critical for success. However, trials designed to preventively inhibit brain inflammation in AD patients have failed which again brings up the question if inflammation is purely detrimental in neurodegenerative disease or may also promote clearance of aggregated protein and cell debris.

1.10. Aim of study

Inflammation, the response of the innate immune system to danger signals, can not only occur in the periphery but also in the central nervous system. Here, processes and molecules associated with the immune response can have protective as well as detrimental effects. Also an acute inflammation in the periphery exclusive of brain invasion can negatively affect neuronal morphology, plasticity and learning behavior in rodents.

To gain knowledge about the influences of the immune system long after or in the chronic phase of an infection or immune stimulation, the focus of the presented study was divided into the following aspects:

1) Different types of lipopolysaccharide as well as peptidoglycan and lipoteichoic acid were applied to examine whether distinct immune-stimulatory components differ in their ability to influence neuronal structure and function in the mice CNS.

2) Adult and old mice were used to address a possible age-dependent vulnerability towards a peripheral immune stimulation.

3) The APP/PS1 mouse model of Alzheimer´s disease was deployed for a systemic immune stimulation to investigate whether the genetically induced neurodegeneration in this model is further driven by the peripheral immune system.

4) The NLRP3 KO mouse model was used to analyze the involvement of the NLRP3 inflammasome in effects of a long-term immune stimulation on neuronal structure and function.

5) The parasite *Toxoplasma gondii* was taken as a model of chronic CNS infection to compare effects of a peripheral immune activation with an infection also spreading into the brain.

2. MATERIAL AND METHODS

2.1. Material

2.1.1. Chemicals

All chemicals used in this thesis were obtained from AppliChem, Invitrogen, PAA, Roth or Sigma. Exceptions were mentioned respectively.

2.1.2. Immune stimulatory reagents

Table 1: Bacterial cell wall components used for peripheral immune stimulations

reagent	description	dose
Lipopolysaccharide, *Salmonella enterica serogroup typhimurium*	Sigma Aldrich, product No. L6511	2 x 0.2 µg/g bodyweight
Lipopolysaccharide, *Escherichia coli* O127:B8	Sigma Aldrich, product No. L3129	2 x 0.2 µg/g bodyweight
Peptidoglycan, *Staphylococcus aureus*	Sigma Aldrich, product No. 77140	2 x 0.5 µg/g bodyweight
Lipoteichoic acid, *Staphylococcus aureus*	Sigma Aldrich, product No. L2515	2 x 0.5 µg/g bodyweight

2.1.3. Buffers and solutions

10 x PBS, pH 7.3		
NaCl	1.37 M	
KCl	0.027 M	
KH_2PO_4	0.015 M	
Na_2HPO_4	0.08 M	pH 7.3

ACSF, pH 7.4	
NaCl	124 mM
KCl	4.9 mM
$MgSO_4$ $7H_2O$	2 mM
$CaCl_2$ $2H_2O$	2 mM
$NaHCO_3$	25.6 mM
D+ Glucose (water free)	10 mM

DNA lysis buffer	
Tris/HCl pH 8.5	100 mM
NaCl	200 mM
EDTA	5 mM
SDS	0.2%
Proteinase K	100 µg/ml (stock solution 1 mg/ml)

Blocking solution for immunohistochemistry	
Triton X-100	0.2%
Goat serum	10 %
BSA	1%
in PBS	

2.1.4. Antibodies

Table 2 | Primary and secondary antibodies for immunohistochemical experiments

	Immunohistochemisty		
antibody	**description**	**manufacturer**	**dilution**
anti - GFAP	mouse monoclonal product number G 3893	Sigma-Aldrich	1:1000
anti - IL-1b	rabbit polyclonal catalogue number AB9722 charge 083M4785	Abcam	1:250
anti - TNF-a	rabbit polyclonal catalogue number R4-6A2	Thermo Scientific	1:250 /1:500
anti - IBA 1	rabbit polyclonal catalogue number 234003	Synaptic Systems	1:1000
anti – CD11b	rat monoclonal catalogue number AB-N05	Advanced Targeting Systems	1:500
anti – rabbit Cy2	goat polyclonal product number 111-225-144 charge 81780	Jackson Immuno Research Laboratories	1:500
anti – mouse Cy3	goat polyclonal product number 115-165-068 charge 95966	Jackson Immuno Research Laboratories	1:500

2.1.5. Mouselines

2.1.5.1. APP/PS1 transgenic mice

The Alzheimer mouse model used in this thesis was the B6C3-Tg (APPswe, PSEN1dE9)85Dbo/Mmjax on C57Bl/6 background of donating investigator David Borchelt, McKnight Brain Institute, University of Florida (Borchelt et al. 1997). The mouse model includes two transgenes inserted at a single locus controlled by the mouse prion protein promotor. One transgene encodes for the chimeric amyloid beta precursor protein (3 mouse aminoacids of the A-beta domain were replaced by the human sequence) with the Swedish mutation K595N/M596L (APPswe). The mutation is found in humans with familial cases of Alzheimer´s disease. The second transgene gives raise to mutated presenilin 1 protein. The “DeltaE9” mutation leads to deletion of exon 9, which is associated with the early-onset of Alzheimer´s disease.

2.1.5.2. NLRP3 knockout mice

NLPR3 knockout (KO) mice lack the NOD-like receptor family, pyrin domain containing 3 inflammasome and therefore also lack IL-18 and IL-1β maturation. NLRP3 KO mice were provided by Michael T. Heneka, German Center for Neurodegenerative Diseases (DZNE) and Dept. of Neurology, Clinical Neuroscience, Bonn, Germany. Breeding, genotyping and the aging of these mice were realized at the DZNE. There, NLRP3-deficient animals (Millennium Pharmaceuticals) were backbred onto C57BL/6 mice genotype to more than 99% C57BL/6, which was confirmed by microsatellite analysis. Aged mice were transported 2 weeks prior to the immune stimulation experiments to the animal facility of the TU Braunschweig.

2.2. Methods

2.2.1. Genotyping of APP/PS1 transgenic mice

For the identification of transgene positive APP/PS1 mice, genotyping experiments were performed by Heike Kessler and Eva Saxinger. Genomic DNA was extracted from short tail pieces digested with 500 µl lysis buffer with proteinase K at 650 rpm and 55°C overnight. Genomic DNA was cleaned from cellular debris by centrifugation at 14.000 g for 10 minutes and precipitated with 500 µl isopropanol. The DNA pellet was washed once

with 70% ethanol. The DNA was stored at -20 °C in 20 mM Tris/ HCl (pH 8). Three µl of genomic DNA was used for one polymerase chain reaction (PCR, table 3 - 5) to detect the presence of the APPswe, PSEN1dE9 transgene. Results were obtained via agarose gel electrophoresis.

Table 3 | PCR protocol for genotyping of APP/PS1 transgenic mice

Reagent	Volume
ddH_2O	37.6 µl
10x PCR buffer	5 µl
$MgCl_2$	1.5 µl (50 mM)
dNTPs	1 µl (5 mM)
BACE HC69	0.2 µl (50 µM)
BACE HC70	0.2 µl (50 µM)
S36	0.1 µl (50 µM)
237F	0.2 µl (50 µM)
Antisense J	0.2 µl (50 µM)
Taq polymerase	1 µl
Genomic DNA	3 µl

Table 4 | PCR program for genotyping of APP/PS1 transgenic mice

Step	Temperature	Time
First Denaturation	94°C	3 min
Denaturation	94°C	30 sec
Annealing	65°C	1 min
Elongation	72°C	1 min
Last Elongation	72°C	4 min
Hold	4°C	infinite

Table 5 | Primer sequences for genotyping of APP/PS1 transgenic mice

Primer	Sequence
BACE HC69	AGGCAGCTTTGTGGAGATGGTG
BACE HC70	CGGGAAATGGAAAGGCTACTCC
S36	CCGAGATCTCTGAAGTGAAGATGGATG
237F	CAGGTGGTGGAGCAAGATG
Antisense J	AGCCTAGACCACGAGAATGC

2.2.2. Immune stimulation with endotoxic bacterial cell wall components

To stimulate the peripheral innate immunity in adult and aged mice, well characterized bacterial endotoxins were used. Prior to the immune stimulation, the mice were weighed and monitored daily for at least 4 days up to one week to acclimate to the balance and to daily handling. The bodyweight one day before injection was taken to calculate the necessary volume of the immune stimulatory component. For intraperitoneal administration 1 ml syringe with an 26 G x 1/2 ” 0.45 x 12 mm cannula with the appropriate volume of LPS *Escherichia coli*, LPS *Salmonella typhimurium*, PGN/LTA or 0.9% NaCl (Table 1) was prepared. Therefore, 25 g of LPS-, PGN- or LTA-powder was diluted in 12.5 ml sterile 0.9% NaCl solution and stored as stock (concentration 2 mg/ml) at -20°C until use. The stock solutions of both LPS types were further diluted 1:10 with 0.9% NaCl directly before use and given for 2 days at a concentration of 0.2 µg per g of bodyweight. The PGN and LTA stock were diluted 1:5 in sterile 0.9% NaCl to a concentration of 0.4 mg/ml. The same volume of PGN and LTA was used to prepare a solution with each 0.2 mg/ml per component. PGN/LTA was given for 2 days at a concentration of 0.5 µg/g bodyweight. The mice were weighed, fixed and the suitable volume was injected in the lower right body quadrant. The needle was pulled out slowly to avoid further injury. The leakage of fluid was controlled to make sure no internal organs were hit.

On the second day of immune stimulation, the mice were weighed and put directly into a rodent restrainer (34 mm in diameter, Süd-Laborbedarf Gauting) to take a blood sample from the tail vein. Subsequently, the mice were fixed and the same dose of immune stimulatory component was administered as on day one. Again the lower right body quadrant was chosen for the injection. On the next 13 consecutive days the body weight and sickness behavior of the mice was documented. These procedures had been conducted in accordance with the applicable European and National regulations (Tierschutzgesetz) and approved by the responsible authority (Nds. Landesamt für Verbraucherschutz und Lebensmittelsicherheit; permit number: 33.9-42502-04-13/1106).

2.2.3. Infections with *Toxoplasma gondii*

The experiments concerning the chronic infections with the protozoan *Toxoplasma gondii* (*T.gondii*) were planned and performed by Dr. Alexandru Parlog and Dr. Ildiko Rita Dunay, Institute of Medical Microbiology, Otto-von-Guericke University Magdeburg. The infections with *T.gondii* were approved, according to German and European legislation by the Landesverwaltungsamt Halle (Sachsen-Anhalt, Germany, approval number IMMB/G/01-

1089/11). Shortly, adult C57BL/6 female mice (8 weeks old, purchased from Janvier) were housed in standard lighting conditions (12:12 h light-dark cycle) and temperature (21-23°C), 4 to 5 animals per cage, with food and water *ad libitum*. *T. gondii* cysts of the ME49 type II strain were harvested from mice of NMRI strain, infected with *T. gondii* cysts 4 to 5 months earlier. Brains were isolated from infected mice and dispersed in 1 ml sterile PBS by mechanical disruption of the tissue followed by several passages through needles with regressing diameter.

Cysts were counted under a light microscope and the total number of cysts per brain was calculated. Three cysts were administered intraperitoneally in a total volume of 200 µl per mouse. Control (noninfected) mice received injections with sterile PBS.

2.2.4. Perfusion of the mouse brain and preparation of fixed brain slices

For the preparation of the brain slices, immune stimulated and control C57Bl/6 wildtype mice or APP/PS1 were sacrificed by CO_2 asphyxiation. The mice were placed in an airtight container with CO_2 fed in from a compressed gas cylinder. The animals were observed until all muscle activity and signs of life have been absent for at least 30 seconds. Quickly the mouse was fixed on a plate and the body cavity was opened. After removing skin and muscles of the abdomen the thorax was opened. The right atrium of the heart was cut and a butterfly needle (0.5 x 13 mm G25) was inserted into the left ventricle. Via this needle about 30 ml of 4°C cold 4% PFA and 4% sucrose was directed into the blood circuit by force of gravity. After 10 minutes of perfusion, the mouse was rapidly decapitated. The skull was opened and the brain was removed. The cerebellum and the olfactory bulb were departed and the brain hemispheres were separated along their longitudinal axis with a razor blade.

The brain hemispheres were incubated in 4% PFA with 4% sucrose at 4°C for 30 minutes and subsequently transferred into phosphate buffered saline. The brain hemispheres were cut into 400 µm thick transversal slices with a vibratome (VT 1000 S, Leica Microsystems, Germany). Therefore, the brain was embedded into 2% agar in phosphate buffered saline and glued onto the sample plate. The cutting was performed in a PBS filled buffer tray. The brain slices were collected in a PBS filled tissue culture plate.

2.2.5. DiOlistic labeling of single neurons

Hippocampal and cortical neurons from C57Bl/6 and APP/PS1 control and immune stimulated mice were labeled, 3 month post-stimulation using DiOlistics on fixed brain

slices. For the preparation of the DiI bullets, tungsten particles (50 mg; 1.7 µm in diameter; Bio-Rad) were spread on a glass slide and merged with 100 µl of dye solution prepared by dissolving 3 mg of lipophilic dye DiI (Invitrogen) in 100 µl of methylene-chloride (Sigma-Aldrich). The dried dye-coated particles were removed from the glass slide, suspended in 3 ml of distilled water, and sonicated. The dye solution was subsequently diluted 1:60, 1:70 and 1:80 and used to coat the inside of a TEFZEL tubing (Bio-Rad). After drying the bullets were stored at room temperature (RT). Before labeling, 400 µm thick coronal sections of both hemispheres were post-fixed with 4% PFA and 4% sucrose in 0.1 M PB for 1 h. Slices were washed with PBS and transferred onto a tissue culture insert (Merk-Millipore). Dye-coated particles were delivered to the brain slices using a hand-held gene gun (Bio-Rad; Helios Gene Gun System) with a pressure of 120 psi. A membrane filter (3 µm; Millipore) was inserted between the gene gun and the slice to prevent clusters of large particles from landing on the tissue. After shooting, brain slices were kept in PBS for 20 h at RT to allow dye diffusion. The consecutive day, slices were stained with DAPI-solution 1:1000 for 10 min and mounted with an anti-fading water-based mounting medium (Biomeda). Because of a strong increase of the tissue back ground fluorescence neurons of the hippocampus and cortex were imaged within one week after mounting to assure best image quality.

2.2.6. Imaging and analysis of DiI stained neurons

To examine the dendritic architecture as well as the spine density of the DiI stained hippocampal and cortical neurons, single neurons were first imaged with a 20x objective (0.8 N.A., Zeiss) with a *z*-sectioning of 1 µm.at an Axioplan 2 imaging microscope (Zeiss) equipped with an ApoTome module (Zeiss) to assess dendritic complexity. Afterwards, mid-apical and basal dendrites were imaged with a BX61WI FluoView 1000 (FV1000) Olympus confocal microscope. Image stacks with z-steps of 0.5 µm were acquired using a 40x oil objective (NA1.3). The dendritic morphology was analyzed via tracing of the neuronal processes in three dimensions using the Neurolucida and Neuroexplorer software (MicroBrightField). The density of dendritic spines was determined by counting of spines with the multipoint tool on a stretch of dendrite defined with help of the segmented line in the ImageJ program (US National Institutes of Health). Data were calculated as mean ± SEM and compared to control conditions with an unpaired two-tailed Student's t-test. P values of less than 0.05 were considered significant and plotted as follows: * = $p < 0.05$; ** = $p < 0.01$; *** = $p < 0.001$.

2.2.7. Immunohistochemical analysis of immune response in the central nervous system

To characterize the phenotype of CNS cells involved in innate immune response, astrocytes and microglia were stained in an immunohistochemical approach. Therefore, 400 µm thick fixed brain slices were dehydrated in 30% sucrose in 0.1 M PB. After slices were sunken to the ground, they were frozen in Tissue-Tek® O.C.T.™ compound (A.Hartenstein Laborversand) on a freezing microtome and cut into 30 µm thick slices. The brain slices were incubated in blocking solution for 1 h RT. Slices were incubated with the primary antibody diluted in 0.2% Triton X-100 and 10% goat serum at 4°C covered in plastic wrap on a shaker overnight. After washing with 1 x PBS, slices were incubated with the secondary antibody diluted in 1x PBS for 2 h at RT. Cell bodies were stained with DAPI-solution 1:1000 for 5 min. Slices were mounted with an anti-fading water-based mounting medium (Biomeda). Images of the *stratum radiatum* within the CA1 area of the hippocampus were taken with a 20x objective (0.8 N.A., Zeiss) with a *z*-sectioning of 1 µm.at an Axioplan 2 imaging microscope (Zeiss) and an ApoTome module (Zeiss). GFAP- and IBA-1 positive cells as well as primary processes of IBA-1 positive cells were counted in overlap with the DAPI signal with the help of the multipoint tool of ImageJ (US National Institutes of Health).Data were analyzed with Microsoft excel as mean ± SEM and compared between control and immune stimulated groups using an unpaired two-tailed Student's t-test. P values of less than 0.05 were considered significant and plotted as follows: * = $p < 0.05$; ** = $p < 0.01$; *** = $p < 0.001$.

2.2.8. Preparation and incubation of hippocampal acute slices

To assure cell survival, acute hippocampal slices were prepared in 4°C cold ACSF. From a 10x ACSF stock solution 1 L of fresh ACSF was complemented with the respective amount of D+Glucose and $NaHCO_3$. The ACSF was purged with carbogen (95% O_2 and 5% CO_2) for 20 min prior to use. The interface chamber was washed with MilliQ-H_2O for 30 min and with ASCF for another 20 min with a flow rate of 0.79 ml per min and heated to 32°C.

Mice were deeply anaesthetized by CO_2 asphyxiation and quickly sacrificed by decapitation. The skull was opened, the brain was removed and rapidly put into 4°C cold carbogenated ACSF. First, the cerebellum as well as the olfactory bulb, prefrontal cortex and striatum were eliminated with a scalpel. Then, the hemispheres were separated and one was immediately put back into the cold ACSF. The hippocampus was prepared with two spatulas by gently removing the midbrain and thalamus. Thereon, the hippocampus

was disconnected from the cortex buy loosening the *fimbria hippocampi* and cleaned with cold ACSF before cutting. Therefore, the hippocampus was placed onto the tissue chopper plate in a 70° angel to the razor blade to maintain intra-hippocampal neuronal circuitry. 400 µm thick slices were cut and collected in cold ACSF with a brush. The slices were placed on a custom made nylon net into the interface brain slice chamber and keep under ACSF (pH 7.3, flow rate 0.7 ml per minute) bathing at 32°C, heated by a proportional temperature controller (PTC) (Scientific System Design). The slices were incubated under these conditions for 2 h prior to the electrophysiological measurements to assure metabolic recovery.

2.2.9. Electrophysiological recordings

Recordings of field excitatory postsynaptic potentials (fEPSPs) were performed on hippocampal acute slices in an interface brain slice chamber (Scientific System Design). After an incubation time of 2h at 32°C under constant carbogenated ACSF flow at 0.7 ml/min in the interface chamber, two stimulating and one recording electrode were placed in the hippocampal acute slice (figure 2.1A). Therefore, one stainless-steel recording electrode (5 MΩ; AM-Systems) was placed at 100 µm depth in the *stratum radiatum* of the CA1 region of the slice. Two monopolar lacquer-coated, stainless-steel electrodes (5 MΩ; AM-Systems) were positioned in this region of apical CA1 dendrites to each side of the recording electrode to allow stimulation of two independent populations of Schaffer collateral axons. Later, one stimulating electrode was used to evoke LTP, one served as control pathway. After an initial fEPSP could be detected with both stimulating electrodes, the slices were incubated for another 20 minutes in the previous mentioned conditions.

2.2.9.1. Input-Output curve

To identify the basal synaptic transmission properties for each channel, an input-output relationship between the given stimulus intensity in µA was correlated to the evoked fEPSP slope as indicator for synaptic output of a certain population of CA1 neurons. fEPSPs were recorded at 100 to 600 µA stimulus intensity in intervals of 50 µA. The maximal size of the fEPSP slope was measured and 40% there from was calculated for the further electrophysiological experiments. For this, the steepest fEPSP slope without dominant population spike as impurification of the maximal fEPSP slope at high stimulus intensities was set as maximum (figure 2.1B). Basal synaptic transmission values were indicated as mean ± SEM and the different experimental conditions were only compared

to controls within the same set of experiments using an unpaired two-tailed Student's t-test. Asterisks show levels of significance as follows: * = $p < 0.05$; ** = $p < 0.01$; *** = $p < 0.001$.

2.2.9.2. Paired pulse facilitation

Paired pulse facilitation (PPF) describes the characteristic increase of the EPSP, population spike and unitary firing of a second response if an afferent pathway is electrically stimulated twice in rapid chronology (Fujita and Sakata 1962, Lømo 1971 b; Bliss and Gardner-Medwin 1973). PPF can be evoked as the small increase in the presynaptic calcium concentration at the first stimulus increases the probability for an action potential upon the second stimulus (reviewed by Zucker, 1989), providing that the transmitter pool is not exhausted by previous release (Debanne et al. 1996). In the present study, PPF ratio of the second over the first fEPSP slope was measured at 40% of the maximum fEPSP slope calculated during the input-output experiments. The two stimuli were given in an increasing inter-stimulus interval (ISI) from 10 ms, 20 ms, 40 ms, 60 ms, 80 ms and 100 ms. PPF values were calculated as mean ± SEM and compared to control conditions via an unpaired two-tailed Student's t-test. P values of less than 0.05 were considered significant and plotted as follows: * = $p < 0.05$; ** = $p < 0.01$; *** = $p < 0.001$.

2.2.9.3. Long-term potentiation

Long-term potentiation (LTP) as enduring enhancement of synaptic efficacy is believed to serve as cellular correlate for learning and memory processes (Bliss and Lømo 1973, Bliss and Gardner-Medwin 1973; Bliss and Collingridge 1993). Therefore, the investigation of long-term synaptic plasticity in the form of LTP was performed subsequent to the PPF as short-term plasticity experiments and the evaluation of the basal synaptic transmission for each hippocampal acute slice. After 20 minutes of baseline recordings at 40% of the maximal fEPSP slope and with four 0.2 Hz biphasic, constant-current pulses (0.1 ms/polarity) per input channel at 0.003 Hz, LTP was induced via theta burst stimulation (TBS, figure 2.1c). The TBS, 10 trains of 4 pulses at 100 Hz with an inter-burst interval of 200 ms, applied 3 times in 10 s interval, was given with the beforehand calculated stimulus intensity and is considered as comparable to physiological changes during learning as it reflects naturally occurring firing patterns in the hippocampus of freely moving rats (Larson and Lynch 1986, Bland 1986). After induction, LTP was measured for

60 minutes and analyzed as [(fEPSP slope LTP / mean fEPSP slope baseline) * 100]. LTP was shown as mean ± SEM of fEPSP slope [%]. Values of immune stimulated mice were compared to controls using an unpaired two two-tailed Student's t-test. Levels of significances were plotted as follows: * = $p < 0.05$; ** = $p < 0.01$; *** = $p < 0.001$.

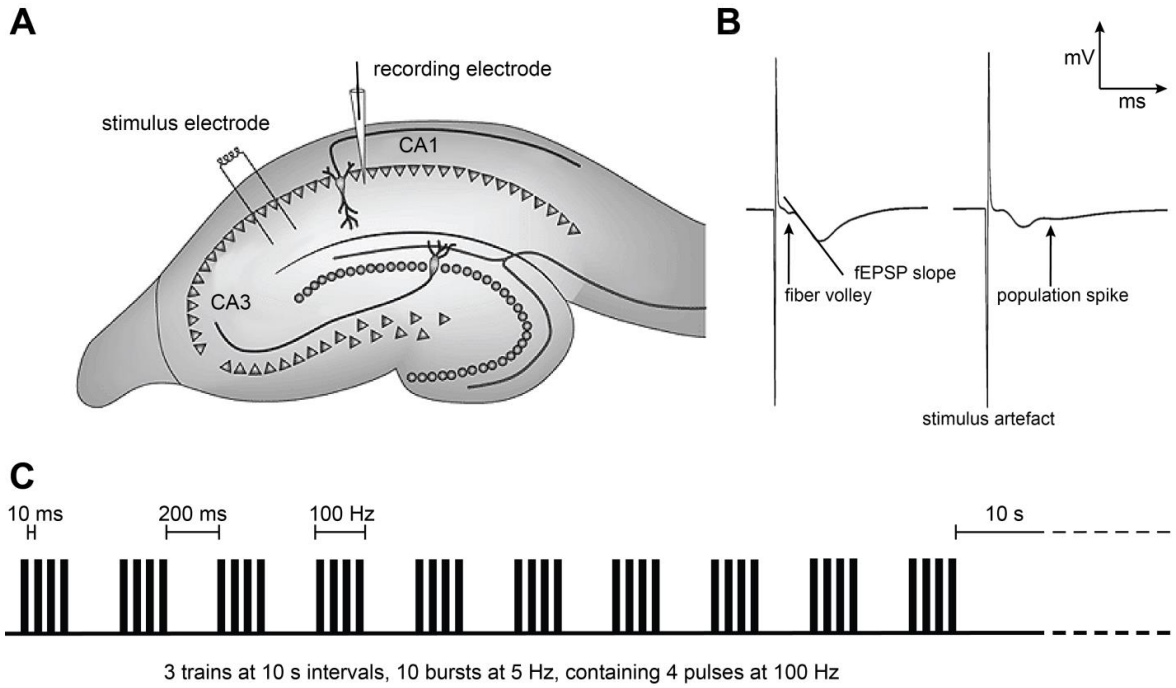

Figure 2.1 | Schematic illustration of the field excitatory postsynaptic potential recorded in the CA1 area of a hippocampal acute slice and theta burst protocol for recordings of long-term potentiation. (A) Transversal hippocampal acute slice with positioning of one stimulating electrode and one recording electrode in the *stratum radiatum* sublayer of CA1 area, adapted from Kim and Diamond 2002. **(B)** Scheme of an exemplary fEPSP signal, fEPSP slope measurement (left) and population spike as criterion of exclusion (right) indicated. **(C)** Theta burst stimulation (TBS) protocol.

2.2.10. Morris water maze navigation task

For the analysis of spatial learning in rodents the water maze of Richard Morris was used (Morris 1981, 1984). The Morris water maze pool with 160 cm in diameter was filled with water at 21 ± 1°C colored opaque with non-toxic white paint (Titanoxid, Euro OTC Pharma) and a white platform was hidden 1 cm under the water surface in the northwest quadrant of the maze in 38 cm distance to the pool wall. Different black and white visual cues (circle, triangle, 4 vertical stripes) were provided an average distance of 30 cm to the maze.

Mice were handled 2 weeks prior to the task for a few minutes every day. The mice were kept on a 12h light/dark cycle with *ad libitum* access to water and food. The training was performed during the light phase of the day. To assess swimming and visual abilities of the animals, a pre-training of 3 days with a cued platform was performed. The mice were

pre-exposed to the platform at 2 trails per day of maximal 45 s. Mice were either placed on the platform or allowed to stay there for 10 s at the end of each trail. The platform position was changed for every trail and the mice were put into the maze on the opposite side of the pool. Mice were trained for 8 consecutive days with 4 trails at a 5 min intertrail interval. Each trail lasted maximum 60 sec and the mice were placed or allowed to stay on the platform for another 15 sec. Entrance into the pool occurred at 4 different position (Northeast, East, South, Southeast, Fig. 2.2) per day.

The mice were tracked with a camera in the ceiling and for each learning day the escape latency, the moved distance and the used search strategies were analyzed. To access memory formation the mice were tested in a probe trail without the hidden platform on day 3 and day 9 of the training. The time spent in the target quadrant as well as the crossings of the former platform position were quantified.

Search strategies were divided into hippocampus-dependent and –independent strategies according to the time spent at the edge of the pool, the annulus zone or the goal corridor as described by Garthe et al. 2009 (Fig. 2.2.). Hippocampus-independent strategies were random search (> 60 % surface coverage), scanning (< 60 % and > 10 % surface coverage) and chaining (> 80 % in the annulus zone). Hippocampus-dependent strategies contained directed search (> 80 % time in 40° goal corridor), focal search (<0.3 x radius to mean distance to the platform, <0.35 x radius to mean distance to swim path centroid) and direct swimming (> 90 % in 10° goal corridor). To access memory formation the mice were tested in a probe trail without the hidden platform on day 3 and day 9 of the training. The time spent in the target quadrant as well as the crossings of the former platform position were quantified.

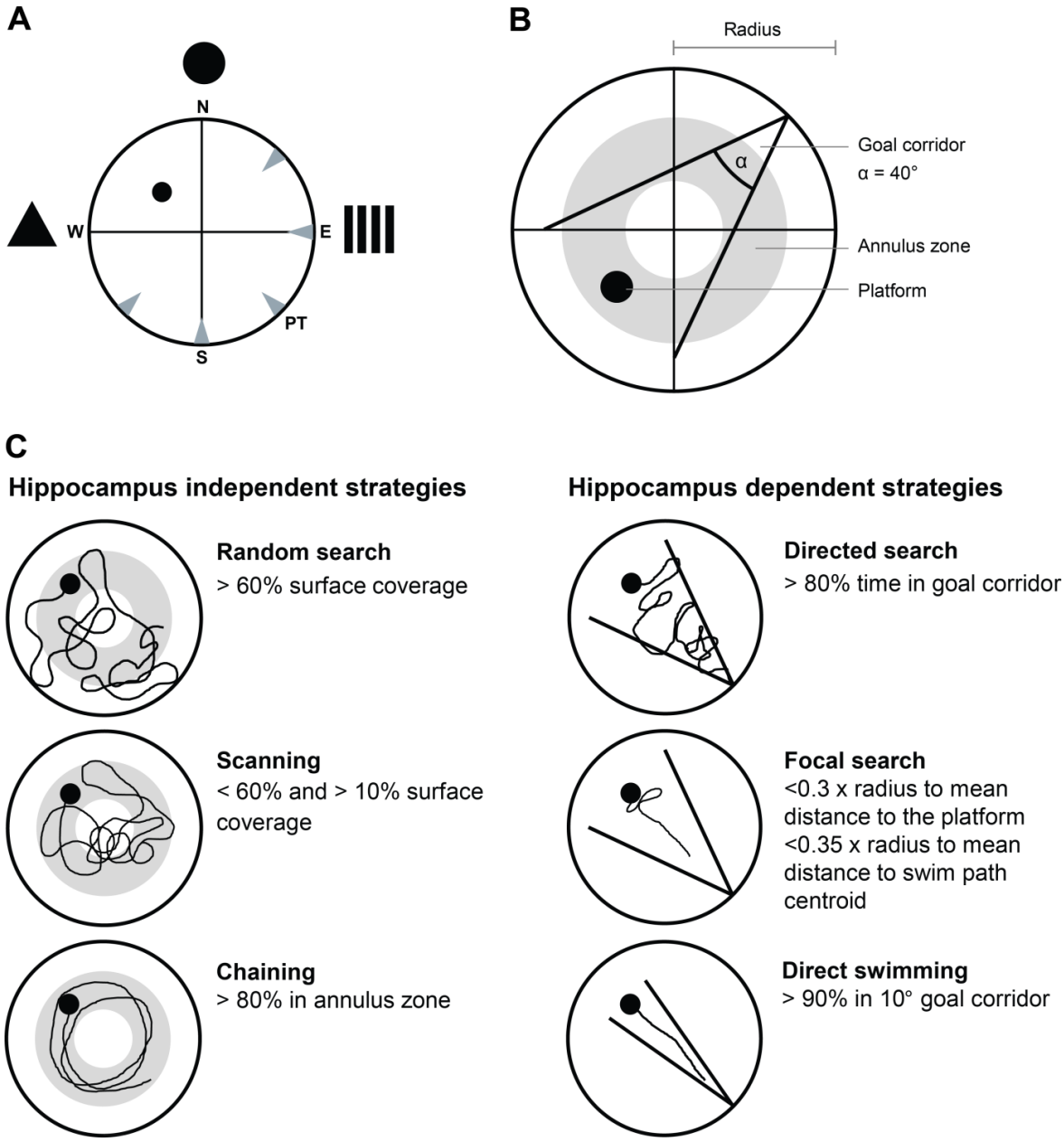

Figure 2.2 | Schematic illustration of the Morris water maze (MWM) arena used for the analysis of spatial learning and memory subclassified in different zones of the arena used for the division into distinct search strategies. (A) MWM arena, hidden platform indicated in the north west quadrant of the maze. Black symbols in the north, west and east serve as visual cues for the animals, starting position of the mice during the training and probe trail (PT) visualized as gray arrows. **(B)** MWM arena divided into the four quadrants, the annulus zone and goal corridor. **(C)** Hippocampus-independent (random search, scanning and chaining) and hippocampus-dependent strategies (directed search, focal search and direct swimming) according to the time spent in the respective area of the MWM arena, adapted from Garthe et al. 2009.

For the Morris water maze experiments, the one way variance ANOVA was used to calculate statistical significance. The search strategy analysis was carried out with using 2-way repeated ANOVA followed by a non-parametric Mann–Whitney U-test. Values of $p < 0.05$ were considered statistically significant (* =$p < 0.05$) p-values lower than 0.01 are

describes as highly significant (** = $p < 0.01$; *** = $p < 0.001$). All data presented in this study are shown as mean ± standard error of the mean (SEM).

2.19 Statistical analysis

All the statistical analyses were performed with Microsoft Excel, Graphpad Prism 5 (Graphpad software) or SPSS (IBM Statistics). A two-tailed student´s t-test was chosen whenever two groups, genotypes, treatments or experimental conditions were compared. This was also the case, when two different treatments were depicted in one graph or figure a comparison was only drawn between the treated and control group, but not the treated groups among themselves as they were considered not dependent on each other.

3. RESULTS

3.1. Long-term effects of an immune stimulation with different kinds of LPS

Sepsis and septic shock as systemic inflammatory response to infection go along with activation of macrophages and massive secretion of pro-inflammatory cytokines like IL-18, IL-6, IL-1β and TNF-α (reviewed in Blackwell and Christman 1996). Symptoms like impairment in attention and memory, delirium and coma can occur and are summarized as septic or sepsis-induced encephalopathy (Pine et al. 1983, Sprung et al. 1990, Wilson and Young 2003). In the rodent model of peripheral LPS injections, the acute consequences of the peripheral LPS administration range from impairment in long-term potentiation (Commins et al. 2001, Jo et al. 2001, Hennigan et al. 2007, Strehl et al. 2014) to deficits in learning and memory (Arai et al. 2001, Shaw et al. 2001, Sparkman et al. 2005). However, long-term influences of a peripheral immune activation have not been satisfyingly addressed so far. In addition to this, also factors like age and the innate immune activation as facilitator of neurodegenerative disease have not been adequately taken into account. Therefore, to investigate the long-term influences of a systemic immune stimulation on neuronal morphology and function, the peripheral immune system of young adult and old C57Bl/6 mice or transgenic APP/PS1 C57Bl/6J mice was activated via intraperitoneal injection of either *Escherichia coli* or *Salmonella enterica* serovar *typhimurium* lipopolysaccharide. In treated mice, 0.2 µg of LPS were given on two consecutive days, while control mice received injections with an equal volume of 0.9% sterile saline (vehicle). The body weight of all animals was controlled over the first two weeks after the immune stimulation to establish the successful injection and subsequent recovery of all immune stimulated mice. Body weight loss of rodents can be correlated to pathogen burden and cytokine release for many infectious diseases as well as to sepsis (Breuillé et al. 1993, Cooney et al. 1999)

With both types of LPS, young immune stimulated WT mice showed a strong loss of body weight up to 15% in the first 2 days after beginning of the immune stimulation with subsequent recovery to about 95% of the initial body weight within another week (Fig. 3.1A, LPS *S.typhimurium*, day 3: 84.92 ± 0.74 % of body weight from day 1, day 15: 95.31 ± 0.74 %; LPS *E.coli*, day 3: 86.57 ± 1.05 % body weight from day 1, day 15: 98,00 ± 0.73 %). The stimulation with LPS of *S.typhimurium* resulted in a slightly stronger reduction in body weight. Control animals showed no change in body weight over the whole period of measurement (Fig. 3.1A, control, day 3: 99.39 ± 0.44 % body weight from day 1, day 15: 101.1 ± 0.83 %).

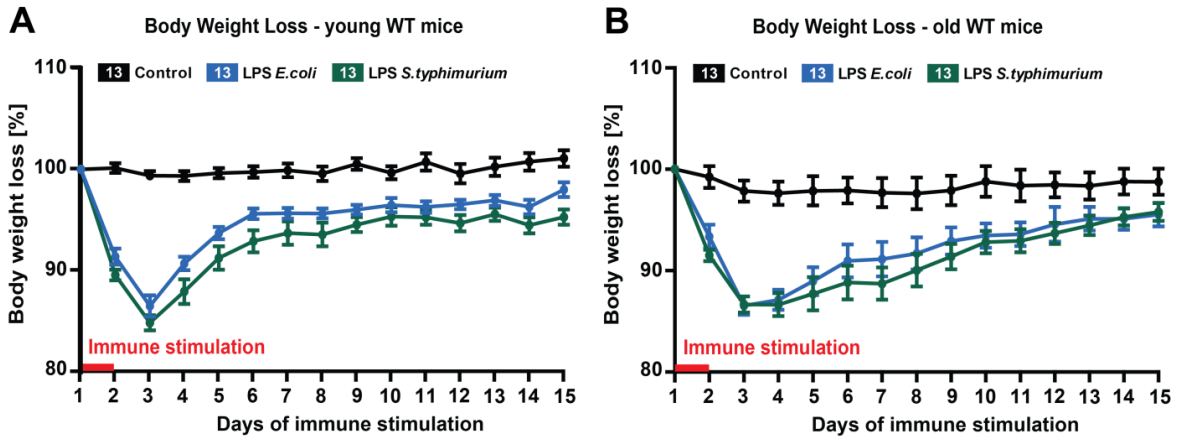

Figure 3.1 | Body weight loss of young adult (4 months) and aged (16 months) C57Bl/6 WT mice during peripheral immune stimulation with *E.coli* or *S.typhimurium* lipopolysaccharide (LPS). Intraperitoneal injections of 0.2 µg/g body weight of LPS from *Escherichia coli* or *Salmonella enterica* serotype *typhimurium* were given for 2 consecutive days (0.4 µg/g body weight in total). Control mice received the injection of the vehicle, sterile 0.9% NaCl solution. (A) Recovery curve of young adult mice documented the first two weeks during and after the immune stimulation. **(B)** Body weight loss of old mice as cause of the immune stimulation on the first two days, indicated in red, and subsequent recovery during the first 15 days. Data presented as mean ± SEM, n = number of animals.

Also the 16 months old WT mice exhibited a rapid loss in body weight on day 2 and 3 of immune activation with both kinds of LPS. However, here the recovery started one day later and proceeded in a less steep fashion. Nevertheless, also the aged WT mice showed a gain of weight up to 95% of the starting body weight in the first two weeks of the experiment (Fig. 3.1B, LPS *S.typhimurium*, day 3: 86.7 ± 0.79 % of body weight from day 1, day 15: 95.60 ± 0.87 %; LPS *E.coli*, day 3: 86.50 ± 0.91 % body weight from day 1, day 15: 95.5 ± 1.17 %). The body weight of the old control mice remained constant over the examined 15 days (Fig. 3.1B, control, day 3: 97.9 ± 1.04 % body weight from day 1, day 15: 98.8 ± 1.39 %). Altogether injections with both LPS of *E.coli* and *S.typhimurium* caused reproducible degree of bodyweight loss in all immune stimulated individuals independent of their age even though the body weight of the 16 months old group of mice showed a higher variation then the 4 months old cohort.

3.1.1. Influence of LPS *E.coli* and LPS *S.typhimurium* on neuronal morphology in aged mice

Systemic inflammation caused by peripheral administration of LPS is able to provoke neuroinflammation (Godbout et al. 2005, Qin et al. 2007), which causes morphological changes of cortical and hippocampal neurons (Milatovic et al. 2010), inhibits long-term potentiation (Vereker et al. 2000, Commins et al. 2001, Hennigan et al. 2007, Min et al.

2009, Strehl et al. 2014) and impairs cognitive function and spatial learning (Pugh et al. 1998, Arai et al. 2001, Sparkman et al. 2005, Chen 2008) during or only shortly after application.

However, the effect of an acute and systemic inflammation on neuronal morphology after the initial sickness behavior and immune activation is overcome has not been investigated so far. In this study, I focused on the architecture of excitatory neurons in different brain regions also known to be susceptible and involved in Alzheimer´s disease. Therefore, I analyzed dendritic complexity and spine density of cortex layer II/III pyramidal neurons as well as pyramidal neurons of the hippocampal CA1 area and the dentate gyrus granule cells. In cortex layer II/III neurons, the Sholl analysis of both, the apical and basal dendrites showed no changes in complexity upon immune stimulation with *E.coli* LPS (Fig. 3.2A) compared to control neurons.

Also the spine density of basal and apical dendrites was only slightly reduced (Fig. 3.2B, 3.2C, basal: control 1.614 ± 0.060 spines/µm dendrite, LPS *E.coli* 1.461 ± 0.091 spines/µm, p = 0.1782; 3.2D, 3.2E, apical: control 1.864 ± 0.063 spines/µm dendrite, LPS *E.coli* 1.690 ± 0.062 spines/µm, p = 0.0626). Three months after the stimulation with LPS from *S.typhimurium* however, there was a slight decrease in the number of intersections of cortex LII/III apical dendrites and significant reduction in the complexity of proximal basal dendrites at a 20 and 30 µm distance from the cell body (Fig. 3.2A). In addition, both the apical and basal compartment exhibited a significantly lower number of dendritic spines per µm than seen in control animals (Fig. 3.2B, 3.2C, basal: control 1.614 ± 0.060 spines/µm dendrite, LPS *S.typhimurium* 1.303 ± 0.100 spines/µm, p = 0.0121; 3.2D, 3.2E, apical: control 1.864 ± 0.063 spines/µm dendrite, LPS *S.typhimurium* 1.487 ± 0.114 spines/µm, p = 0.0096).

Also the basal and apical compartments of CA1 pyramidal neurons were analyzed separately. Again, the treatment with *E.coli* LPS had no effect on basal dendritic complexity after 3 months incubation, but in contrast a significant reduction of intersections in the Sholl analysis of the apical dendritic tree was revealed between 60 and 110 µm from the soma (Fig 3.2F). While the spine density of the basal CA1 dendrites was not altered, the mid-apical dendrites have fewer spines per dendrite in comparison to control neurons (Fig 3.2I, 3.2J, control: 2.025 ± 0.06 spines/µm dendrite, LPS *E.coli*: 1.849 ± 0.049 spines/µm, p = 0.0303).

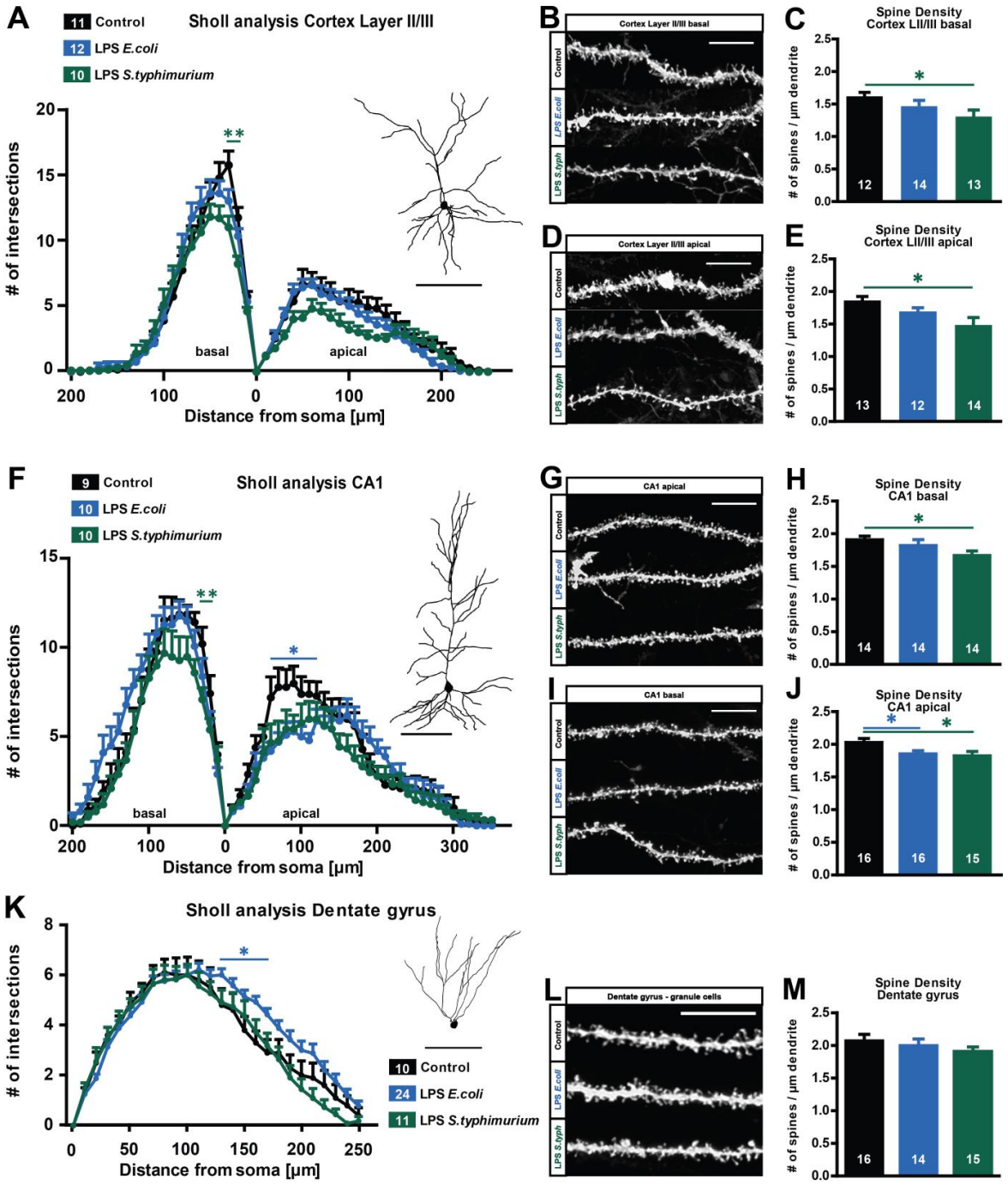

Figure 3.2 | Long-term effects of an immune stimulation with lipopolysaccharide from *Escherichia coli* or *Salmonella typhimurium* on dendritic morphology and spine density of hippocampal and cortical neurons in 19 months old C57Bl/6 mice. (A) Exemplified tracings and Sholl analysis of cortical layer II/III neurons. **(B, D)** Confocal microscopic images from basal and apical cortex LII/III dendrites. **(C, E)** Spine density of basal and apical dendrites from cortex LII/III pyramidal neurons. **(F)** Dendritic complexity of CA1 pyramidal neurons of immune stimulated and control mice, **(G, H)** Confocal image of basal CA1 dendrites and respective spine density. **(I, J)** Exemplified confocal images of CA1 apical dendrites and quantification of the spine density. **(K)** Sholl analysis of dentate gyrus granule cells. **(L, M)** Spine density of granule cells from the dentate gyrus, confocal image. Data presented as mean ± SEM, n = number of neurons and dendrites respectively, scale bar of tracings 100 µm, scale bar confocal microscopic images 10 µm, * = $p < 0.05$; ** = $p < 0.01$.

The treatment with LPS from *S.typhimurium* resulted in a slight reduction in the number of proximal apical dendrites from CA1 pyramidal neurons and in a highly significant reduction in the proximal basal ones at a 30 and 40 µm distance from the cell body. The spine density was significantly lower in apical and basal CA1 dendrites after LPS *S.typhimurium* treatment if compared to control neurons (Fig. 3.2G, 3.2H, basal: control 1.906 ± 0.055 spines/µm dendrite, LPS *S.typhimurium* 1.663 ± 0.069 spines/µm, p = 0.0104; 3.2I, 3.2J, apical: control 2.025 ± 0.060 spines/µm dendrite, LPS *S.typhimurium* 1.819 ± 0.063 spines/µm, p = 0.0241).

The granule cells of the dentate gyrus manifested a significant higher dendritic complexity 3 months after stimulation with LPS of *E.coli* between 130 and 170 µm from the soma while the spine density was not altered (Fig. 3.2K, 3.2L, 3.2M, control: 2.093 ± 0.77 spines/µm dendrite, LPS *E.coli*: 2.019 ± 0.080 spines/µm, p = 0.5057). In comparison, dendritic complexity of granule cells from LPS *S.typhimurium* treated animals was on control level (Fig. XK) and the spine density was only slightly reduced (Fig 3.2L, 3.2M, control: 2.093 ± 0.77 spines/µm dendrite, LPS *S.typhimurium*: 1.932 ± 0.045 spines/µm, p = 0.0845).

Taken together, 3 months after an immune stimulation performed in old C57Bl/6 mice with two different types of LPS resulted, 3 months later in changes in dendritic complexity and spine density of different types of excitatory neurons. The treatment with LPS from *Salmonella typhimurium* caused more pronounced alterations.

3.1.2. Effects of LPS *E.coli* and LPS *S.typhimurium* on synaptic plasticity in old mice

Several studies showed the acute influences of a systemic immune stimulation on synaptic plasticity. For example, long-term potentiation was impaired 6 to 24 hours after treatment with *E.coli* LPS (Arai *et al.* 2001, Commins *et al.* 2001, Di Filippo et al. 2013, Strehl et al. 2014).

In this study, short term as well as long-term plasticity was investigated in hippocampal acute slices of 19 months old C57Bl/6 mice 3 months after peripheral injection of either *E.coli* or *S.typhimurium* LPS. After 20 minutes of baseline recordings E-LTP was induced via TBS and recorded for 1 h. In control slices, it was possible to induce a stable LTP with a mean value of 139.4 ± 8.2 % for the last 10 minutes of recording (Fig 3.3A, 3.3B). Compared to the controls, no change could be observed for LTP in acute slices from *E.coli* LPS treated animals with a mean LTP of 146.2 ± 14.2 % for the last 10 minutes of recording. Interestingly however, the induction as well as the maintenance of LTP after

S.typhimurium LPS treatment was significantly impaired at all time points of the recording (Fig 3.3A, 3.3B, 119.0 ± 4.0 % for the last 3 time points of measurement, p = 0.02).

To examine whether the defect in LTP induction and maintenance is caused by impaired basal synaptic transmission, the input-output properties of the Schaffer collateral pathway were addressed. Here, with increasing stimulus intensities also the negative fEPSP slope increased in all treatments. While there was a perfect overlap of input-output curves under control and LPS *S.typhimurium* treated conditions, surprisingly the slices of *E.coli* LPS treated animals showed significantly lower response at stimulus intensities of 200 to 600 µA in comparison to controls (Fig 3.3C).

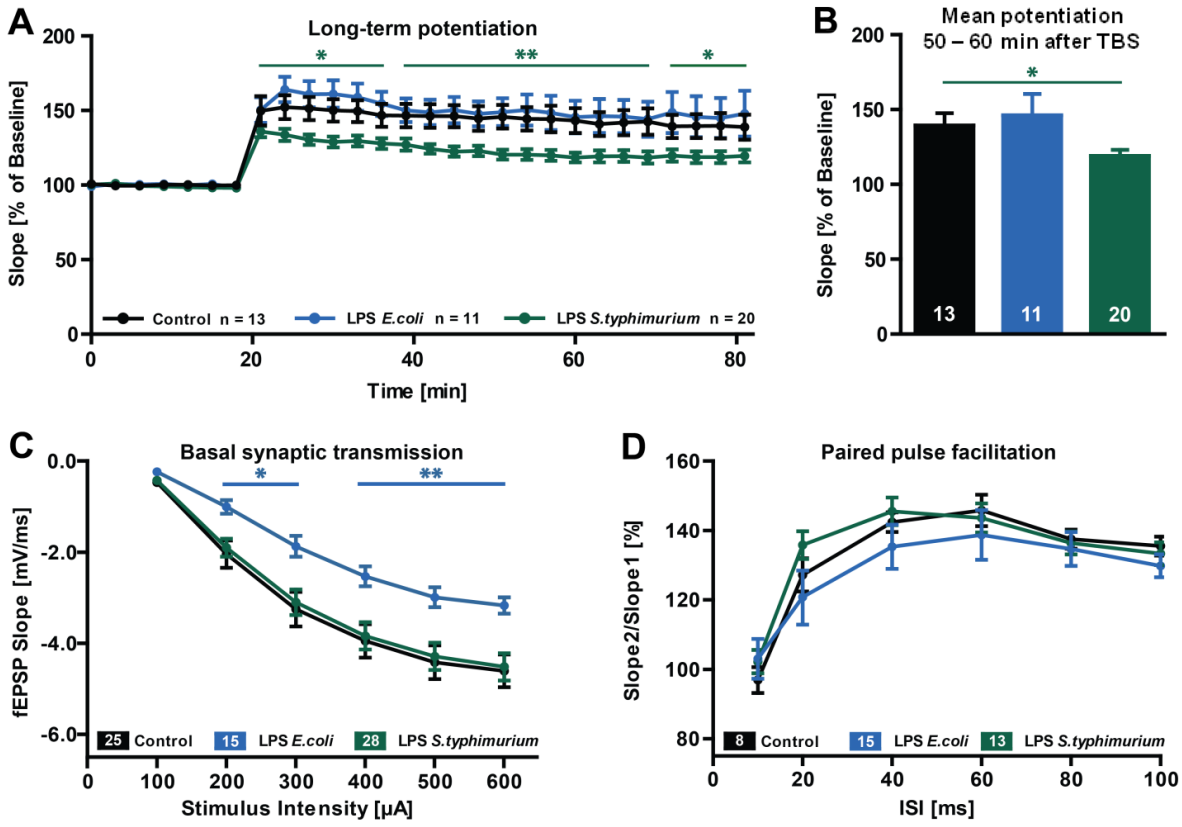

Figure 3.3 | Short-term and long-term synaptic plasticity at the CA3-CA1 pathway in hippocampal acute slices of aged C57Bl/6 WT mice 3 months after peripheral immune stimulation with lipopolysaccharide (LPS) of *Salmonella typhimurium* or *Escherichia coli*. (A) Long-term potentiation induced via TBS after 20 minutes of stable baseline recordings. **(B)** Mean LTP value for the last 3 repeats. **(C)** Input-Output curve. **(D)** Presynaptic properties, paired pulse facilitation with increasing inter stimulus interval (ISI). All data shown as mean ± SEM; n = number of acute slices, * = $p < 0.05$; ** = $p < 0.01$

With the help of the input-output relationship within a certain slice, 40% of the maximal fEPSP slope was calculated and the correlating stimulus intensity was adjusted for a second experiment, the paired pulse facilitation (PPF) to test whether a presynaptic defect is responsible for an altered LTP upon LPS *S.typhimurium* stimulation. Here, two pulses with increasing inter stimulus interval (ISI) were given and the slope of the second fEPSP

was compared to the first slope (fEPSP slope2/ fEPSP slope1). The PPF observed in slices derived from mice treated with both kinds of LPS was not distinguishable from the one in control slices (Fig 3.3D).

In summary, treatment with LPS of *S.typhimurium* leaded 3 months later to a LTP defect which cannot be explained with impaired basal synaptic transmission or paired pulse facilitation. Upon immune stimulation with *E.coli* LPS only the basal synaptic transmission was altered.

3.1.3. Influence of LPS *E.coli* and LPS *S.typhimurium* on learning behavior of aged mice

As a decrease in neuronal complexity, spine density and LTP was observed in aged mice 3 months after immune stimulation with *S.typhimurium* LPS, subsequently the Morris water maze navigation task was used to evaluate the behavioral consequences of the peripheral immune stimulation on spatial learning (Morris 1982, 1984). Sixteen months old C57Bl/6 mice were immune stimulated with intraperitoneal injections of 0.2 µg LPS of either *E.coli* or *S.typhimurium* per g body weight for 2 days for a total of 0.4 µg LPS per g body weight and tested in the Morris water maze navigation task at 19 months of age. After a pre-training period of 3 days, the mice were trained to locate the hidden platform in the northwest quadrant of the maze for 8 consecutive days. A probe trial experiment without platform was performed on day 3 prior to the training session and on day 9 after the entire training period. Independently of the treatment, all mice managed to learn the position of the hidden platform as a progressive improvement in the escape latency was documented over the training time (Fig. 3.4A: Controls 32.8 ± 2.9 s (day 1), 8.0 ± 1.3 s (day 8), $F_{(7,48)}$= 11.001 $p < 0.001$; LPS *E.coli* 38.6 ± 2.9 (day 1), 9.8 ± 1.2 (day 8), $F_{(7,48)}$ = 9.310, $p < 0.01$; LPS *S.typhimurium* 33.2 ± 5.0 (day 1), 11.0 ± 1.6 (day 8), $F_{(7,64)}$ = 6.538, $p < 0.01$). Interestingly, even though the escape latencies decreased in both controls and LPS *S.typhimurium* about the same degree during the whole training, the immune stimulated mice took a significantly longer time to find the hidden platform on day 4 of the training period (Fig 3.4A, Controls 17.2 ± 3.5 s, LPS *S.typhimurium* treated 30.7 ± 4 s, $p = 0.0262$) and show slightly elevated escape latencies also on day 5 and 6 of the training (Fig 3.4A).

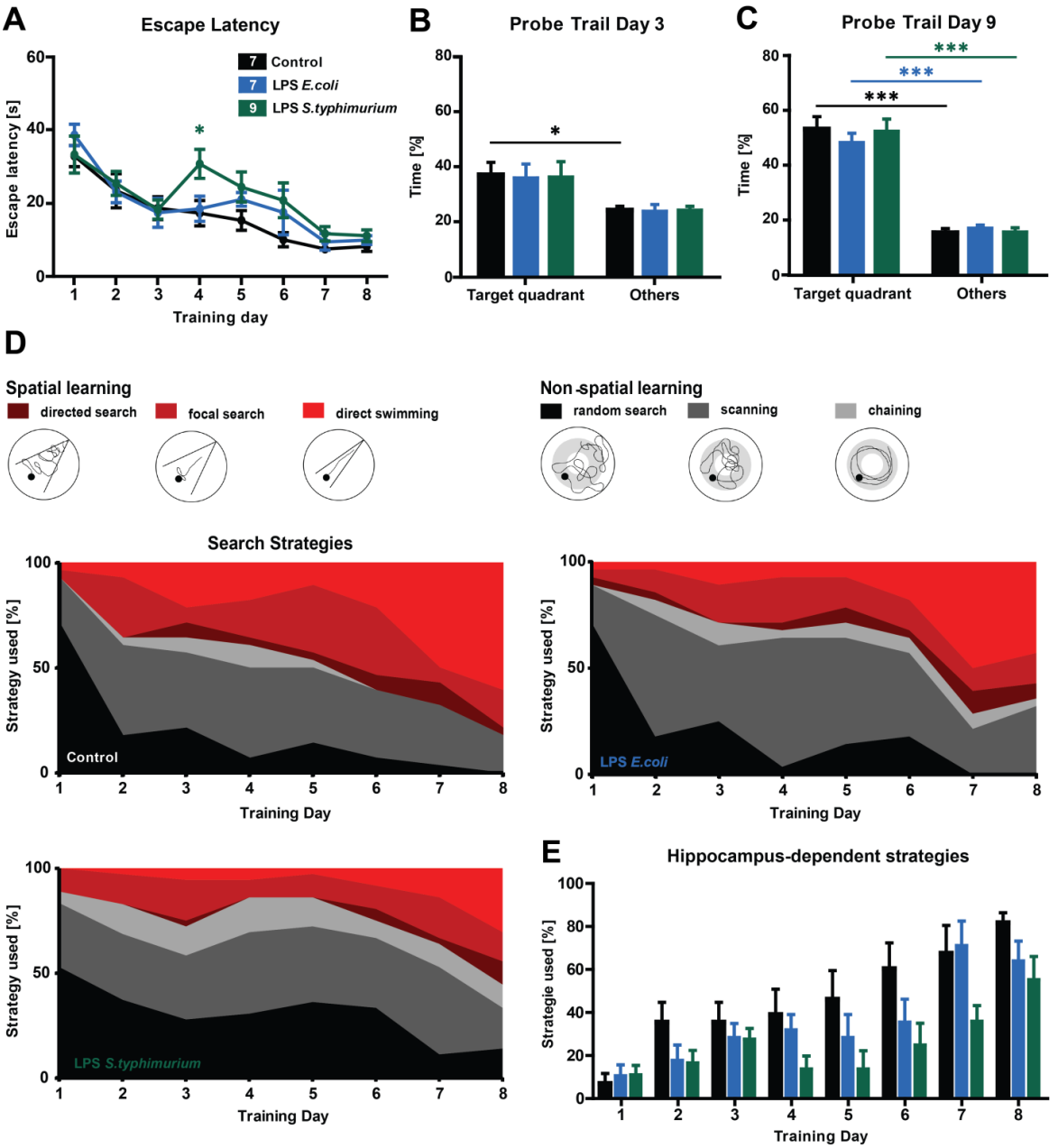

Figure 3.4 | Peripherally immune stimulated mice challenged in the Morris water maze. Control, LPS *E.coli* and LPS *S.typhimurium* stimulated C57Bl/6 mice (19 months old) were trained in the Morris water maze arena with a submerged platform for 8 consecutive days with 4 trials per mouse and day. The escape latency, target quadrant preference of two probe trials on day 3 and 9 and the executed search strategies were analyzed. (A) Escape latency, mean values of 4 trials per mouse per day **(B)** Target quadrant preference in comparison to time spent in other quadrants on day 3 of the training**. (C)** Percent time spent in the target quadrant in comparison to the mean time spent in other quadrants without platform on day 9. **(D)** Illustration and quantification of the six different search strategies random search, scanning, chaining, directed search, focal search and direct swimming as mean of 4 trials per mouse per day. **(E)** Quantification of the hippocampus-dependent search strategies for every single training day. All data shown as mean ± SEM, n = number of mice, * = $p < 0.05$.

To test early memory formation during the Morris water maze, the first probe trial experiment was performed after two days of learning, on the third day of the training period. In absence of the hidden platform, control mice spent significantly more time in the target quadrant, when compared to the other quadrants (Fig 3.4B, controls: other

quadrants 24.1 ± 1.4 % vs. target quadrant 36.9 ± 4.6 %, p = 0.0199). Notably, LPS treated mice did not show this early target quadrant preference (Fig 3.4B). In the probe trial on day 9, all mice spent significantly more time in the target quadrant than in the other 3 quadrants (Fig 3.4C, controls 53.5 ± 4.5 %, p = 0.0001; LPS *E.coli* 48.5 ± 3.4 %, p = 0.0001; LPS *S.typhimurium* 52.6 ± 4.5 %, p = 0.0001). Here, a difference between the three groups is not perceptible.

These data confirm the observation from the platform escape latencies, that LPS *S.typhimurium* treated animals show some deficits in memory formation or consolidation earlier during the training period (day 4 to day 6), but are undistinguishable from the controls during the last days of training (day 7 & 8) and complete the training session with a probe trial on control level.

To investigate the quality of spatial learning during these critical days for the LPS *S.typhimurium* treated group and to emphasize possible differences in the learning behavior of the immune stimulated mice, the search strategies during the learning period were analyzed. For this purpose, the search tracks of each mouse and trial were analyzed. The quantification of the time spent in the middle of the pool, the outer regions, the annulus zone or the goal corridor (Fig. 2.2., Material and Methods chapter 2.2.10.), gives the opportunity to divide the search strategies used by the mice into hippocampus-dependent or spatial learning, allocentric search strategies including focal search, directed search and direct swimming, with increasing accuracy and hippocampus-independent or non-spatial learning, egocentric strategies like chaining, scanning and random search (Fig. 3.4D, Garthe et al 2009, Garthe and Kempermann 2013). In control mice, random search and scanning progressively decreased over the 8 days of training. Chaining was only marginally used. These hippocampus-independent strategies decreased especially in favor of direct swimming, which increased from 3.6 ± 3.6 % (day 1) to 60.7 ± 13.2 % (day 8). Also the LPS *E.coli* treated mice showed a steady decrease of random search and scanning. These mice however, applied chaining in about 6 % of all cases on every training day (Fig 3.4C). Also here, a dramatic increase of direct swimming from 3.6 ± 3.6 % (day 1) to 42.9 ± 4.6 % (day 8) was visible.

In the LPS *S.typhimurium* treated mice, from day 1 to day 5 of the training there was nearly no change in the proportion of the six evaluated search strategies. Only from day 6 to day 8 of learning, random search and scanning were used less, but still to a higher extend then in control or LPS *E.coli* treated mice. The most precise search strategy, direct swimming, increased from 0.0 ± 0.0 % (day 1) to 30.6 ± 6.9 % (day 8) in *Salmonella typhimurium* LPS treated aged WT mice (Fig. 3.5A, day 7: controls 50.0 ± 12.2 %, LPS *S.typhimurium* 13.9 ± 4.4 %, p = 0.023). Altogether, the hippocampus-dependent strategies increased dramatically from 7.1 ± 4.6 % (day 1) to 82.1 ± 4.6 % (day 8) in controls ($F_{(7,48)}$= 7.77, p = 0.0001) and substantially from 10.7 ± 5.1 % (day 1) to 64.3 ±

9.2 % (day 8) in LPS *E.coli* ($F_{(7,48)}$ = 7.333, p = 0.001), while *LPS S.typhimurium* treated mice showed a less pronounced increase from 11.1 ± 4.4 % (day 1) to 55.6 ± 10.8 % (day 8) ($F_{(7,64)}$ = 4.610, p = 0.001). Even though the differences in the distribution of search strategies was not significant for a single training day, the observation that control mice used hippocampus-dependent strategies in about half of the trials in contrast to one fourth of HC-dependent strategies in LPS *S.typhimurium* treated mice is worth mentioning.

In a second approach only the first trial of every mouse per day was analyzed. As mice were trained for 4 trials per day, a bad performance in the first trial speaking for impaired long-term memory could be balanced via the last 3 trials taking advantage of short term memory as well.

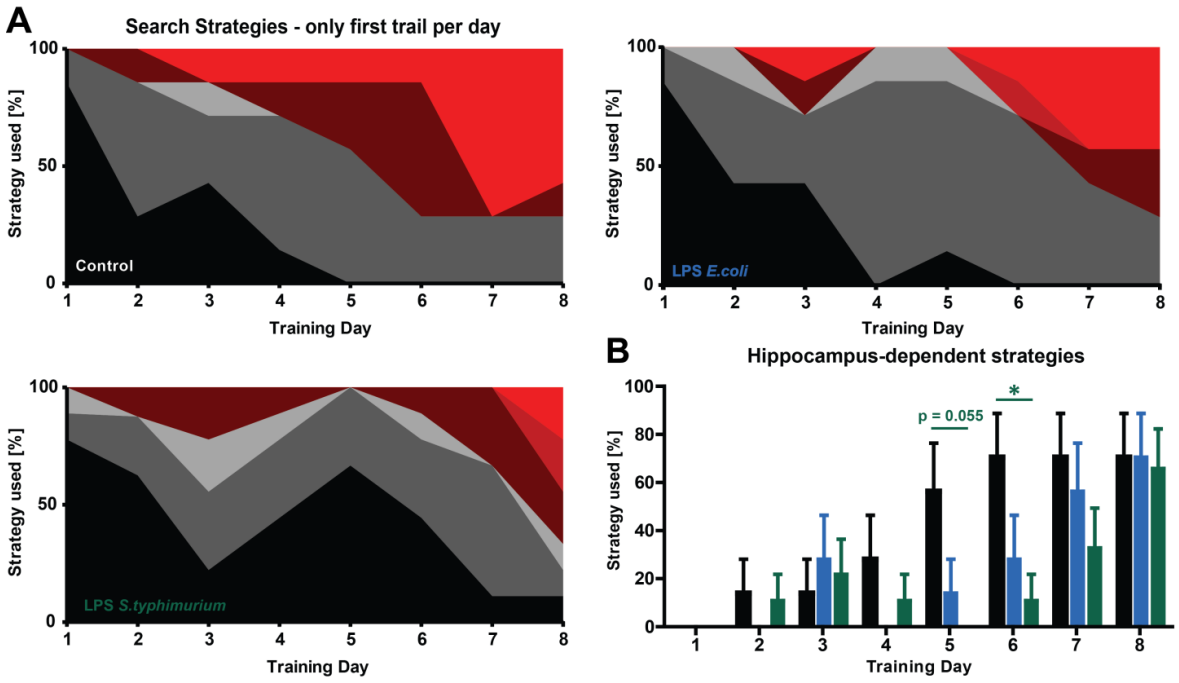

Figure 3.5 | Search strategies in the Morris water maze applied by 19 months old C57Bl/6 mice 3 months after peripheral immune stimulation with LPS of *E.coli* or LPS of *S.typhimurium.* Control (n = 7), LPS *E.coli* (n = 7) and LPS *S.typhimurium* (n = 9) treated mice were trained in the Morris water maze arena with a submerged platform for 8 consecutive days with 4 trials per mouse and day. (A) Illustration of the 3 hippocampus-dependent search strategies directed search, focal search and direct swimming and 3 hippocampus-independent random search, scanning and chaining. Quantification of search strategies of the first trial per mouse and day **(B)** Quantification of the hippocampus-dependent search strategies for every single training day, only the first trial was taken into account. All data shown as mean ± SEM. * = p < 0.05**.**

In control mice, the search strategy proportions of only the first trial are highly comparable to the results from all 4 trials per day. Random search and scanning decreased progressively and from day 5, no random search was shown at all (Fig. 3.5A). Scanning was reduced to 28.6 ± 18.4 % for the days 6 to 8. Chaining was again only shown marginally. The hippocampus-dependent strategy directed search was not shown on day 3 and 7 of the training, while focal search was not used at all. Direct swimming was

increased from 14.3 ± 14.3 % on day 3 to 57.1 ± 20.2 % on day 8 of the learning period (Fig 3.5A). In contrast to that, the LPS *E.coli* and *S.typhimurium* treated mice show a dramatically different pattern of search strategies. The LPS *E.coli* treated mice did not show hippocampus-dependent strategies on day 1, 2, 4 and 5 of the training. Even though random search was rapidly decreased, scanning was shown to a very high extent until day 6 of the learning period (Fig 3.5A, LPS *E.coli*, day 6: 71.4 ± 18.4 %). The implementation of the hippocampus-dependent strategies increased appreciable only from day 6 (28.6 ± 18.4 %) to day 8 (71.4 ± 18.4 %). The *Salmonella* LPS treated mice showed even less hippocampus-dependent learning (Fig 3.5A). In the first 5 days, only directed search was executed as hippocampus-dependent strategy with the highest amount on day 3 with 22.2 ± 14.7 %. Focal search and direct swimming were only used on day 8 of learning. Altogether, LPS *S.typhimurium* treated mice showed slightly less hippocampus-dependent searching on day 5 (Fig 3.5B, controls: 42.9 ± 20.2 % vs. LPS *S.typhimurium*: 0.0 ± 0.0 %, $p = 0.055$) and significantly less on day 6 (Fig 3.5B, controls: 71.4 ± 18.4 % vs. LPS *S.typhimurium*: 11.1 ± 11.1 %, $p = 0.042$).

The analysis of the 1st trial resulted in even more pronounced effects, showing deficits in hippocampus-dependent spatial learning for LPS *S.typhimurium* treated aged WT mice. Amazingly however, they were identical to the control mice on the last day of training and finished the Morris water maze with a probe trial comparable to controls. One possible explanation for this learning impairment is the heavy production of pro-inflammatory cytokines by either brain resident microglia and astrocytes or invading immune cells.

3.1.4. Quantification of glial immune response in the brain of old immune stimulated mice

Even though some studies already suggest long lasting inflammatory events and enhanced classical activation of microglia and astrocytes happening in the brain of aged individuals upon a peripheral immune stimulation (Godbout et al., 2005; Barrientos et al., 2009a), time courses longer than two weeks, have not been investigated so far. In the present study, I immunostained microglia and astrocytes in the hippocampus of 19 months old C57Bl/6 mice 3 months after a peripheral immune stimulation with lipopolysaccharide of *Escherichia coli* or *Salmonella enterica* serovar *typhimurium*. For this purpose, hippocampi of immune stimulated and control mice were fixed, deep frozen and cut into 30 µm thick transversal slices. To visualize astrocytes in the tissue, an antibody against the glial fibrillary acidic protein (GFAP) was used. GFAP-positive cells were counted in a defined region of interest (ROI) and compared to the control samples, which were normalized to 1. The number of astrocytes quantified via GFAP staining, was

not elevated in the *stratum radiatum* of CA1 in hippocampi of immune stimulated mice 3 months after incubation independent of the LPS component used (Fig 3.6B, controls: 1.00 ± 0.08 GFAP$^+$ cells/ROI; LPS *E.coli*: 1.04 ± 0.07, p = 0.898; LPS *S.typhimurium*: 1.06 ± 0.09, p = 0.6402).

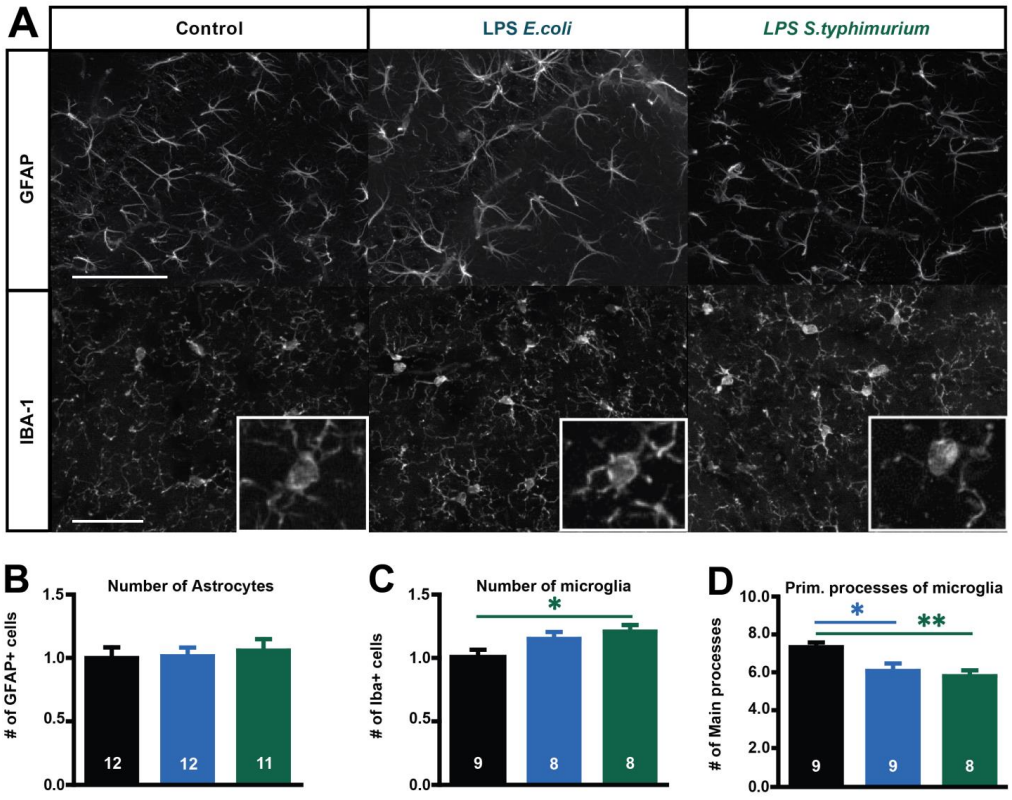

Figure 3.6 | Astrocyte and microglia phenotype of 19 months old C57Bl/6 mice 3 months after peripheral immune stimulation with lipopolysaccharide (LPS) of *Escherichia coli* or *Salmonella typhimurium* in 30 µm hippocampal transversal slices (A) Maximum intensity projection of staining of astrocytes and microglia/macrophages in the *stratum radiatum* of the CA1 area with primary antibodies against Glial fibrillary acidic protein (GFAP) and ionized calcium-binding adapter molecule 1 (IBA-1) respectively, scale bar large frame 100 µm, smaller detail 10 µm. **(B)** Quantification of GFAP$^+$ cells, normalized to controls. **(C)** Number of microglia/macrophages of immune stimulated mice CA1 area compared to controls, n = number of ROIs analyzed (D) Number of primary branches of IBA1$^+$ cells in control and immune stimulated aged WT mice, n = number of cells. All data are presented as mean ± SEM, * = $p < 0.05$; ** = $p < 0.01$.

The second cell type analyzed was the IBA1-positive cell population. IBA1 or ionized calcium-binding adapter molecule 1 is also known as allograft inflammatory factor 1 (AIF-1). It is expressed on microglia and macrophages and up regulated upon inflammation.

Counting of IBA-1-positive cells revealed a significant increase in the number of microglia/macrophages only upon stimulation with LPS from *S.typhimurium*, whereas there was only a slight increase with *E.coli* LPS (Fig 3.6C, controls: 1.00 ± 0.07 IBA1$^+$ cells/ROI; LPS *S.typhimurium*: 1.21 ± 0.05, p = 0.0310; LPS *E.coli*: 1.15 ± 0.06, p = 0.1119).

In a following approach, the number of primary microglia/macrophage branches was counted per IBA1-positive cell. In microglia, a very complex, branched structure indicates the resting housekeeping function, which is rapidly transformed into a macrophage like amoeboid structure upon proinflammatory activation (reviewed by Kettenmann 2011).
The activation status of the microglia/macrophages quantified counting the number of primary branches of IBA-1-positive cells was altered in the hippocampi of aged mice with both types of LPS. The number of primary processes was significantly decreased upon immune stimulation with *E.coli* LPS (Fig 3.6D, controls: 7.33 ± 0.24 prim. processes/IBA1$^+$ cell; LPS *E.coli*: 6.07 ± 0.40, p = 0.0200). The reduction of primary branches was even more pronounced and highly significant 3 months after the treatment with LPS from *S.typhimurium* (Fig 3.6D, controls: 7.33 ± 0.24 prim. processes/IBA1$^+$ cell; LPS *S.typhimurium*: 5.79 ± 0.31, p = 0.0013).
In summary, even though there was no astrogliosis detectable in hippocampi of aged mice, the microglia/macrophage phenotype indicates a pro-inflammatory activation even 3 months after the immune stimulation with LPS of either *E.coli* or *S.typhimurium* with a more severe activation seen in the later.

3.1.5. Influence of *E.coli* and *S.typhimurium* LPS on neuronal morphology in adult mice

The analysis of neuronal structure and signaling revealed a sensitivity of aged mice towards a peripheral immune stimulation with LPS of *S.typhimurium*. To examine, whether also young adult mice show alterations in neuronal architecture as long-term consequence of a systemic immune stimulation, 4 months old C57Bl/6 mice were peripherally immune stimulated with lipopolysaccharide of either *Escherichia coli* or *Salmonella enterica* serovar *typhimurium* and 3 months after incubation neuronal architecture was analyzed using a DiOlistic approach.

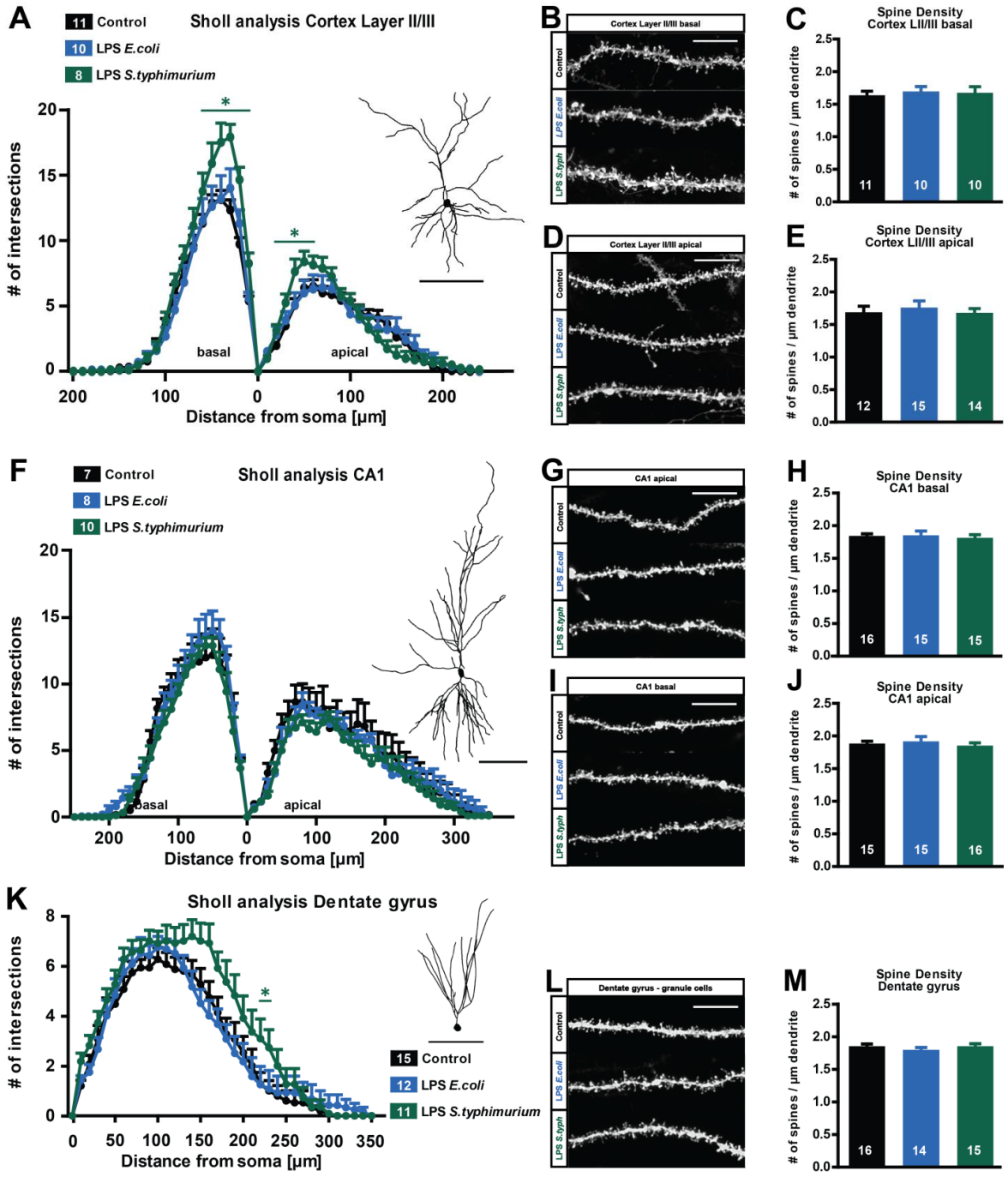

Figure 3.7 | Dendritic architecture and spine density of hippocampal and cortical neurons 3 months after immune stimulation of 4 months old C57Bl/6 mice with LPS *S.typhimurium* or LPS *E.coli.* (A) Dendritic complexity of cortex layer II/III cells of immune stimulated and control mice, scale bar of exemplified tracing 100 µm. **(B, C)** Confocal microscopic image and density of basal cortex LII/III spines, scale bar 10 µm. **(D, E)** Spine density of cortex layer II/III cells upon immune stimulation, scale bar of DiI stained dendrites in confocal images 10 µm. **(F)** Dendritic morphology of CA1 hippocampal neurons, scale bar 100 µm **(G, H)** Spine density of basal CA1 dendrites, 10 µm scale bar of confocal images. **(I, J)** Apical CA1 dendrites, confocal microscopic images, scale bar 10 µm and quantified spine density. **(K)** Sholl analysis of dentate gyrus granule cells, scale bar of tracing 50 µm. **(L, M)** Spine density and exemplified image of granule cells, scale bar 10 µm. Data presented as mean ± SEM, n = number of neurons or dendrites respectively, * = $p < 0.05$.

Similarly to the experiments with aged mice, pyramidal neurons of the CA1 area and cortex layer II/III as well as dentate gyrus granule cells were examined. In the cortex layer

II/III, 3 months after immune stimulation with LPS of *E.coli*, the Sholl analysis revealed a dendritic complexity on control level for both apical and basal dendrites (Fig 3.7A). Also there was no change in spine density of either apical or basal dendrites (Fig 3.7B, 3.7C, basal: control 1.619 ± 0.064 spines/µm dendrite, LPS *E.coli* 1.673 ± 0.081 spines/µm, p = 0.6010, 3.7D, 3.7E apical: control 1.692 ± 0.94 spines/µm dendrite, LPS *E.coli* 1.766 ± 0.101 spines/µm, p = 0.6029). While the number of spines per µm apical or basal Cortex LII/III dendrites in *S.typhimurium* LPS treated mice was equal to the controls (Fig 3.7B, 3.7C, basal: control 1.619 ± 0.064 spines/µm dendrite, LPS *S.typhimurium* 1.658 ± 0.093 spines/µm, p = 0.7250, 3.7D, 3.7E apical: control 1.692 ± 0.94 spines/µm dendrite, LPS *S.typhimurium* 1.684 ± 0.064 spines/µm, p = 0.9395), the dendritic complexity was significantly elevated in the basal and proximal apical compartment, between 10 and 60 µm and 20 and 60 µm from the soma respectively (Fig 3.7A).

The Sholl analysis of the CA1 pyramidal neurons showed an almost perfect overlap for both LPS *E.coli* and *S.typhimurium* treatment (Fig 3.7F). Furthermore, the spine densities for apical and basal dendrites were on control level for both kinds of immune stimulation (Fig 3.7G, 3.7H, basal: control 1.825 ± 0.033 spines/µm dendrite, LPS *E.coli* 1.834 ± 0.064 spines/µm, p = 0.8988; LPS *S.typhimurium* 1.796 ± 0.047 spines/µm, p = 0.6162; Fig 3.7I, 3.7J, apical: control 1.866 ± 0.34 spines/µm dendrite, LPS *E.coli* 1.900 ± 0.071 spines/µm, p = 0.6692; LPS *S.typhimurium* 1.835 ± 0.041 spines/µm, p = 0.5589).

In the dendritic complexity of the granule cells of the dentate gyrus, the treatment with *S.typhimurium* LPS caused a stronger increase in intersections, which was significant between 220 and 230 µm from the cell body, while the *E.coli* LPS treatment resulted in a complexity at control level (Fig 3.7K). The spine density of these granule cells was not affected by either treatment (Fig 3.7L, 3.7M, control 1.832 ± 0.034 spines/µm dendrite, LPS *E.coli* 1.775 ± 0.038 spines/µm, p = 0.2777; LPS *S.typhimurium* 1.832± 0.037 spines/µm, p = 0.9957).

Taken together, independently of the kind of LPS, the immune stimulation of young adult mice did not cause any detrimental long-term influences on neuronal structure. Due to this absence of a clear structural phenotype, the consequences for neuronal function or the spatial learning of younger mice were not addressed in this study.

3.1.6. Comparison of the glial phenotype in young and old mice

To investigate whether the glial immune response to a peripheral immune stimulation is as long lasting in adult as seen in aged mice, microglia and astrocytes were immunostained in the hippocampus of 7 months old C57Bl/6 mice 3 months after a peripheral immune stimulation with lipopolysaccharide of *Escherichia coli* or *Salmonella enterica* serogroup

typhimurium. The number of astrocytes in the *stratum radiatum* of CA1 in hippocampi of immune stimulated mice 3 months after incubation was not different from the one observed in control mice (Fig 3.8B, controls: 1.00 ± 0.10 GFAP$^+$ cells/ROI; LPS *E.coli*: 1.00 ± 0.08, p = 1.0000; LPS *S.typhimurium*: 0.98 ± 0.11, p = 0.9073).

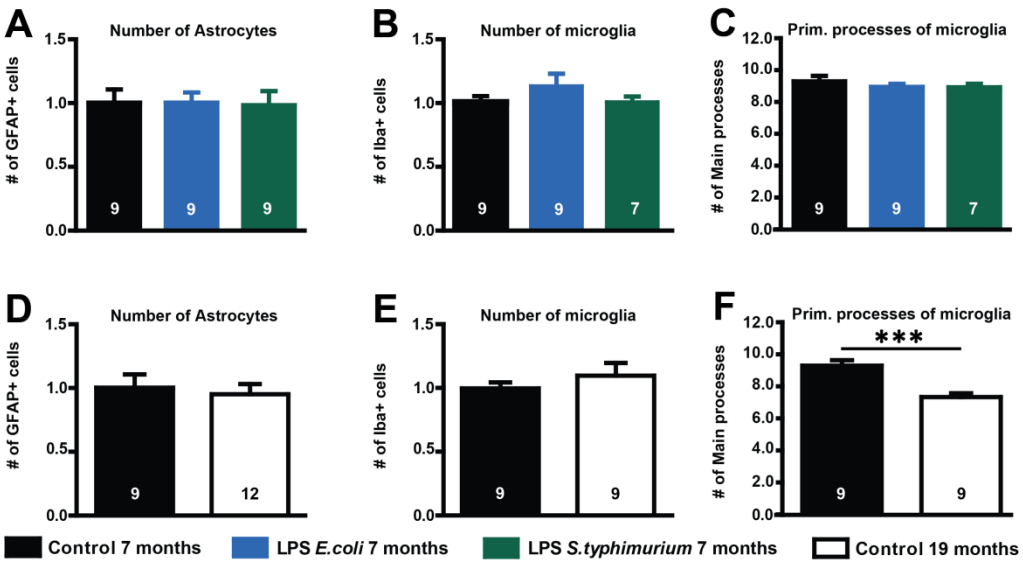

Figure 3.8 | Astrocyte and microglia phenotype of 7 months old C57Bl/6 mice 3 months after peripheral immune stimulation with LPS of *Escherichia coli* or *Salmonella typhimurium* in 30 µm hippocampal transversal slices (A) Quantification of astrocytes in the *stratum radiatum* of the CA1 area with primary antibodies against GFAP (Glial fibrillary acidic protein), normalized to controls, n = number of ROIs analyzed. **(B)** Number of microglia/macrophages of immune stimulated mice analyzed via IBA-1 (ionized calcium-binding adapter molecule 1) antibody staining in the CA1 area compared to controls, n = number of ROIs analyzed **(C)** Number of primary branches of IBA1$^+$ cells in control and immune stimulated adult WT mice, n = number of cells. **(D)** Comparison of astrocyte numbers in 7 and 19 months old mice under control conditions via GFAP-staining. **(E)** Number of microglia/macrophages of 7 and 19 months old control mice, n = # of ROIs. **(F)** Quantification of primary processes of IBA-1-positive cells in adult and aged controls, n = # of cells. All data are presented as mean ± SEM, *** = p < 0.001.

Also the number of IBA-1-positive microglia/macrophages was not altered in adult mice 3 months after immune stimulation when compared to the control conditions (Fig 3.8C, controls: 1.00 ± 0.05 IBA-1$^+$ cells/ROI; LPS *E.coli*: 1.13 ± 0.10, p = 0.2788; LPS *S.typhimurium*: 1.00 ± 0.05, p = 0.9864). The activation of these immune cells was not different from controls in the CA1 area of young adult immune stimulated mice (Fig 3.8D, controls: 9.30 ± 0.34 prim. processes/IBA-1$^+$ cell; LPS *E.coli*: 8.94 ± 0.96, p = 0.3764; LPS *S.typhimurium*: 8.93 ± 0.96, p = 0.3253).

As the microglia/macrophage phenotype seen in old mice indicates a pro-inflammatory activation even 3 months after the immune stimulation with LPS, which was not visible in their young counterparts, the basal level of astrocytes and microglia was compared between young and old individuals. The number of astrocytes was only mildly reduced with age (Fig 3.8E, controls 7 months: 1.00 ± 0.10 GFAP$^+$/ROI; controls 19 months: 0.95 ±

0.08, p = 0.7179), whereas the quantification of microglia showed a slight increase (Fig 3.8F, controls 7 months: 1.00 ± 0.05 IBA-1$^+$ cells/ROI; controls 19 months: 1.13 ± 0.16, p = 0.1618). The pro-inflammatory activation of these microglia cells however, was heavily increased in old control mice seen in a highly significant reduction of primary microglia processes (Fig 3.8G, controls 7 months: 9.30 ± 0.34 primary processes/IBA-1$^+$ cell; controls 19 months: 7.33 ± 0.24, p = 0.0002). This supports the hypothesis of an age-dependent “primed status” of immune cells in the brain, which leads to a prolonged activation in response to a peripheral immune stimulation not seen in young mice.

3.1.7. Changes in neuronal morphology upon LPS stimulation in aged APP/PS1 mice

In the context of an additional activation of the innate immune system in promoting the progression of Alzheimer´s disease, some studies suggest a worsening of Aβ accumulation, tau pathology and even cognitive function in AD models upon peripheral immune stimulation with LPS (Qiao et al. 2001, Sheng et al. 2003, Lee et al. 2010, Valero et al. 2014). Other studies report an enhanced clearance of Aβ plaques and improved AD pathology under pro-inflammatory conditions (DiCarlo et al. 2001, Michaud et al. 2012). However, time points longer than one month after immune stimulation and consequences for neuronal morphology and synapse loss were not examined and a short-term improvement or worsening cannot be excluded. In addition to that, all studies were performed with young adult mice and the influence of age was neglected so far. It was tempting to hypothesize, that the immune stimulation of old AD mice with a proinflammatory priming of the brain leads to an even more severe neurodegenerative phenotype than seen in WT mice with the same stimulation protocol.

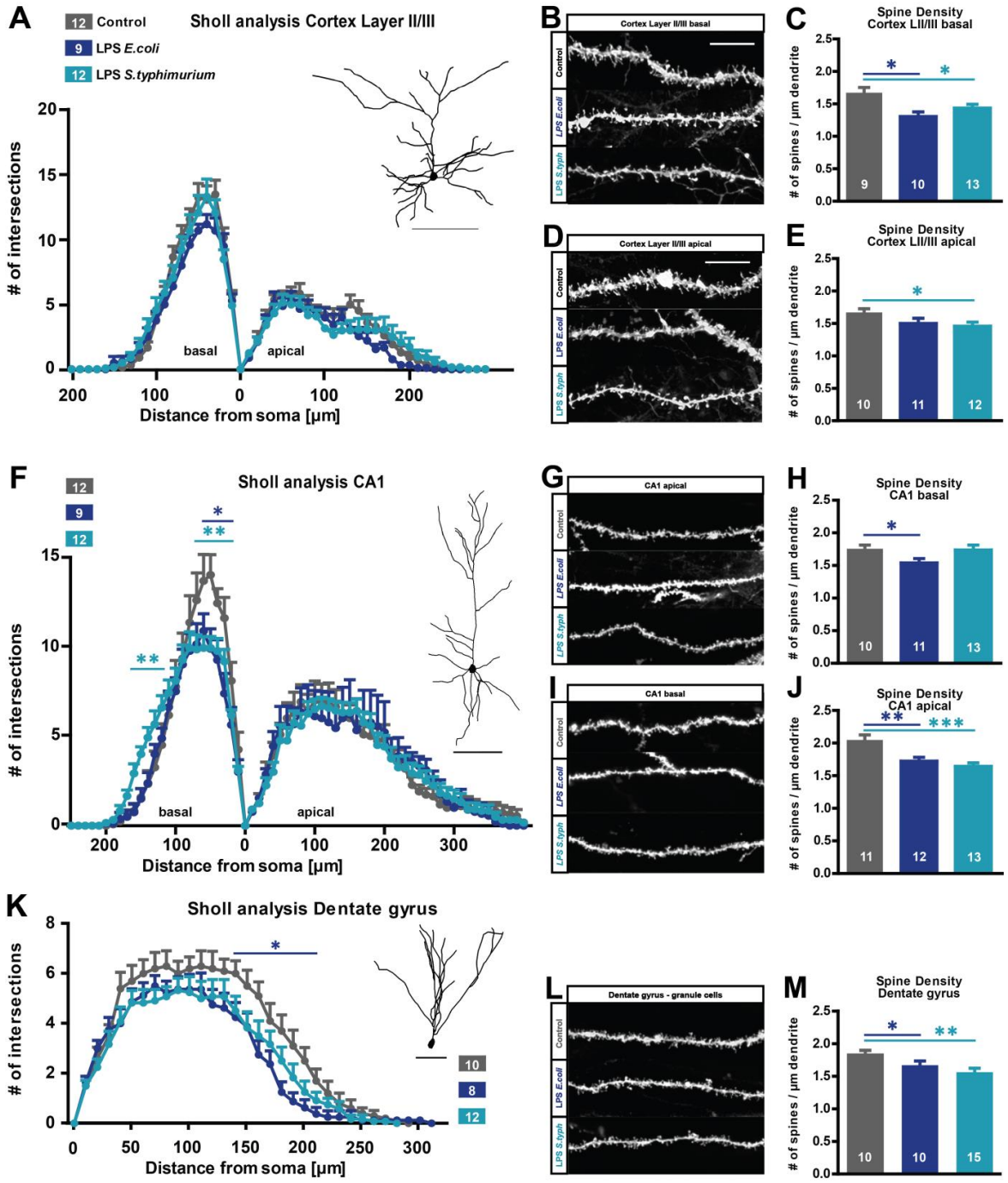

Figure 3.9 | Effect of an immune stimulation with lipopolysaccharide (LPS) from *E.coli* or *S.typhimurium* on neuronal morphology in 19 months old APP/PS1 mice 3 months after treatment. (A) Dendritic complexity of cortex layer II/III neurons, 100 µm scale bar. **(B, C)** Basal dendritic spine density of cortical pyramidal neurons, confocal image scale bar 10 µm **(D, E)** Apical spine density of cortex LII/III cells, image scale bar 10 µm **(F)** Sholl analysis and exemplified tracing of CA1 pyramidal neurons, scale bar 100 µm. **(G, H)** Spine density of basal CA1 dendrites, scale bar 10 µm**. (I, J)** Spines/µm of mid-apical CA1 dendrites **(K)** Dendritic architecture of granule cells of the dentate gyrus. **(L, M)** Spine density of DG, scale bar 10 µm. Data presented as mean ± SEM, n = number of cell/dendrites, * = $p < 0.05$; ** = $p < 0.01$).

Therefore, I used LPS of *Escherichia coli* or *Salmonella typhimurium* to stimulate the peripheral immune system of 16 months old APP/PS1 mice. Three months later dendritic morphology and spine density were analyzed for hippocampal CA1 and dentate gyrus granule cells as well as cortex layer II/III neurons via Diolistics. Tracings of cortical neurons of the layer II and III showed no differences in dendritic complexity 3 months after the immune stimulation with either LPS from *E.coli* or *S.typhimurium* when compared to control cells of non-immune stimulated old APP/PS1 mice (Fig 3.9A). On the synaptic level, both types of LPS caused a significant decrease in spine density of basal dendrites (Fig 3.9B, 3.9C, control: 1.670 ± 0.082 spines/µm dendrite; LPS *E.coli*: 1.306 ± 0.069 spines/µm, p = 0.0033; LPS *S.typhimurium*: 1.435 ± 0.058 spines/µm, p = 0.0262). But apical dendrites of Cortex LII/III cells only had lower numbers of spines per µm when the mice were treated with *S.typhimurium* LPS (Fig 3.9D, 3.9E, control: 1.667 ± 0.056 spines/µm dendrite; LPS *E.coli*: 1.499 ± 0.079 spines/µm, p = 0.1058; LPS *S.typhimurium*: 1.457 ± 0.063 spines/µm, p = 0.0244).

In the CA1 area of the hippocampus, pyramidal neurons showed no change in dendritic complexity in the apical dendrites to both LPS treatments. In the basal compartment, LPS from *E.coli* and *S.typhimurium* caused a significant reduction in complexity in the close proximity to the soma. In the *S.typhimurium* LPS treatment however, a higher dendritic complexity is visible in the more distal part of the basal dendritic tree (Fig 3.9F). In contrast to the dendritic level, the more severe changes in spine density occurred in the apical dendritic tree of the CA1 pyramidal neurons. Here, the spine density was significantly reduced with both kinds of LPS when compared to control conditions (Fig 3.9I, 3.9J, control: 2.038 ± 0.077 spines/µm dendrite; LPS *E.coli*: 1.716 ± 0.059 spines/µm, p = 0.0030; LPS *S.typhimurium*: 1.636 ± 0.052 spines/µm, p = 0.0002). The basal dendritic spine density was significantly reduced only upon stimulation with LPS from *E.coli* in aged APP/PS1 mice (Fig 3.9G, 3.9H, control: 1.756 ± 0.056 spines/µm dendrite; LPS *E.coli*: 1.539 ± 0.067 spines/µm, p = 0.0238; LPS *S.typhimurium*: 1.736 ± 0.076 spines/µm, p = 0.8424).

The granule cells of the dentate gyrus exhibited a reduced number of intersections in the Sholl analysis upon treatment with either LPS from *E.coli* or *S.typhimurium* over the whole length of the dendritic tree, which was statistically significant for the *E.coli* treatment at a distance between 140 and 210 µm from the cell body (Fig 3.9K). The spine density of these cells was significantly reduced under both treatment conditions (Fig 3.9L, 3.9M, control: 1.851 ± 0.053 spines/µm dendrite; LPS *E.coli*: 1.672 ± 0.066 spines/µm, p = 0.0485; LPS *S.typhimurium*: 1.565 ± 0.062 spines/µm, p = 0.0035). Taken together, both LPS types caused changes in the dendritic complexity and spine density of CA1 and Cortex pyramidal neurons and dentate gyrus granule cells in aged APP/PS1 mice with unequal pattern and degree.

3.1.8. Synaptic plasticity in aged APP/PS1 mice 3 months after stimulation with LPS

The APP/PS1 mouse model for Alzheimer´s disease is characterized by an increasing Aβ plaque load starting with about 6 months of age which leads to neurodegenerative phenotype with neuronal death, synapse loss and learning and memory deficits. Also synaptic plasticity was investigated in this and other AD models. Studies showed that an elevation in aggregated Aβ causes impairment in LTP (Nalbantoglu et al. 1997, Chapman et al. 1999). This observation was also made for the APP/PS1 mouse model used in this study (Kummer et al. 2011, Heneka et al. 2013).

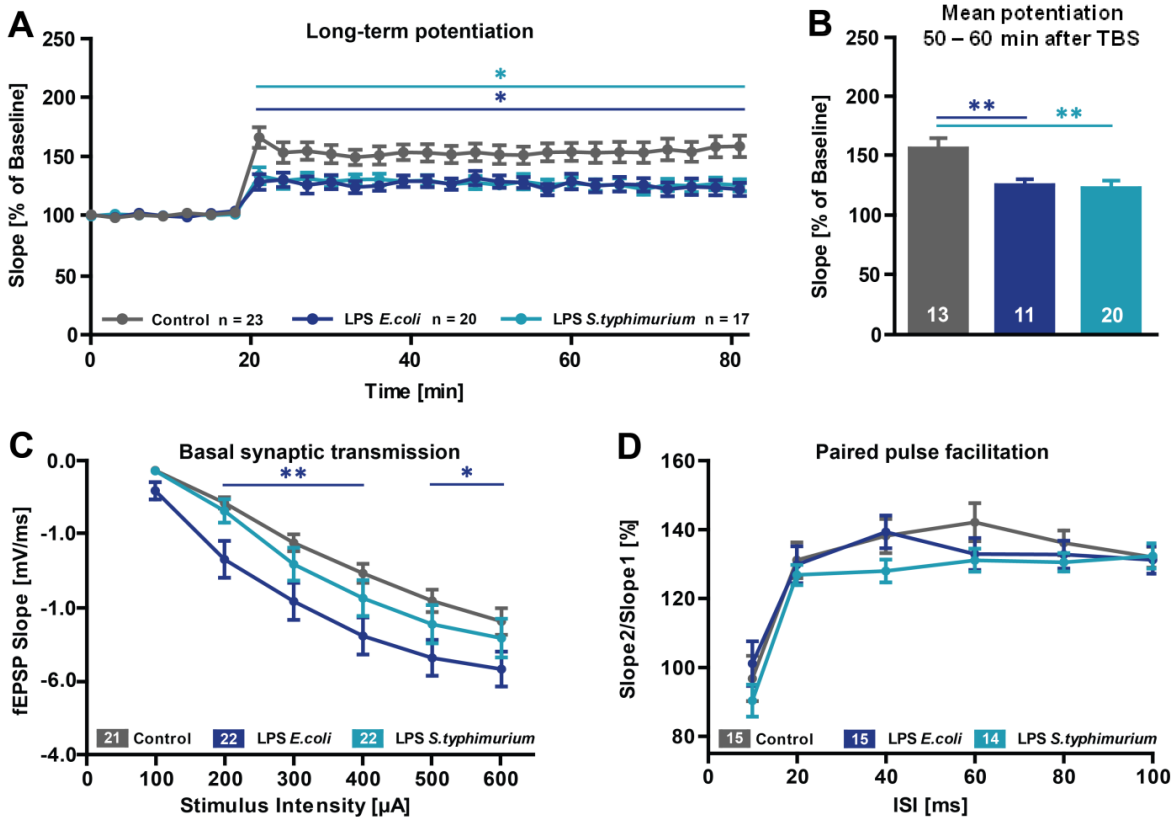

Figure 3.10 | Changes in short-term and long-term synaptic plasticity in the hippocampus of 19 months old APP/PS1 mice immune stimulated with lipopolysaccharide (LPS) of *E.coli* or *S.typhimurium* 3 months after the peripheral application. (A) Long-term potentiation at Schaffer Collateral pathway measured at stimulus intensity of 40% maximal fEPSP slope, LTP induction after 20 minutes of baseline recording via TBS (3 trains with 10 s interval of 10 bursts containing 4 pulses at 100 Hz with 200 ms interval), recording for 1 hour. **(B)** Mean LTP of the last 10 minutes of recording. **(C)** Input-Out-relationship, fEPSP slope measured in the CA1 area at increasing stimulus intensities. **(D)** Short-term synaptic plasticity, paired pulse facilitation at 40% of the maximal fEPSP slope. n = number of hippocampal acute slices, * = $p < 0.05$; ** = $p < 0.01$.

In the present study, the effect of a peripheral immune stimulation with LPS was examined in old APP/PS1 mice. Here, the morphological phenotype of CA1 and dentate gyrus neurons suggests also a functional consequence for the hippocampal circuitry. Therefore, basal synaptic transmission as well as short and long-term synaptic plasticity was

measured as mentioned above (Fig. 2.2.9., 3.1.2). After 20 minutes of stable baseline recordings LTP was successfully induced via TBS and maintained stable over 1 hour recording under all experimental conditions. When compared to control injection in APP/PS1 mice, the induction of LTP was significantly lower 3 months after treatment with both LPS from *E.coli* and from *S.typhimurium* (Fig 3.10A), which resulted in a highly significant reduction also in the stable phase of the LTP, here indicated as mean value of the last 10 minutes of recording (Fig 3.10B, control: 156.2 ± 8.6 fEPSP slope in % of baseline; LPS *E.coli*: 125.3 ± 5.1, p = 0.007; LPS *S.typhimurium*: 122.8 ± 6.2 %, p = 0.009). Basal synaptic transmission was not altered in the LPS *S.typhimurium* treated group, but in slices from LPS *E.coli* treated old APP/PS1 mice the fEPSP slope was significantly higher than control signals at stimulus intensities between 200 and 600 µA (Fig 3.10C). The ratio of the second to the first fEPSP slope in the paired pulse facilitation paradigm was on control level with both types of LPS (Fig 3.10D), which indicates normal presynaptic function and ready releasable neurotransmitter pool despite the peripheral immune stimulation.

Conclusively, a peripheral immune activation in old APP/PS1 mice led to impairment in LTP with normal presynaptic properties independent of the type of stimulatory LPS. So, in contrast to the aged WT mice, APP/PS1 mice were more vulnerable towards stimulation with *E.coli* LPS. As the formation of Aβ plaques starts already at 6 months of age, it was interesting to see whether also young adult APP/PS1 show detrimental effects of an innate immune activation while their age matched WT counterparts show no reduction in dendritic complexity or spine density 3 months after the immune stimulation (3.1.5).

3.1.9. Neuronal architecture of young APP/PS1 mice 3 months after stimulation with LPS

In this study, I saw detrimental effects of a peripheral immune stimulation with LPS on neuronal morphology and signaling in aged WT as well as APP/PS1 mice, but adult WT mice seemed unaffected. Therefore, I aimed to analyze the long-term effects of a peripheral immune stimulation with LPS on neuronal morphology in young adult APP/PS1 mice to see whether neurodegeneration is enhanced upon pro-inflammatory conditions in the periphery.

Young adult (4 months old) APP/PS1 mice were intraperitoneally injected with 0.4 µg/g bodyweight LPS of either *Escherichia coli* or *Salmonella typhimurium*. 3 months after incubation dendritic morphology and spine density of cortex layer II/III, CA1 and dentate gyrus cells were analyzed after neurons were stained with the fluorescent dye DiI. In the cortex layer II/III pyramidal neurons did not show any differences in dendritic complexity of

basal or apical dendrites with both types of LPS (Fig 3.11A). The spine density was not changed with LPS *S.typhimurium* either, but the LPS *E.coli* treatment caused a significant reduction in the spine number of basal and apical dendrites (Fig 3.11B, 3.11C basal: control 1.852 ± 0.080 spines/µm dendrite; LPS *E.coli*: 1.560 ± 0.059 spines/µm, p = 0.0146; LPS *S.typhimurium*: 1.701 ± 0.052 spines/µm, p = 0.1277, Fig 3.11D, 3.11E apical: control 1.763 ± 0.076 spines/µm dendrite; LPS *E.coli*: 1.533 ± 0.063 spines/µm, p = 0.0394; LPS *S.typhimurium*: 1.706 ± 0.088 spines/µm, p = 0.6281). Also the dendritic complexity of the CA1 pyramidal neurons showed no significant differences upon immune stimulation with LPS of *E.coli* or *S.typhimurium* in young APP/PS1 mice (Fig 3.11F). Only the basal CA1 spine density was significantly reduced in the LPS *S.typhimurium* treated group (Fig 3.11G, 3.11H, basal: control 1.668 ± 0.055 spines/µm dendrite; LPS *E.coli*: 1.721 ± 0.041 spines/µm, p = 0.4815; LPS *S.typhimurium*: 1.486 ± 0.041 spines/µm, p = 0.0126), while the apical dendrites and the *E.coli* LPS treatment resulted in spine densities at control level (Fig 3.11I, 3.11J, apical: control 1.771 ± 0.029 spines/µm dendrite; LPS *E.coli*: 1.765 ± 0.032 spines/µm, p = 0.8999; LPS *S.typhimurium*: 1.756 ± 0.045 spines/µm, p = 0.7753). The Sholl analysis of the granule cells from the dentate gyrus showed a perfect overlap in the LPS *S.typhimurium* and control treatment, while the neurons in the LPS *E.coli* treatment showed a shift in morphology with slightly higher numbers of intersections in the proximal and slightly less intersections in the distal part of the dendritic tree (Fig 3.11K). Here, the spine density was affected with both kinds of LPS. The LPS of *E.coli* caused a significant reduction in the spine density of dentate gyrus granule cells of young adult APP/PS1 mice 3 months after incubation and the LPS *S.typhimurium* caused an even stronger decrease (Fig 3.11L, 3.11M, control: 1.990 ± 0.045 spines/µm dendrite, LPS *E.coli*: 1.825 ± 0.064 spines/µm, p = 0.0389; LPS *S.typhimurium*: 1.687 ± 0.075 spines/µm, p = 0.0019).

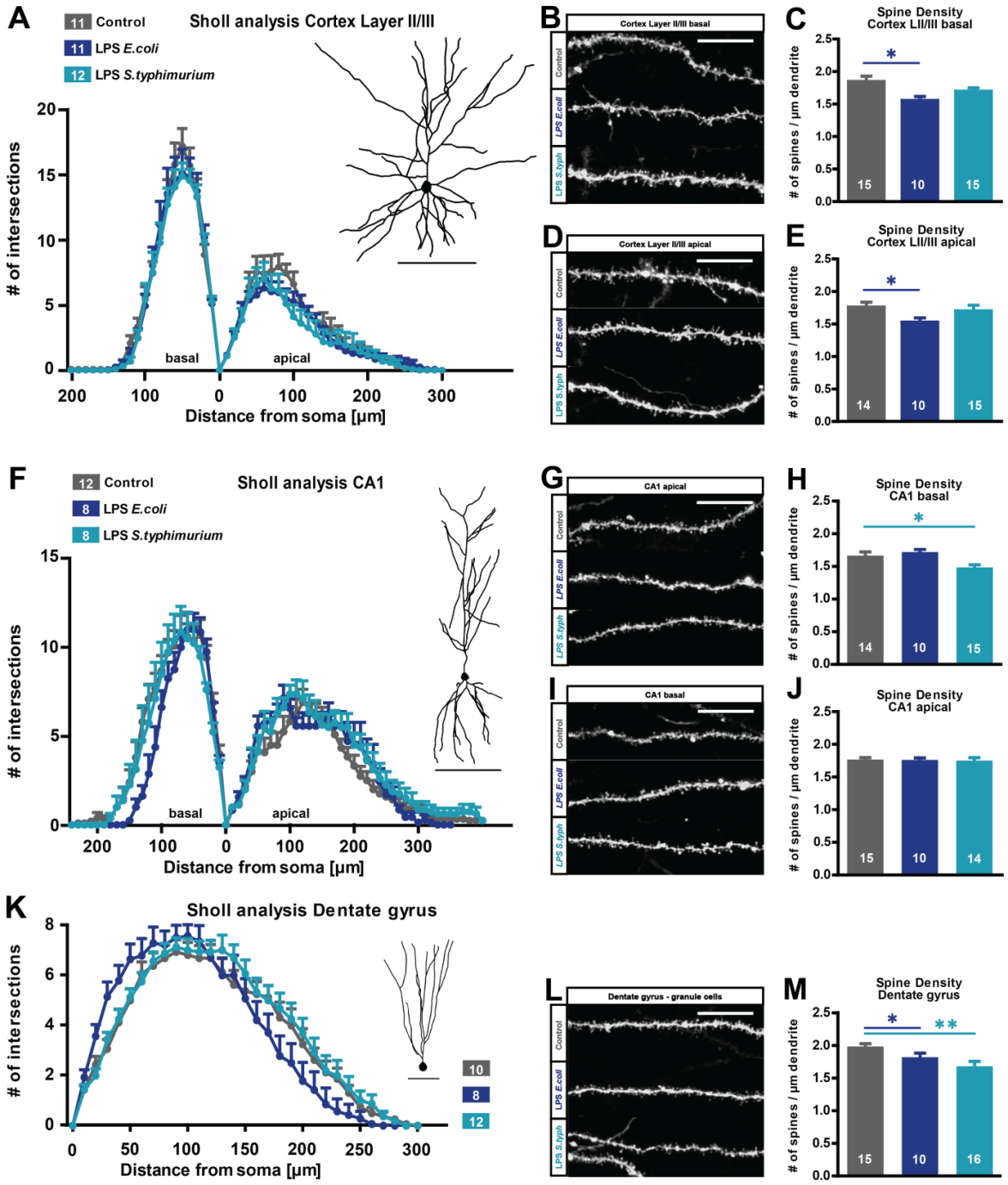

Figure 3.11 | Immune stimulation with lipopolysaccharide (LPS) from *E.coli* and *S.typhimurium* causes changes in neuronal morphology of hippocampal and cortical neurons in 19 months old APP/PS1 mice 3 months after the treatment. (A) Dendritic complexity of cortex Layer II/III neurons, 100 µm scale bar. **(B, C)** Spine number per µm of basal dendrites, 10 µm scale bar in microscopic image **(D, E)** Apical spine density of neurons from cortex LII/III, confocal microscopic images, 10 µm scale bar **(F)** Sholl analysis and exemplified tracing of CA1 pyramidal neurons, scale bar 100 µm. **(G, H)** Spine density of basal CA1 dendrites, scale bar of confocal images 10 µm. (**I, J)** Number of spines per µm of mid-apical CA1 dendrites, scale bar 10 µm in confocal images **(K)** Dendritic architecture of granule cells of the dentate gyrus. **(L, M)** Spine density of DG, scale bar 10 µm. Data presented as mean ± SEM, n = number of cells or dendrites respectively, * = $p < 0.05$; ** = $p < 0.01$.

In summary, the changes in neuronal morphology in young APP/PS1 mice after immune stimulation with LPS were less dramatic than in the aged APP/PS1 mice but stronger than in the young adult WT counterparts suggesting a synergizing effect of amyloid β plaque deposition and an activation of the peripheral innate immunity in this AD mouse model. Functional consequences for the neuronal signaling or the learning behavior were not analyzed in the present study.

3.1.10 Changes in neuronal architecture of aged NLRP3 knockout mice after peripheral immune stimulation

It was shown that deficiency of the NLRP3 inflammasome and the maturation of IL-1β and IL-18 prevents neurodegeneration in the APP/PS1 mouse model of Alzheimer´s disease (Heneka et al. 2013). As impaired neuronal signaling and learning in aged C57Bl/6 WT mice were paralleled by an increase of microglia numbers and activation 3 months after immune stimulation with LPS *S.typhimurium*, the hypothesis that the absence of the NLRP3 inflammasome could also be beneficial in the context of a peripheral immune activation was addressed next.

Therefore, 16 months old NLRP3 knockout (KO) mice were immune stimulated via peripheral administration of 0.4 µg LPS of *S.typhimurium* or control injected with saline. Three months later neuronal morphology and spine density were analyzed in cortex layer II/III, CA1 and dentate gyrus. And indeed, there was neither a change in the dendritic morphology (Fig. 3.12A) nor the spine density of basal (Fig 3.12B, 3.12C, basal: control 1.425 ± 0.092 spines/µm dendrite; LPS *S.typhimurium*: 1.397 ± 0.086 spines/µm, p = 0.8295) and apical dendrites (Fig 3.12D, 3.12E, apical: control 1.450 ± 0.048 spines/µm dendrite; LPS *S.typhimurium*: 1.434 ± 0.058 spines/µm, p = 0.8391) in cortex layer II/III upon immune stimulation of aged NLRP3 KO mice. Likewise, the dendritic architecture of CA1 neurons was not altered upon immune stimulation (Fig. 3.12F). In the basal compartment, even an increase in the number of intersections could be observed. In contrast to that, the spine density of basal CA1 dendrites was significantly reduced (Fig 3.12G, 3.12H, basal: control 1.796 ± 0.050 spines/µm dendrite; LPS *S.typhimurium*: 1.597 ± 0.056 spines/µm, p = 0.0156). The spine density of apical dendrites was at control level (Fig 3.12I, 3.12J, apical: control 1.682 ± 0.057 spines/µm dendrite; LPS *S.typhimurium*: 1.572 ± 0.065 spines/µm, p = 0.2194).

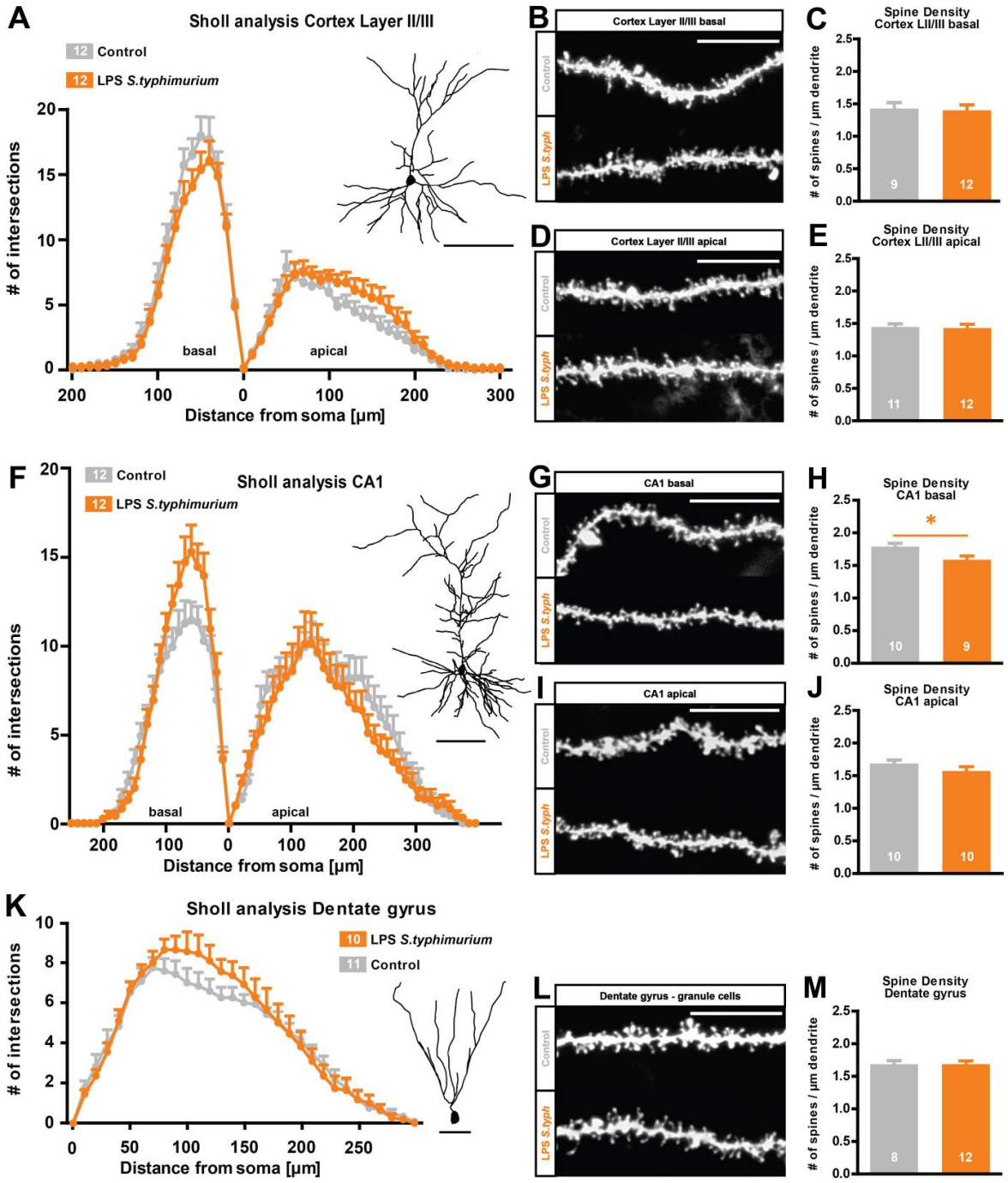

Figure 3.12 | Changes in neuronal morphology in 19 months old NLRP3 KO mice 3 months after immune stimulation with LPS of *S.typhimurium.* (A) Dendritic complexity of cortex layer II/III pyramidal neurons, tracing scale bar 100 µm. **(B, D)** Confocal fluorescent microscopic images of DiI stained cortical basal and apical dendrites, scale bar 10 µm. **(C, E)** Spine density of basal and apical cortex layer II/III dendrites, NLRP3KO controls vs. LPS *S.typhimurium.* **(F)** Sholl analysis of CA1 pyramidal, scale bar 100 µm. **(G, H)** Microscopic image and quantification of the spine density from CA1 basal dendrites. **(I, J) S**pine density and representative image of CA1 apical dendrites, scale bar 10 µm. **(K)** Dendritic architecture of dentate gyrus granule cells. **(L, M)** Confocal microscopic images and spine density of granule neurons of the dentate gyrus. Data presented as mean ± SEM, n = number of cells and number of dendrites, respectively, * = $p < 0.05$.

In the dentate gyrus, after immune simulation in aged NLRP3 KO mice with LPS *S.typhimurium* the granule cells exhibited a similar dendritic architecture as the control

cells (Fig. 3.12 K). Also the spine density was not altered here (Fig 3.12L, 3.12M: control 1.688 ± 0.057 spines/µm dendrite; LPS *S.typhimurium*: 1.690 ± 0.050 spines/µm, p = 0.9733).

Taken together, it can be concluded, that NLRP3 inflammasome deficiency led to a partial rescue of the morphological degeneration observed in age matched WT mice.

3.1.11 Synaptic plasticity of aged NLRP3 KO mice 3 months after stimulation with LPS

It was found that a neurodegenerative phenotype in the morphology of CA1 neurons seen in AD mice could be rescued upon deletion of the NLRP3 inflammasome (Heneka et al. 2013). Likewise, also impairment in cognitive function and synaptic plasticity could be prevented via NLRP3 or ASC deficiency (Heneka et al. 2013). In this study, NLRP3 KO mice showed a partial rescue of the detrimental effects on neuronal morphology seen upon immune stimulation in aged mice. It was hypothesized that the properties of synaptic plasticity could be at control level despite a peripheral immune stimulation as well. Therefore, 16 months old NLRP3 KO mice were immune stimulated via peripheral administration of 0.4 µg LPS of *S.typhimurium* or control injected with saline. Three months later hippocampal acute slices were prepared and synaptic plasticity was measured at the CA3-CA1 Schaffer-collateral pathway. After 20 minutes of baseline recordings LTP was induced via theta burst stimulation and recorded for another 60 minutes. In both control and LPS *S.typhimurium* stimulated aged NLRP3 KO mice the potentiation was stable for the whole recording period (Fig. 3.13A). There was no change in the level of LTP in the last 10 minutes of recording between control and immune stimulated mice (Fig 3.13B, control: 132.9 ± 8.4 % fEPSP slope of baseline, LPS *S.typhimurium*: 129.3 ± 8.7 %, p = 0.621). Also the basal synaptic transmission within the CA3-CA1 pathway was not altered after immune stimulation with *S.typhimurium* LPS (Fig 3.13C). The presynaptic properties were not affected either as there is no change in the paired pulse facilitation paradigm (Fig 3.13 D). Taken together, the deficiency of the NLRP3 inflammasome prevented detrimental effects on synaptic plasticity caused by peripheral immune stimulation with LPS of *S.typhimurium* as seen in this study with old WT animals.

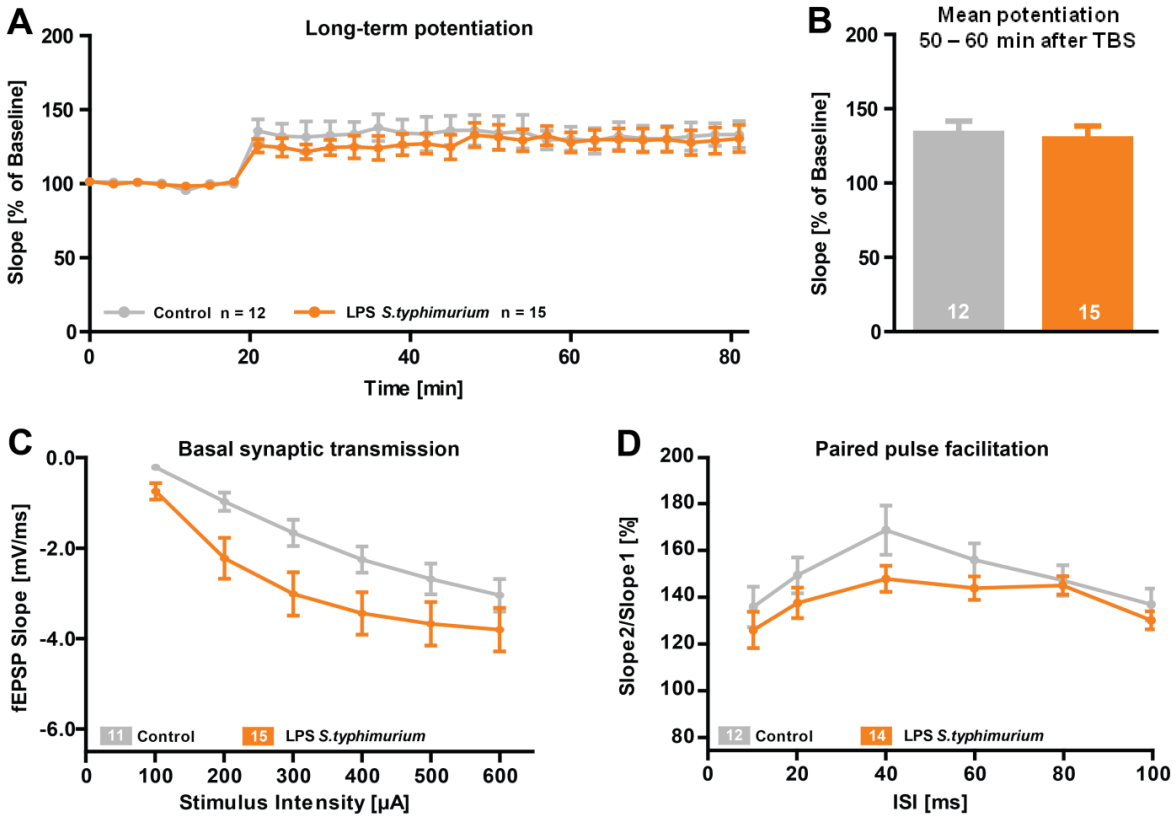

Fig 3.13 | Long-term synaptic plasticity at Schaffer-collateral CA3-CA1 pathway in hippocampal acute slices of 19 months old NLRP3 KO mice 3 months after peripheral immune stimulation with lipopolysaccharide (LPS) from *Salmonella enterica* serogroup *typhimurium*. (A) Long-term potentiation (LTP) was induced via theta burst stimulation (10 bursts containing 4 pulses at 100 Hz at an inter burst interval of 200 ms, repeated 3 times with 10 s interval) after 20 minutes of baseline recording **(B)** Quantification of the last 10 minutes of LTP **(C)** Basal synaptic transmission measured as input-output relationship at increasing stimulus intensities **(D)** Presynaptic properties addressed in the paired pulse facilitation with increasing ISI = interstimulus intervals. All data shown as mean ± SEM, n = number of slices.

3.2. Peripheral immune stimulation with components of Gram positive bacteria

Until the 1990s, sepsis was considered to be specific for Gram negative bacteria (Parrillo et al. 1990). Today, we know that most cases of sepsis are actually caused by Gram positive bacteria (Martin et al. 2003). In the present study, PGN and LTA as major endotoxic components of the Gram positive cell were given intraperitoneally at concentrations of 0.5 µg/g bodyweight each on two consecutive days. That made a total of 1.0 µg/g body weight for each component. These relatively low doses were chosen to avoid a high rate of lethality in aged WT mice. The groups used for the Gram-positive immune stimulations were adult (4 months) WT and APP/PS1 and old (16 months) WT and APP/PS1 mice.

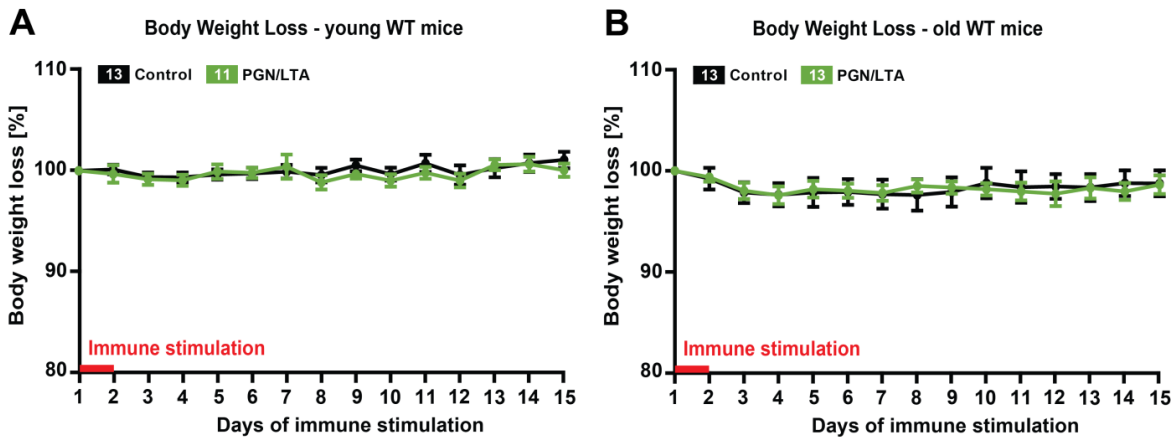

Figure 3.14 | Body weight (BW) loss of young adult (4 months) and aged (16 months) C57Bl/6 WT mice during peripheral immune stimulation with peptidoglycan (PGN) and lipoteichoic acid (LTA) from *Staphylococcus aureus*. The immune stimulation with 1.0 µg/g BW was realized by intraperitoneal injection of 0.5 µg/g BW of each LTA and PGN for 2 consecutive days. Control animals received injections of sterile 0.9% NaCl solution. (A) BW of adult mice in % of starting weight during the first 15 days of immune stimulation **(B)** Body weight of old control and PGN/LTA stimulated mice during and two weeks after the immune stimulation. Data presented as mean ± SEM, n = number of mice.

In comparison to control animals, neither the younger nor the old WT mice showed body weight loss after the application of the full dose PGN/LTA on day 3 of immune stimulation (Fig 3.14A, young adult mice, control: 99.39 ± 0.44 %, PGN/LTA: 99.15 ± 0.55 %; Fig 3.14B, old mice, control: 97.86 ± 1.04 % body weight from day 1, PGN/LTA: 98.03 ± 0.81 %). Also in the course of the following days, there was no change in the body weight loss of PGN/LTA treated or control mice until day 15 of the immune stimulation (Fig. 3.14A, day 15, control: 101.08 ± 0.81 % body weight from day 1, PGN/LTA: 100.07 ± 0.64 %). This indicated no dramatic inflammatory response in the initial phase of the immune stimulation. Certainly, the used doses were not comparable with a severe sepsis or septic

shock as seen for higher concentrations (De Kimpe et al. 1995) or with the classical LPS application, but a milder pro-inflammatory response cannot be excluded, since a correlation between Gram positive induced sepsis and body weight loss in rodents has not been described so far.

3.2.1. Long-term effects of PGN/LTA from *S.aureus* on neuronal morphology in aged mice

As in not many studies the Gram positive bacterial cell wall components peptidoglycan and lipoteichoic acid were used to provoke a stimulation of the innate immune system, even less is known about the influence of such an immune stimulation on the central nervous system. Here, for the first time I investigated the impact of a Gram positive peripheral immune stimulation on neuronal morphology of aged WT mice. Therefore, 16 months old C57Bl/6 mice were intraperitoneally injected with 1 µg PGN and LTA per g body weight each. After 3 months of incubation single neurons in the cortex and hippocampus were labeled with the lipophilic fluorescent dye DiI. Tracings of cortex layer II/III neurons showed only a slightly reduced complexity in the apical dendrites whereas the basal dendritic tree was highly significantly less complex in PGN/LTA treated old WT mice compared to control neurons (Fig 3.15A). The spine density of basal as well as apical dendrites was highly significantly reduced upon PGN/LTA treatment in an analogous manner (Fig 3.15B, 3.15C basal: control 1.614 ± 0.06; PGN/LTA 1.166 ± 0.099, $p = 0.0001$; Fig 3.15D, 3.15E apical: control 1.864 ± 0.063, PGN/LTA 1.364 ± 0.080, $p = 0.00007$). CA1 neurons of the hippocampus reacted with a decrease in intersections in the proximal part of the apical dendritic tree, while basal dendrites were not affected (Fig 3.15F). In an opposite way, the spine density of CA1 pyramidal neurons was highly significantly reduced in the basal dendrites (Fig 3.15G, 3.15H control: 1.906 ± 0.055, PGN/LTA: 1.647 ± 0.066 spines/µm dendrite, $p = 0.0056$), while apical dendrites showed only a slight reduction in the number of spines per µm dendrite (Fig 3.15I, 3.15J control: 2.025 ± 0.060, PGN/LTA: 1.874 ± 0.062 spines/µm dendrite, $p = 0.0917$). The dentate gyrus granule cells as second cell type evaluated in the hippocampus exhibited significantly more intersections between 140 and 170 µm from the soma (Fig 3.15K).

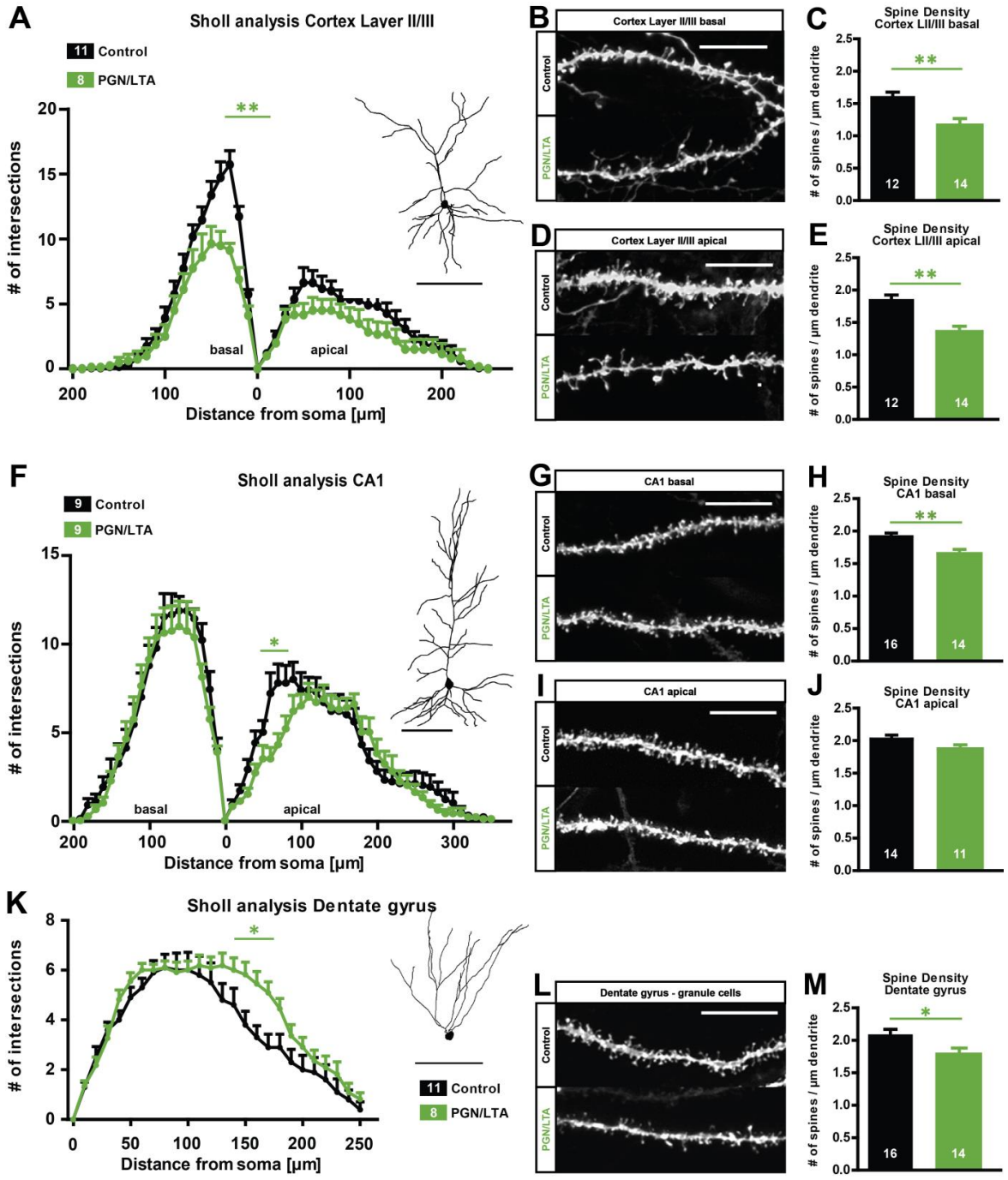

Figure 3.15 | Long-term effects of an immune stimulation with 1µg/g bodyweight peptidoglycan (PGN) and lipoteichoic acid (LTA) on dendritic morphology and spine density of hippocampal and cortical neurons of aged C57Bl/6 mice. (A) Sholl analysis of cortex layer II/III neurons. **(B, D)** Representative basal and apical dendrites of cortex layer II/III cells in control and treated mice. **(C, E)** Quantification of dendritic spine density in basal and mid-apical dendrites. **(F)** Number of intersections of apical and basal dendritic tree of hippocampal CA1 pyramidal neurons in relationship to the distance from the cell body. **(G, H, I, J)** Confocal images of CA1 apical and basal dendrites and the number of spines per µm of dendrite. **(K)** Sholl analysis of dentate gyrus granule cells of control and PGN/LTA treated old WT mice. **(L, M)** Confocal images and counting of dendritic spines of granule cells of the dentate gyrus in control and PGN/LTA treated animals. Data presented as mean ± SEM, scale bar tracings 100 µm, scale bar microscopic images 10 µm, n = number of cells/dendrites, * = $p < 0.05$; ** = $p < 0.01$.

In contrast to that, the spine density was significantly reduced (Fig 3.15L, 3.14M control: 2.093 ± 0.077, PGN/LTA: 1.812 ± 0.071 spines/µm dendrite, p = 0.0127), which indicates that the overall number of synapses might be stable in granule cells of the dentate.
In summary, while cortical pyramidal neurons of old WT mice showed a severe reduction in dendritic complexity and spine density upon immune stimulation with PGN and LTA, the CA1 area showed a milder reduction of both criteria. The dentate gyrus granule cells were less sensitive towards the treatment with PGN/LTA.

3.2.2. Enduring changes of PGN/LTA of *S. aureus* on synaptic plasticity in old mice

In contrast to the wealth of experiments with Gram negative cell wall components as stimulator of the innate immune system, not as many were performed with peptidoglycan (PGN) and/or lipoteichoic acid (LTA) as major constituents of the Gram positive cell wall. The influence - whether acute or chronic - of the application of Gram positive endotoxins on synaptic plasticity in rodents has not been addressed at all.
Here, I investigated whether a peripheral immune stimulation with an equal mixture of PGN and LTA can induce long-term changes in neuronal signaling the hippocampus in old WT mice. Therefore, 16 months old C57Bl/6 mice were injected with 0.5 µg of each LTA and PGN per g bodyweight for two days (1 µg/g bodyweight each in total). After 3 months of incubation, hippocampal acute slices were prepared and synaptic plasticity was measured at the CA3-CA1 Schaffer collateral pathway in an interface setup. TBS-induced LTP was measured for 1 hour after baseline recording.
LTP was significantly lower in slices of PGN/LTA treated mice starting at 10 minutes after LTP induction and during the maintenance phase of the potentiation (Fig 3.16A). Hence, the mean LTP value of the stable phase was significantly reduced upon PGN/LTA treatment (Fig 3.16B, controls: 139.4 ± 8.2 fEPSP % of baseline, PGN/LTA: 121.0 ± 5.6 %, p = 0.033). Basal synaptic transmission and the presynaptic properties addressed via paired pulse facilitation were similar in control and PGN/LTA treated old WT mice (Fig 3.16C, 3.16D). Therefore, no obvious defect in the post- or presynaptic signaling accounted for a lower level of LTP in PGN/LTA treated aged WT mice 3 months after peripheral immune stimulation when compared to control slices.

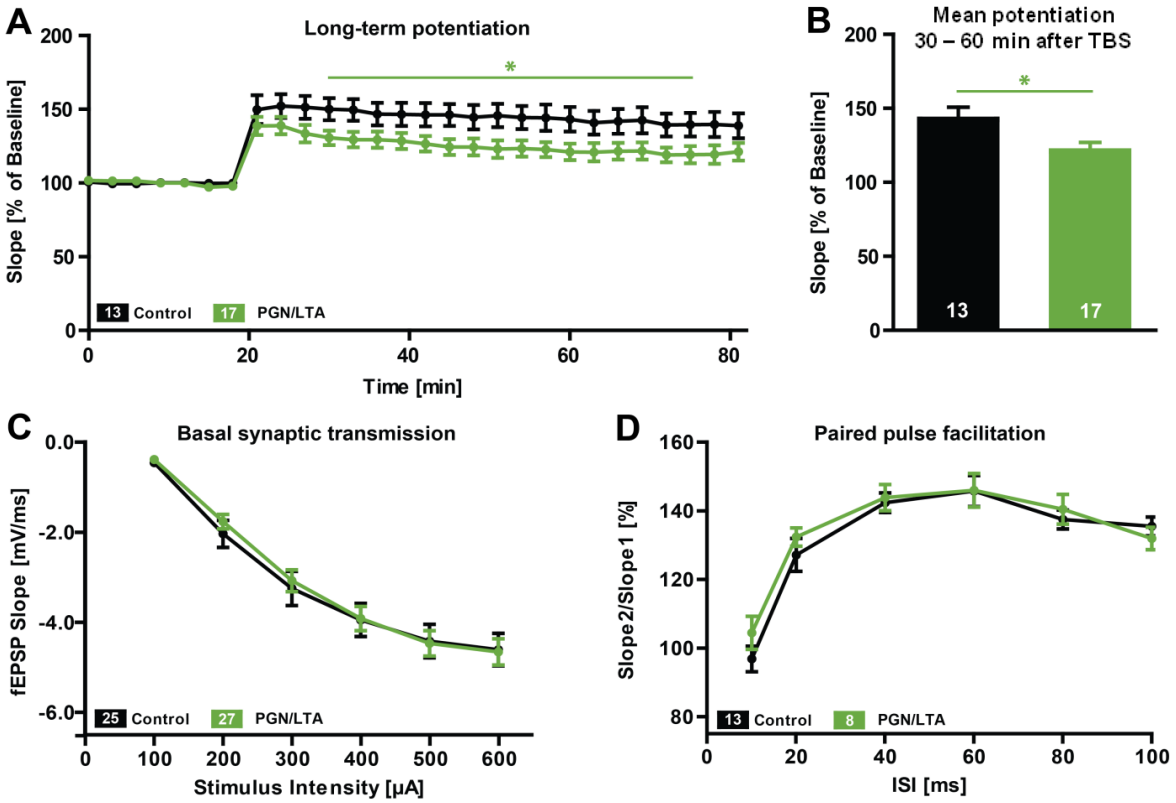

Figure 3.16 | Long-term synaptic plasticity in hippocampal acute slices of aged C57Bl/6 mice 3 months after peripheral immune stimulation with lipoteichoic acid (LTA) and peptidoglycan (PGN) from *Staphylococcus aureus*. (A) Long-term potentiation, recorded 1 hour after induction via TBS and 20 minutes baseline recording. **(B)** Quantification of the last 30 minutes, the stable phase of LTP, control vs. PGN/LTA treatment **(C)** Basal synaptic transmission of PGN/LTA vs. control slices**. (D)** Paired pulse facilitation, ratio of the second over the first stimulus with increasing ISI = interstimulus interval, Data presented as mean ± SEM, n = number of acute slices, * = $p < 0.05$.

3.2.3. Peptidoglycan/lipoteichoic acid treatment affects learning behavior of aged mice

Even though peripheral administration of peptidoglycan and lipoteichoic acid did not cause bodyweight loss in aged WT mice, the dendritic complexity and spine density was negatively affected in different brain areas 3 months after. This most likely is the reason for a slightly impaired long-term potentiation in hippocampal acute slices of these animals. Therefore, it was interesting to see whether the structural and functional alterations in the hippocampus influence the hippocampus-dependent learning in the Morris water maze. Spatial learning was never addressed in mice immune stimulated with both PGN and LTA from *Staphylococcus aureus*. One study with adult mice induced meningitis via application of PCWs (pneumocoocal cell wall) of *Streptococcus pneumoniae* which of course contains both PGN and LTA as major constituent did not find any changes in the learning behavior of these mice in the Morris water maze (Hoffmann et al. 2007). Only after induction of meningitis with living *Streptococcus pneumoniae* impaired

spatial learning and memory was documented (Wellmer et al. 2000). However, studies with aged mice have not been undertaken so far.

Therefore, the performance of 19 months old C57Bl/6 mice treated by peripheral immune stimulation with 1µg PGN and LTA per g body weight at 16 months of age was analyzed in the Morris water maze. After a pre-training period of 3 days, the mice were trained for 8 consecutive days to find the submerged platform in the Morris water maze arena. A probe trial experiment was performed after 2 days and after 8 days of training. Controls and PGN/LTA treated mice managed to learn the position of the hidden platform as the documented escape latency decreased significantly during the training in both cases (Fig. 3.17A: controls 32.8 ± 2.9 s (day 1), 8.0 ± 1.3 s (day 8), $F_{(7,48)}$= 11.001 p < 0.001; PGN/LTA 36.7 ± 3.6 (day 1), 10.2 ± 1.2 (day 8), $F_{(7,64)}$ = 13.765, p < 0.001).

Even though there were no significant differences, PGN/LTA treated mice showed a slightly higher escape latency then control mice on day 7 of the training (Fig 3.17A, controls 7.3 ± 0.9 s, PGN/LTA treated 11.8 ± 0.9 s, p = 0.08871) and mildly elevated escape latencies also on day 4 and 6 of the training (Fig 3.17A). On day 3 and 9, after the second and eighth training session respectively, memory formation was tested in absence of the hidden platform. In these probe trial experiments, control mice spent significantly more time in the target quadrant, when compared to the other quadrants on day 3 (Fig 3.17B, controls: other quadrants 24.1 ± 1.4 % vs. target quadrant 36.9 ± 4.6 %, p = 0.01999) and day 9 (Fig 3.17C, controls: mean value of other quadrants 15.5 ± 1.5 % vs. target quadrant 53.5 ± 4.5 %, p < 0.0001). PGN/LTA treated mice showed a significant preference for the target quadrant on day 9 as well (Fig 3.17 C, PGN/LTA: 15.3 ± 2.2. s in other quadrants compared to 54.1 ± 6.7 s in the target quadrant, p < 0.0001). In the probe trial on day 3 however, PGN/LTA treated mice spent the time almost equally in all 4 virtual quadrants of the water maze pool (platform quadrant 31.7 ± 6.5 % vs. other quadrants 26.1 ± 1.0 %, p = 0.40377).

Although PGN/LTA treated mice were able to successfully complete the Morris water maze task similarly to controls, they showed a slightly impaired early memory formation. To evaluate whether this is due to a difference in the quality of the learning and the used search strategies during the learning period, the search tracks of each mouse and trial were analyzed. Here, the time spent in the middle of the pool, the outer regions, the annulus zone or the goal corridor were quantified (Fig 2.2). The search strategies were divided into hippocampus-dependent, allocentric search strategies including focal search, directed search and direct swimming, with increasing accuracy and hippocampus-independent, egocentric strategies like chaining, scanning and random search (Fig. 3.17D, Garthe et al 2009, Garthe and Kempermann 2013).

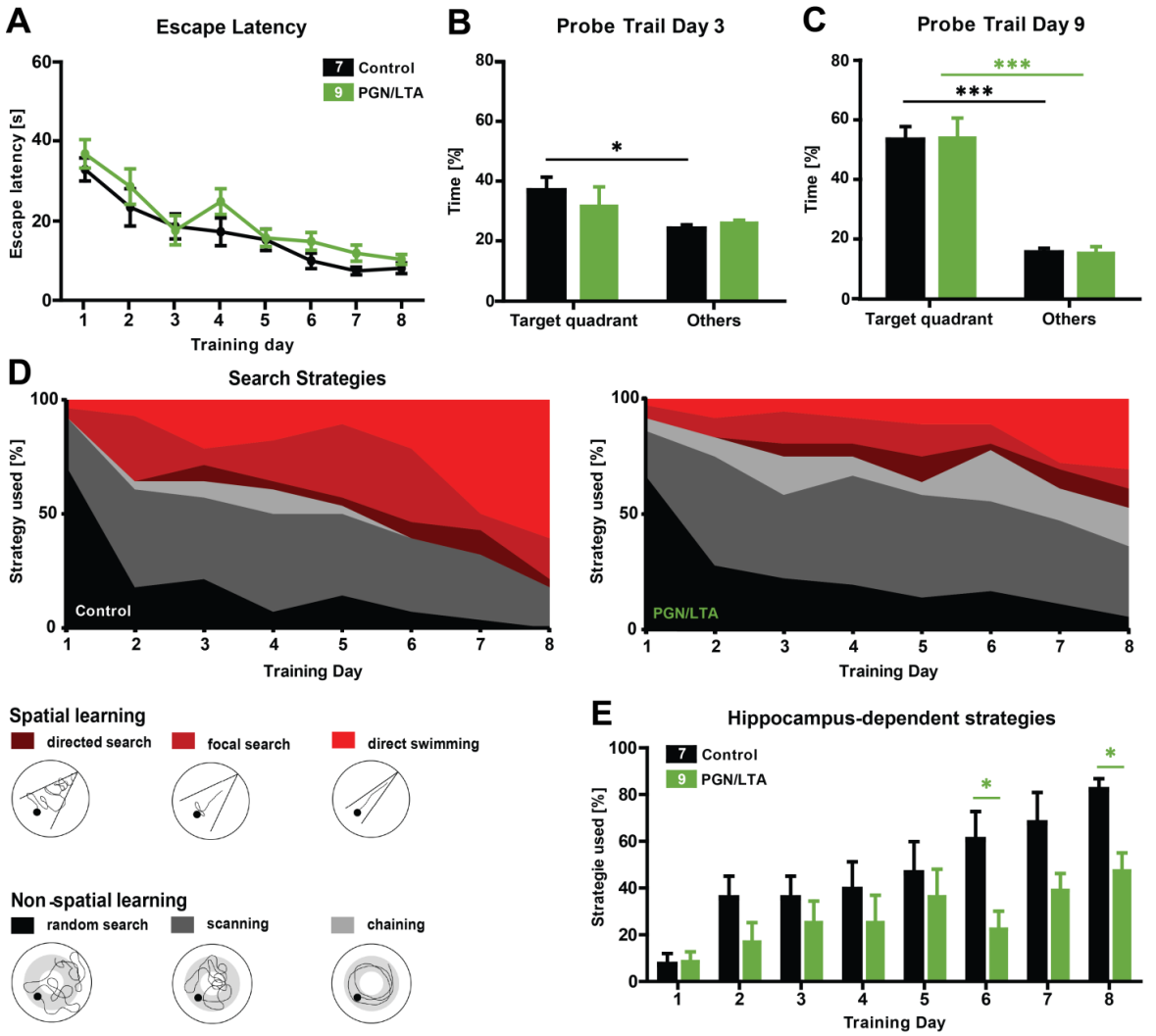

Figure 3.17 | Performance of 19 months old C57Bl/6 mice in the Morris water maze 3 months after peripheral immune stimulation with each 1 µg peptidoglycan (PGN) and lipoteichoic acid (LTA) per g bodyweight. Control and PGN/LTA treated mice were trained in the Morris water maze arena with a submerged platform for 8 consecutive days with 4 trials per mouse and day. The escape latencies, target quadrant preferences and search strategies were analyzed: (A) Escape latency of control (n = 7) as well as PGN/LTA (n = 9) stimulated mice. **(B, C)** Probe trial experiment without platform on day 3 and day 9 respectively. **(D)** Illustration and comparison of the usage of different search strategies. **(E)** Quantification of hippocampus-dependent search between control and PGN/LTA stimulated mice. * = $p < 0.05$.

In control mice random search, chaining and scanning progressively decreased over the 8 days of training. Instead, direct swimming was shown to increase (Fig 3.17 D, controls 3.6 ± 3.6 % (day 1) vs. 60.7 ± 13.2 % (day 8)). Altogether, hippocampus-dependent strategies increased significantly in control mice from 7.1 ± 4.6 % to 82.1 ± 4.6 % (($F_{(7,48)}$= 7.77, $p < 0.001$). The PGN/LTA treated animals showed a decrease in random search and scanning as well, but in a less steep fashion when compared to control mice. Chaining was shown to a higher extent in this treated group. As a consequence, the hippocampus-dependent strategies did not increase as strongly as seen in controls. PGN/LTA mice showed significantly less focal search, directed search and direct swimming on day 6 and

8 of the training in comparison to control animals (day 6, PGN/LTA: 22.2 ± 7.7 %, controls: 60.7 ± 12.0 %, p = 0.014; day 8, PGN/LTA: 47.2 ± 7.7 %, controls: 82.1 ± 4.6 %, p = 0.003).

Altogether, PGN/LTA treated mice showed subtle deficits in spatial learning during the whole 8 training days as seen in a combination of the probe trial experiments and evaluation of the executed search strategies.

As overproduction of pro-inflammatory cytokines can account for learning and memory deficits in a situation of a systemic or CNS localized infection or immune stimulation (Matsumoto et al. 2004, Moore et al. 2009, Silva et al. 2015), the activation of astrocytes and microglia as brain resident monocytes were evaluated next.

3.2.4. Influence of an immune stimulation with PGN/LTA on the glial immune response

Infections with Gram positive bacteria are of increasing importance and *Staphylococcus aureus* is of particular interest in the context of nosocomial infections. While the characteristics of an infection with Gram negative bacteria with their major endotoxic component LPS and the triggering of neuroinflammation are described well, the mechanisms underlying an infection with Gram positive bacteria, a Gram positive sepsis or septic shock and the influences on the brains immune system are not sufficiently illuminated yet. Therefore, it was of high interest to investigate whether the phenotype of brain cells participating in innate immune response is altered 3 months after the intraperitoneal administration of *S.aureus* peptidoglycan and lipoteichoic acid in aged WT mice. Therefore, the PFA fixed hippocampus was deep frozen and cut into 30 µm slices transversally and immunostained for GFAP and IBA-1.

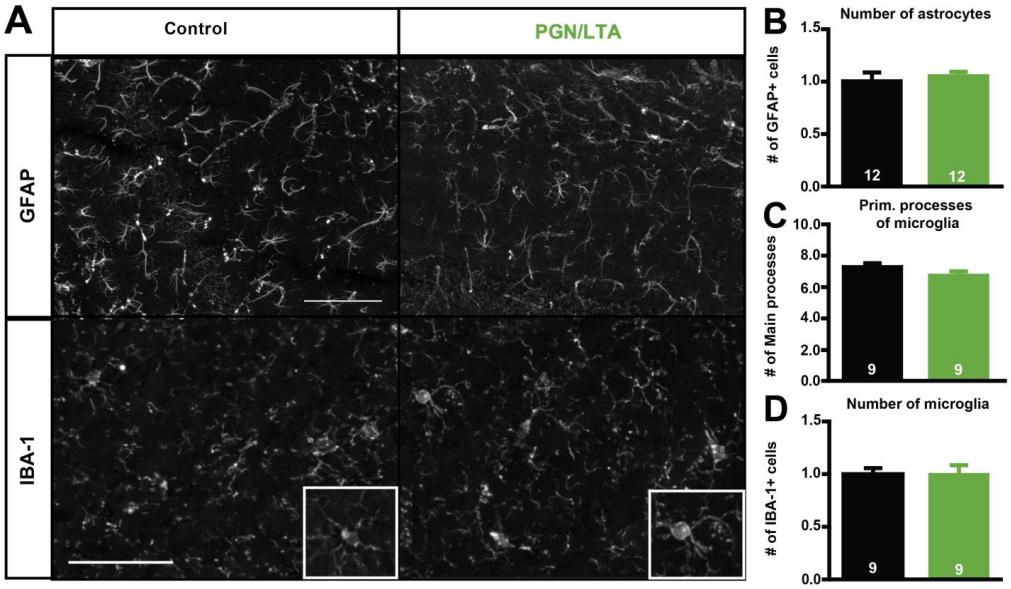

Figure 3.18 | Quantification of astrocytes and microglia/macrophages in hippocampal tissue of 19 months old C57Bl/6 mice immune stimulated with lipoteichoic acid (LTA) and peptidoglycan (PGN) at 16 months of age. (A) Immunohistochemistry of *stratum radiatum* CA1 area of control vs. PGN/LTA stimulated 19 months old WT mice 3 months after incubation. Primary antibodies against GFAP (Glial fibrillary acidic protein) and IBA-1 (ionized calcium-binding adapter molecule 1) were used to visualize astrocytes and microglia/macrophages respectively, scale bar larger section 100 µm, scale bar smaller frame 10 µm. **(B)** Quantification of GFAP-positive cells upon PGN/LTA treatment vs. control (normalized to 1). **(C)** The number of IBA-1 in PGN/LTA stimulated mice compared to controls, normalized to 1. **(D)** Number of primary microglia/macrophage processes in the CA1 area of PGN/LTA treated mice 3 months after application vs. control.

The number of GFAP-positive cells was quantified in the *stratum radiatum* of the CA1 area and the number of astrocytes in control sections was normalized to 1.

There was no change in the relative number of GFAP-positive cells in the hippocampal tissue of PGN/LTA treated mice after 3 months incubation (Fig 3.18B, control: 1.0 ± 0.08 $GFAP^+$ cells; PGN/LTA: 1.05 ± 0.04 $GFAP^+$ cells, p = 0.6059). In addition, the number of microglia/macrophages in the *stratum radiatum* of the CA1 area of PGN/LTA stimulated mice was not different from control tissue either (Fig 3.18C, control: 1.0 ± 0.07 $IBA\text{-}1^+$ cells; PGN/LTA: 1.0 ± 0.09 $IBA1^+$ cells, p = 1.000). Also the activation status of these cells seems to be alike, as the number of primary processes of the IBA-1-positive cell population was only very slightly decreased (Fig 3.18D, control: 7.3 ± 0.2 primary processes, PGN/LTA: 6.8 ± 0.3, p = 0.1512).

Taken together, a dramatic long-term activation of astrocytes and microglia as seen in the neuroinflammation model with LPS was not detectable in aged WT mice 3 months after immune stimulation with PGN and LTA.

3.2.5. Long-term influences of PGN/LTA on neuronal morphology in young mice

In aged mice already higher basal levels of proinflammatory cytokines like IL1β or TNF-α are detectable (Arumugam et al. 2010). After peripheral immune activation with the endotoxic cell wall components LTA and PGN these levels are even higher (Linge et al. 2010). This might explain why the 19 months old mice in the present study showed morphological as well as functional alteration on neurons with detrimental outcome for the spatial learning ability of the mice in response to a subclinical PGN/LTA dose. To examine whether indeed, this strong vulnerability towards stimulation with Gram positive cell wall components is age dependent, young adult mice at 4 months of age were studied. C57Bl/6 mice were immune stimulated with 1.0 µg/g body weight each of LTA and PGN via intraperitoneal injection and after a 3 months incubation period, the neuronal architecture of cortical and hippocampal neurons was examined using the Diolistic technique.

In the cortex layer II/III pyramidal neurons with their characteristic short but strongly ramified basal dendrites, the dendritic complexity was slightly elevated in PGN/LTA treated mice over the whole distance of the dendritic tree when compared to control neurons (Fig 3.19A). The Sholl analysis of the apical dendrites in cortex layer II/III showed a perfect overlap in the number of intersections between control and neurons of PGN/LTA treated mice (Fig 3.19A). The spine density is not altered for basal nor for apical dendrites in cortex layer II/III of PGN/LTA treated animals vs. controls (Fig 3.19 C, basal: control 1.629 ± 0.064 spines/µm of dendrite; PGN/LTA 1.570 ± 0.060 spines/µm dendrite, $p = 0.5854$; Fig 3.19 E, apical: control 1.692 ± 0.094 spines/µm of dendrite; PGN/LTA 1.617 ± 0.058 spines/µm dendrite, $p = 0.4915$).

The number of intersections of apical or basal dendrites in the hippocampal CA1 area was not altered upon treatment with PGN/LTA 3 months after incubation in adult C57Bl/6 mice (Fig 3.19F). The same was true for the spine density of these neurons (Fig 3.19H, basal: control 1.825 ± 0.033 spines/µm dendrite; PGN/LTA 1.767 ± 0.050 spines/µm, $p = 0.3431$; Fig 3.19J, apical: control 1.866 ± 0.034 spines/µm dendrite; PGN/LTA 1.838 ± 0.037 spines/µm, $p = 0.5811$).

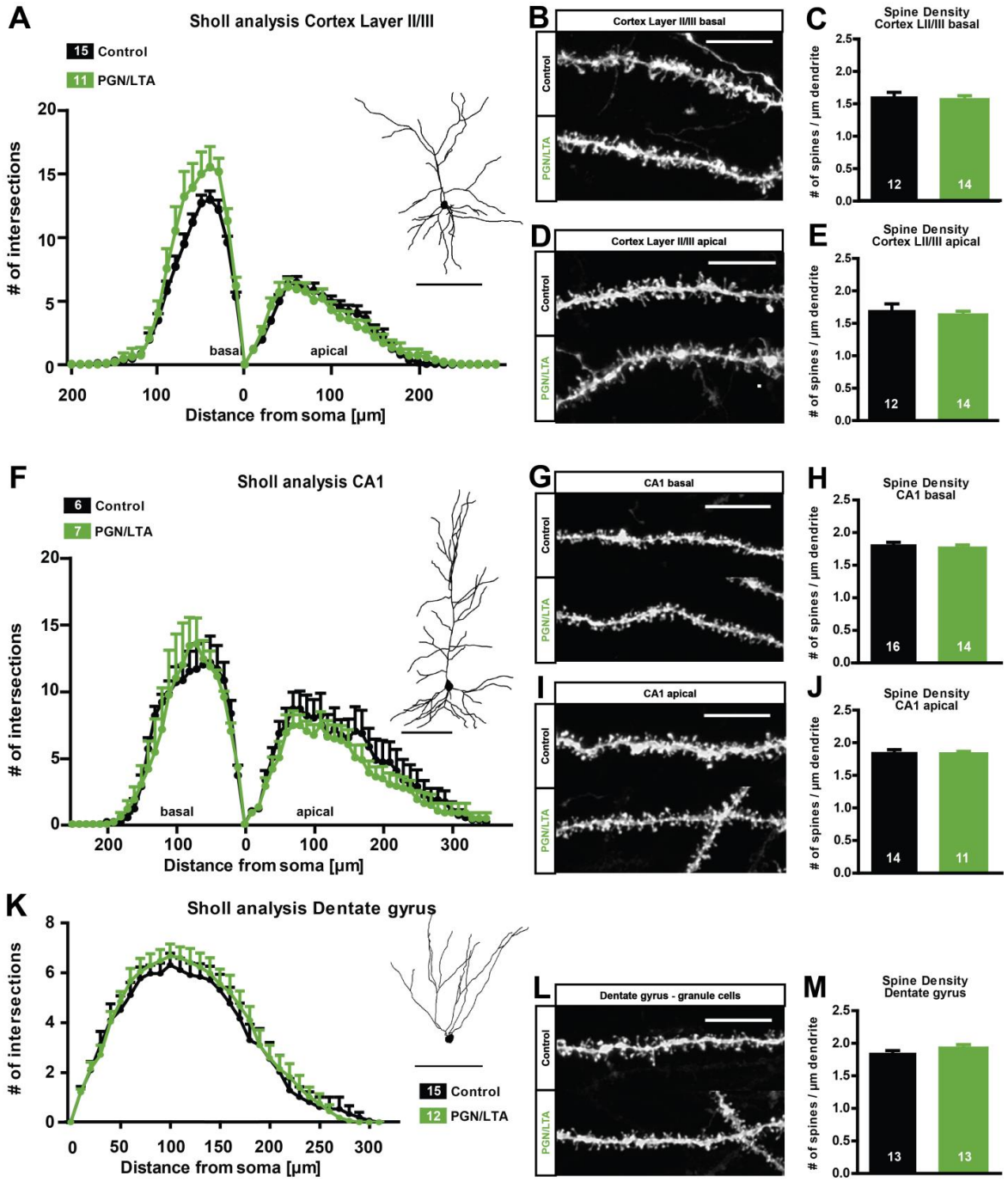

Figure 3.19 | Dendritic morphology and spine density of hippocampal and cortical neurons in adult C57Bl/6 mice 3 months after immune stimulation with 1µg/g bodyweight of lipoteichoic acid (LTA) and peptidoglycan (PGN) - (A) Tracing and Sholl analysis of cortex layer II/III pyramidal neurons, scale bar 100 µm. **(B, C)** Confocal microscopic image and quantification of basal dendritic spines of cortex LII/III cells, scale bar 10 µm. **(D, E)** Spine density and exemplified confocal images, scale bar 10 µm, of apical cortex LII/III neurons **(F)** Dendritic complexity of CA1 pyramidal neurons with tracing example, scale bar 100 µm. **(G, H)** Spine density and confocal microscopic images of basal CA1 dendrites, scale bar 10 µm. **(I, J)** Quantification of dendritic spines of mid-apical CA1 dendrites, representative images, scale bar 10 µm. **(K)** Sholl analysis of dentate gyrus granule cells, scale bar 100 µm. **(L, M)** Spine density of dentate gyrus granule cells, confocal image, scale bar 10 µm**.** Data presented as mean ± SEM, n = number of neurons/dendrites

Also tracings of the granule cells of the dentate gyrus revealed no changes in dendritic architecture upon stimulation with PGN/LTA of young adult WT mice (Fig 3.19K). In the

dentate gyrus, if anything, a slight increase in the spine density of granule cells was visible (Fig 3.19M, control: 1.832 ± 0.034 spines/µm dendrite; PGN/LTA: 1.904 ± 0.051 spines/µm, p = 0.2466).

Summarized, young adult WT mice showed no long-term consequences of an immune stimulation with the Gram positive bacterial cell wall components PGN and LTA 3 months after peripheral application. Therefore, effects on synaptic transmission and the learning behavior of the mice were not further addressed in this study.

3.2.6. Changes in neuronal morphology upon PGN/LTA stimulation in old APP/PS1 mice

In the present study I saw reduced neuronal complexity and functional deficits leading to impaired spatial learning in aged WT mice 3 months after peripheral immune stimulation with the Gram positive cell wall components peptidoglycan (PGN) and lipoteichoic acid (LTA). The consequences of the same peripheral immune stimulation for an already challenged system like the AD brains of old APP/PS1 mice were therefore interesting to explore.

Thus, 16 months old APP/PS1 mice were injected i.p. with 1 µg/g body weight of each PGN and LTA or NaCl solution for control. After 3 months of incubation, single neurons in the cortex and hippocampus were stained with the fluorescent dye DiI and analyzed for dendritic morphology and spine density.

The pyramidal neurons of the cortex layer II/III showed a significant lower number of intersections in the Sholl analysis between 70 and 90 µm from the soma in the basal and between130 and 210 µm from the soma in the apical dendritic compartment (Fig 3.20A). The spine density was significantly reduced in both apical and basal dendrites as well (Fig 3.20B, 3.20C, basal: control 1.670 ± 0.082 spines/µm dendrite, PGN/LTA 1.316 ± 0.056 spines/µm, p = 0.0016; Fig 3.20D, 3.20 E apical: control 1.667 ± 0.056 spines/µm dendrite, PGN/LTA 1.338 ± 0.071 spines/µm, p = 0.0021).

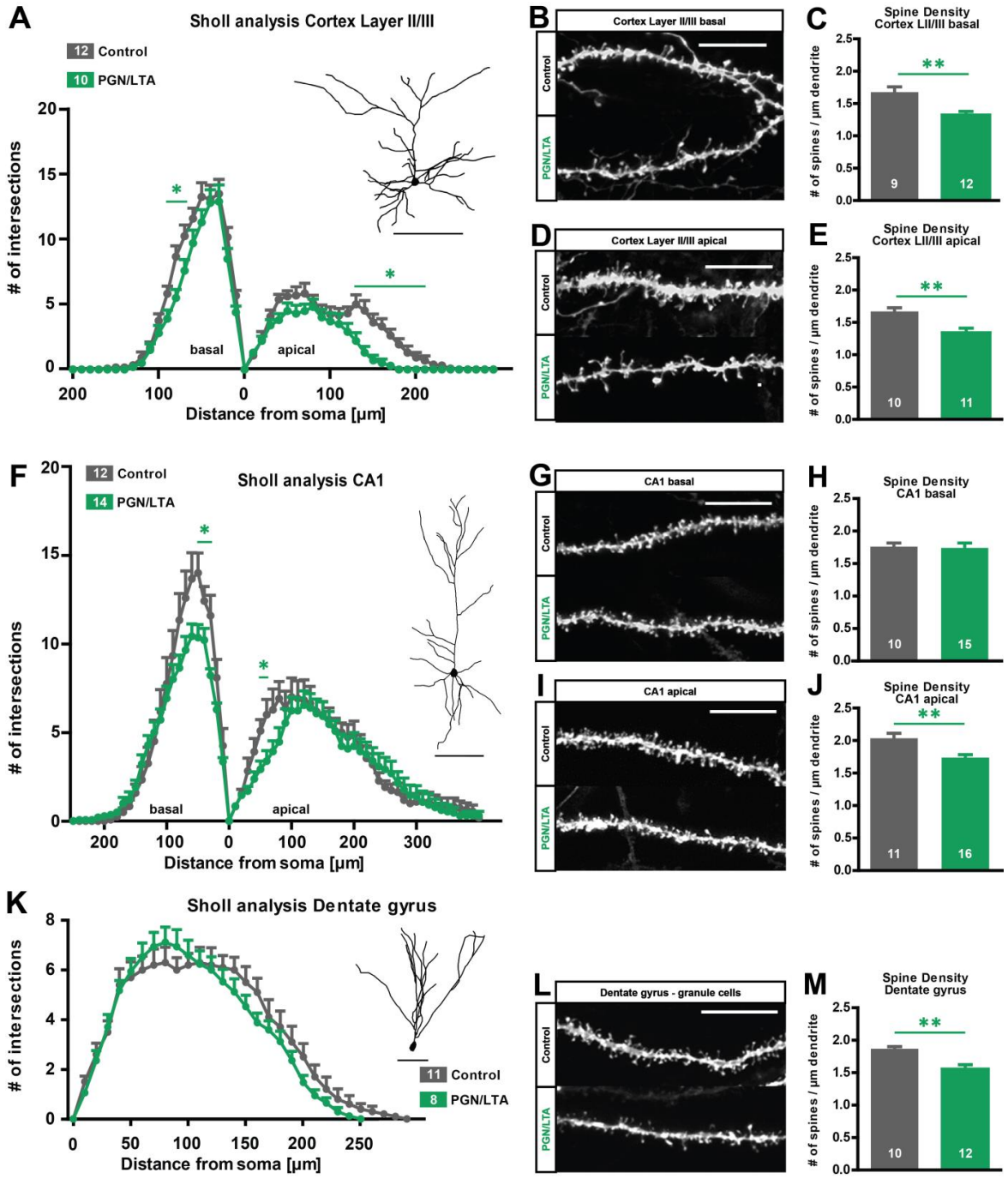

Figure 3.20 | Cortical and hippocampal dendritic architecture and spine density of 19 months old APP/PS1 mice 3 months after immune stimulation with peptidoglycan (PGN) and lipoteichoic acid (LTA). – (A) Tracings and quantification of dendritic complexity of cortex layer II/III neurons, scale bar 100 µm. **(B, D)** Confocal microscopic images of DiI stained basal and apical dendrites of cortex LII/III, scale bar 10 µm. **(C, E)** Basal and apical spine density of cortex LII/III neurons. **(F)** Sholl analysis and exemplified tracing of CA1 pyramidal neurons, scale bar 100 µm. **(G, H)** Spine density and representative image of CA1 basal dendrites, scale bar 10 µm. **(I, J)** Spine density and confocal microscopic image of CA1 apical dendrites, scale bar 10 µm. **(K)** Sholl analysis of granule cells of the dentate gyrus, tracing scale bar 50 µm. **(L, M)** Spine density and image of dentate gyrus granule cells. Data presented as mean ± SEM, n = number of cells or dendrites respectively, * = $p < 0.05$; ** = $p < 0.01$.

Also the dendritic complexity of CA1 pyramidal neurons was reduced between 30 and 50 µm from the soma for the basal dendrites and at 60 and 70 µm from the cell body for the apical dendrites (Fig 3.20F). The number of spines per µm basal dendrite was not altered,

while the apical dendrites had a highly significantly reduced spine density (Fig 3.20G, 3.20H, basal: control 1.756 ± 0.056 spines/µm dendrite, PGN/LTA 1.711 ± 0.044 spines/µm, p = 0.5286; Fig 3.20I, 3.20J, apical: control 2.038 ± 0.077 spines/µm dendrite, PGN/LTA 1.741 ± 0.046 spines/µm, p = 0.0016). In comparison to the CA1 pyramidal neurons, the granule cells of the dentate gyrus did not react with a decrease in dendritic complexity upon PGN/LTA treatment (Fig 3.20K). The spine density here however, was strongly reduced in the granule cells of old APP/PS1 mice (Fig 3.20L, 3.20M, controls: 1.851 ± 0.053 spines/µm dendrite, PGN/LTA: 1.615 ± 0.057 spines/µm, p = 0.0092). Compared to age matched WT mice, the AD mice showed a more dramatic impact of the peripheral immune stimulation with PGN/LTA on the granule cells of the dentate gyrus. The cortical and hippocampal pyramidal neurons showed a reduction in dendritic complexity and spine density, which was not stronger than the one observed for aged WT mice.

3.2.7. Synaptic plasticity in old APP/PS1 mice 3 months after stimulation with PGN/LTA

While several studies suggest detrimental effects of a peripheral immune activation with lipopolysaccharide of Gram negative bacteria in WT mice, only some draw the connection to the onset and progression of Alzheimer´s disease. The involvement of Gram positive bacteria and infections with Gram positive bacteria as risk factor or facilitator of neurodegeneration and cognitive impairment in an AD mouse model has not been addressed at all. I found, that 19 months old WT mice were vulnerable towards a peripheral immune stimulation with the Gram positive bacterial cell wall components peptidoglycan (PGN) and lipoteichoic acid (LTA) as they showed a decrease in neuronal complexity and spine density as well as in long-term potentiation even 3 months after the stimulation. I further saw that 19 months old APP/PS1 mice exhibited an even stronger effect on the dendritic architecture in some cell types of the cortex and hippocampus. The impact on neuronal function and plasticity should therefore be investigated.

Thus, 16 months old APP/PS1 mice were immune stimulated via peripheral administration of 1 µg/g bodyweight of LTA and PGN. 3 months later, basal synaptic transmission as well as short- and long-term plasticity was addressed at the Schaffer collateral CA3-CA1 pathway of hippocampal acute slices in an interface electrophysiology setup.

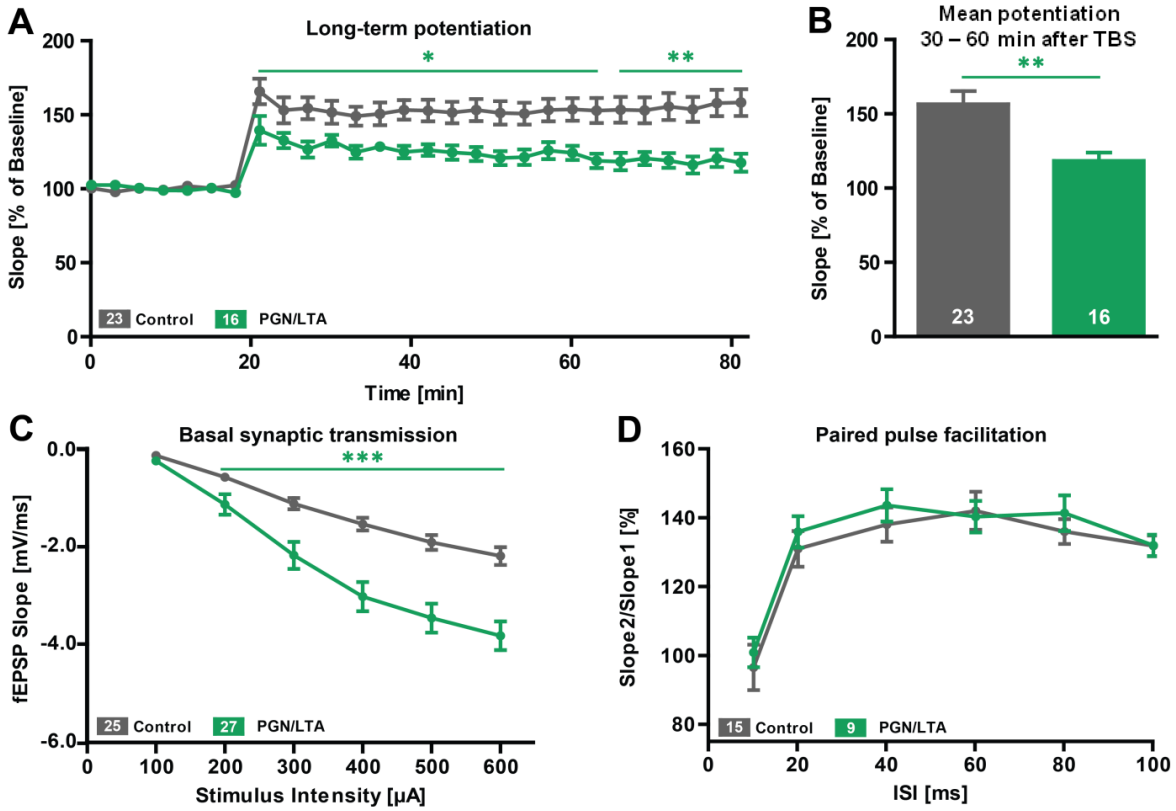

Figure 3.21 | Long-term synaptic plasticity of the CA3-CA1 Schaffer collateral pathway of 19 months old APP/PS1 mice 3 months after peripheral immune stimulation with lipoteichoic acid (LTA) and peptidoglycan (PGN) from *Staphylococcus aureus*. (A) Long-term potentiation (LTP) after 20 minutes baseline recording, induced via TBS (3 trains with 10 s interval of 10 bursts containing 4 pulses at 100 Hz with 200 ms inter burst interval), shown as fEPSP slope % of baseline of control APP/PS1 and PGN/LTA treated APP/PS1 mice. **(B)** Quantification of the last 30 minutes, the stable phase of LTP, in control and PGN/LTA treatment. **(C)** Input-Output relationship and **(D)** short-term plasticity of CA3-CA1 pathway after control and PGN/LTA treatment in old APP/PS1 mice. ISI = interstimulus interval, All data are shown as mean ± SEM; * = $p < 0.05$, ** = $p < 0.01$, *** = $p < 0.001$

After 20 minutes of baseline recordings, LTP was induced via TBS. In control as well as PGN/LTA treated aged APP/PS1 mice LTP was successfully induced and maintained stable for 60 minutes of recording (Fig 3.21A). However, in PGN/LTA treated mice the LTP was significantly lower for the whole measured period (Fig 3.21A) and highly significant reduced during the stable phase of recording (Fig 3.21B, control: 157.2 ± 8.6 fEPSP slope % of baseline, PGN/LTA: 117.9 ± 5.6 % fEPSP slope, $p = 0.0051$). Also the basal synaptic transmission within the CA3-CA1 signaling was altered upon PGN/LTA treatment, but here a steeper fEPSP slope could be evoked at stimulus intensities 200 to 600 µA when compared to control slices (Fig 3.21C). The presynaptic properties like the neurotransmitter vesicle capacity seemed not to be affected as there was no change in paired pulse facilitation upon immune stimulation with PGN/LTA in old APP/PS1 mice (Fig 3.21D).

Even though hippocampal acute slice of immune stimulated aged APP/PS1 mice show higher fEPSP slopes in the input-output curve, the induction and maintenance of LTP was even lower than in age matched WT mice.

3.2.8. Changes in neuronal structure upon PGN/LTA treatment in adult APP/PS1 mice

While most studies dealing with the communication between the peripheral immune system and the central nervous system use lipopolysaccharide of Gram negative bacteria to stimulate the innate immunity, not much is known about mechanisms underlying Gram positive based immune stimulation. In this study I could show, that aged WT as well as aged APP/PS1 mice exhibited a reduction in the neuronal complexity and spine density in different brain areas which led to impairment of long-term potentiation and even the spatial learning ability of the old WT mice actually 3 months after the treatment. Young WT mice on the other hand showed no effect or even an increase in the dendritic complexity of cortical and hippocampal neurons.

Therefore, it was of special interest to examine the impact of a Gram positive bacterial immune stimulation on the neuronal architecture of adult APP/PS1 mice. Hence, I stimulated the peripheral immune system of 4 months old APP/PS1 mice with the intraperitoneal application of 1 µg LTA and PGN per g bodyweight. 3 months later the dendritic morphology and spine density of cortical and hippocampal neurons were analyzed with the help of the DiOlistic technique.

Cortex layer II/III pyramidal neurons showed only a slight decrease in the number of intersections in the Sholl analysis of the basal dendritic tree (Fig 3.22A) but a significant reduction in the spine density at this level (Fig 3.22B, 3.22C, control: 1.852 ± 0.080 spines/µm dendrite, PGN/LTA: 1.540 ± 0.070 spines/µm, $p = 0.0066$). The complexity (Fig 3.22A) and also the spine density of the apical dendritic tree was only mildly reduced 3 months after PGN/LTA treatment (Fig 3.22D, 3.22E, control: 1.763 ± 0.076 spines/ µm dendrite; PGN/LTA: 1.637 ± 0.065 spines/µm, $p = 0.2137$).

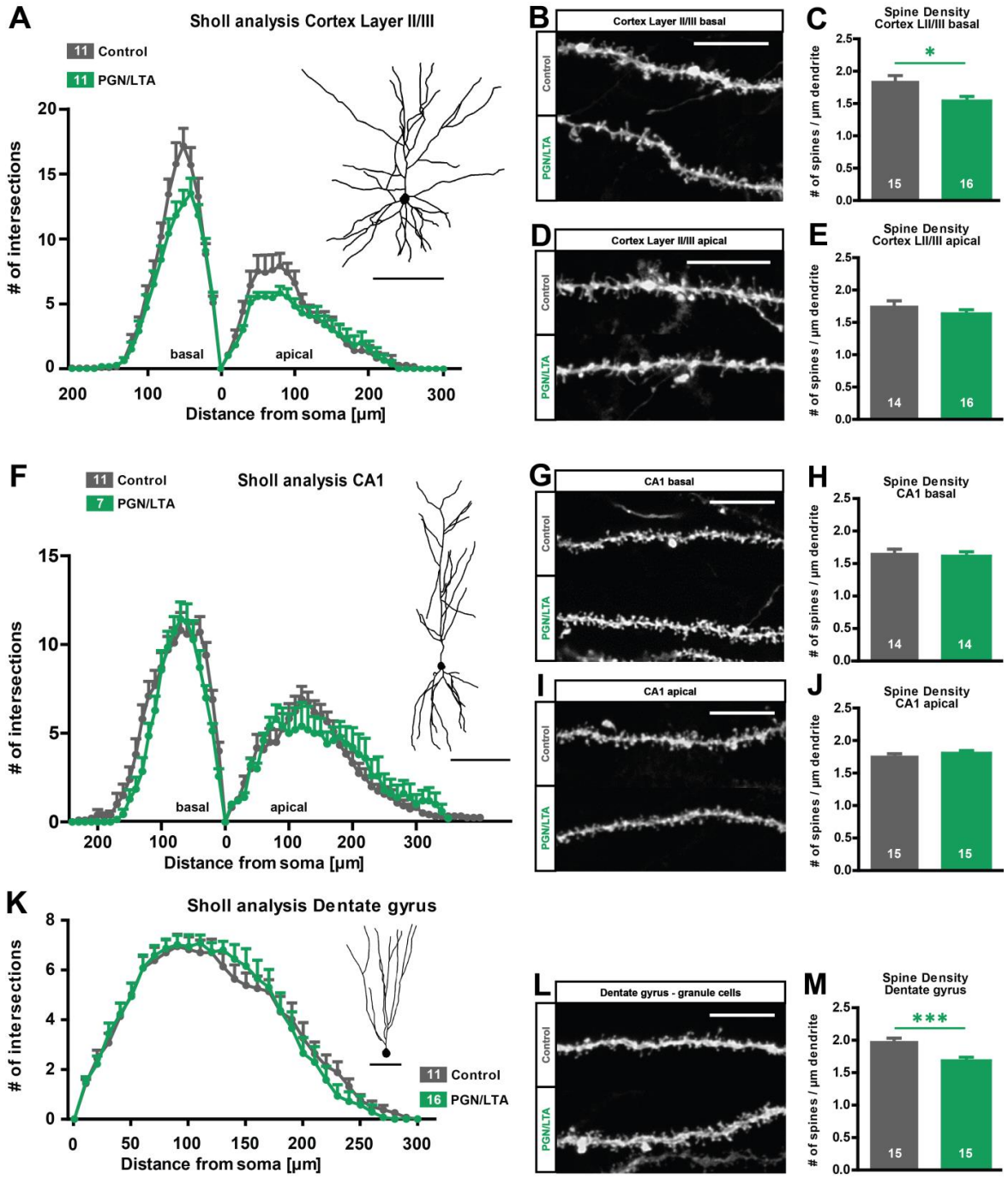

Figure 3.22 | Dendritic architecture and spine density in cortex and hippocampus of 7 months old APP/PS1 mice 3 months after immune stimulation with peptidoglycan (PGN) and lipoteichoic acid (LTA). – (A) Sholl analysis of cortex layer II/III pyramidal neurons, tracing scale bar 100 µm. **(B, D)** Confocal microscopic images of basal and apical dendrites PGN/LTA vs. control, 10 µm scale bar. **(C, E)** Quantification of spine density from basal and apical cortex LII/III dendrites. **(F)** Dendritic morphology and exemplified tracing of CA1 pyramidal neurons. **(G, H)** Spine density of basal CA1 dendrites, confocal image, scale bar 10 µm. **(I, J)** Images of apical CA1 dendrites and respective spine density, scale bar 10 µm. **(K)** Sholl analysis of granule cells of the dentate gyrus, tracing 50 µm scale bar. **(L, M)** Representative confocal microscopic images and evaluation of spine density from dentate gyrus granule cells. Data presented as mean ± SEM, n = # of neurons/dendrites * = $p < 0.05$; *** = $p < 0.001$.

In contrast, CA1 pyramidal neurons showed no change in dendritic complexity (Fig 3.22F) or spine density of basal (Fig 3.22G, 3.22H control: 1.668 ± 0.055 spines/µm dendrite, PGN/LTA: 1.616 ± 0.068, p = 0.5611) or mid-apical dendrites (Fig 3.22I, 3.22J control: 1.771 ± 0.029 spines/µm dendrite, PGN/LTA: 1.807± 0.042, p = 0.4767). The granule cells of the dentate gyrus exhibited no alteration in the dendritic architecture upon stimulation with PGN/LTA in young APP/PS1 (Fig 3.22K), but a highly significantly decreased spine density (Fig 3.22L, 3.22M, control: 1.990 ± 0.45 spines/µm dendrite; PGN/LTA: 1.684 ± 0.056 spines/µm, p = 0.0002).

Conclusively, adult APP/PS1 showed slightly detrimental effects of a peripheral immune stimulation with PGN and LTA while their WT counterparts showed a tendency toward more beneficial effects. Therefore, the immune homeostasis of the young APP/PS1 is likely either easier to disturb or takes longer to revert into an anti-inflammatory status. However, CNS immune response of adult APP/PS1 mice and the effects on neuronal function and spatial learning of the mice were not examined in this study.

3.3. Changes in neuronal morphology upon infection with *Toxoplasma gondii*

In rodents, the chronic infection with the protozoan parasite *T.gondii* leads to subtle neurological and behavioral changes such as a more active behavior (Hay et al. 1985, Webster et al. 1994) and infected animals lose their innate fear of cat odors (Berdoy et al. 2000). Some studies already suggested that inflammation (Hermes et al. 2008), neurotransmitter imbalance (Gatkowska et al. 2012) or dopamine overproduction (Prandovszky et al. 2011) are involved in this phenotype. However, underlying mechanisms and effects on neuronal architecture and signaling have not been explored yet.

To investigate the impact of chronic *Toxoplasma gondii* infection on neuronal morphology in adult mice, the dendritic arborization was analyzed in different brain regions 8 weeks after infection via intraperitoneal application of 3 tissue cysts from brain homogenate of infected mice. A Diolistic approach was used to analyze the morphology of single excitatory neurons in cortex layer II/III, the CA1 area and dentate gyrus of the hippocampus. To determine the effect of chronic *T.gondii* infection on inhibitory neurons, the medium spiny neurons of the striatum were examined. For the evaluation of the dendritic complexity the Sholl analysis was used (Sholl 1953).

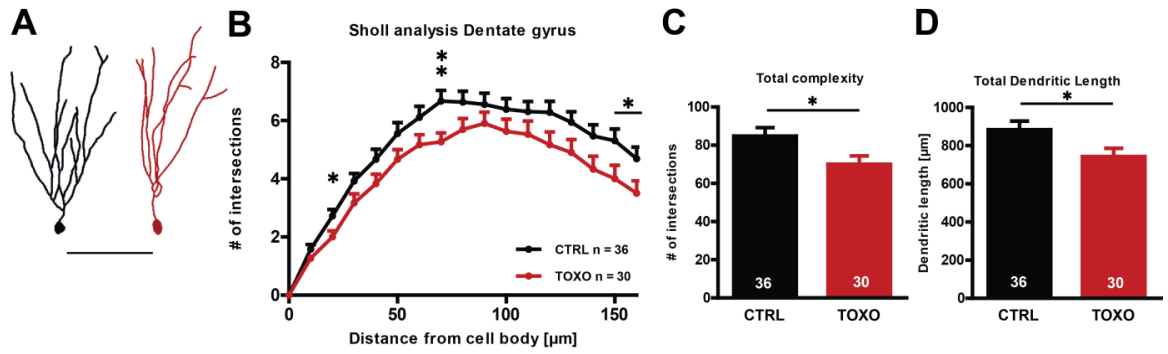

Figure 3.23: Dendritic complexity of hippocampal granule cells of the dentate gyrus during chronic *Toxoplasma gondii* infection – (A) Examples for the morphology of granule cells of the dentate gyrus of control vs. *T.gondii* infected mice (scale bar, 100 µm). **(B)** Sholl analysis of DG granule cells **(C)** Total complexity of DG granule cells **(D)** Total dendritic length of *T.gondii* infected vs. control DG cells, Data presented as mean ± SEM, n = numbers of cells, * = $p < 0.05$; ** = $p > 0.01$.

In *T.gondii* infected mice, the granule cells of the dentate gyrus showed a reduction in the number of intersections over the whole dendritic tree (Fig. 3.23A and Fig. 3.23B), which was significant at 20, 70, 150 and 160 µm from the soma. This resulted in a significant reduction in total dendritic complexity (Fig. 3.23C, control = 84.8 ± 4.4 intersections; infected: 70.1 ± 4.4 intersections; $p = 0.021$). Also the total dendritic length was

significantly reduced in comparison to control neurons (Fig. 3.23D, control: 890.7 ± 46.0 µm; infected: 742.5 ± 44.0 µm, p = 0.025).

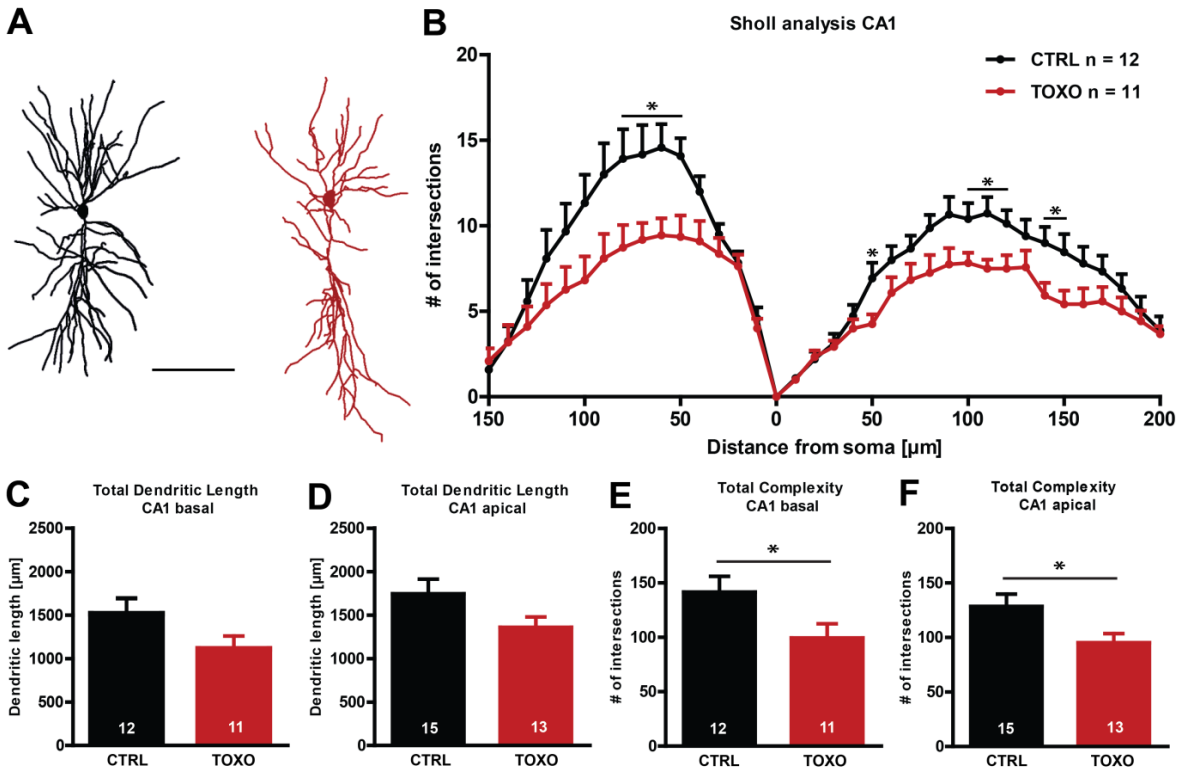

Figure 3.24: Dendritic complexity of hippocampal CA1 pyramidal neurons in mice chronically infected with *Toxoplasma gondii* – (A) Exemplified morphology of a CA1 neuron of a control vs. *Toxoplasma* infected animal (scale bar, 100 µm). **(B)** Dendritic complexity (Sholl analysis) of CA1 pyramidal neurons. **(C)** Total dendritic length of CA1 apical dendrites. **(D)** Total length of CA1 basal dendritic tree. **(E)** Total complexity of CA1 basal dendrites. **(F)** Total complexity of infected vs. control CA1 neurons of the apical tree, Data presented as mean ± SEM, n = number of neurons, * = p < 0.05

Also the dendritic morphology of pyramidal neurons in the CA1 area of the hippocampus was altered in *Toxoplasma gondii* infected mice. The Sholl analysis of apical as well as the basal dendritic tree revealed a reduction in the number of intersections, which was statistically significant between 50 and 80 µm from the soma for the basal and at 50, 90, 100, 110, 140 and 150 µm from the cell body for the apical tree (Fig. 3.24B). This led to a signficant reduction in total complexity for both the apical and the basal CA1 dendrites in *T.gondii* infected mice in comparison to the control neurons (Fig. 3.24E basal, control: 141.6 ± 14.5 intersections, infected: 99.5 ± 13.0, p = 0.044; Fig. 3.24F apical, control: 128.5 ± 11.2 intersections, infected: 95.2 ± 8.3, p = 0.037). The total dendritic length was only slightly reduced in the two different dendritic compartments (Fig. 3.24C, basal, control: 1514.7 ± 172.9 µm, infected: 1111.2 ± 148.3 µm, p = 0.094; Fig 3.24D apical, control: 1744.5 ± 169.1 µm, infected: 1359.1 ± 119.1, p = 0.088).

To determine whether the infection with *T.gondii* induces reduction in dendritic complexity in a cell type specific manner, inhibitory medium spiny neurons of the striatum were analyzed. Although a slight decrease in dendritic complexity was visible for the more proximal part of the dendritic tree in MSN of *Toxoplasma gondii* infected mice (Fig. 3.25B), there were no significant changes in the total complexity (Fig. 3.25C, control: 165.4 ± 19.1 intersections, infected: 137.1 ± 16.2 intersections, p = 0.3025) and total dendritic length (Fig 3.25D, control: 1933.1 ± 213.7 µm, infected: 1708.1 ± 173.1, p = 0.4904) upon *T.gondii* infection in comparison to control neurons.

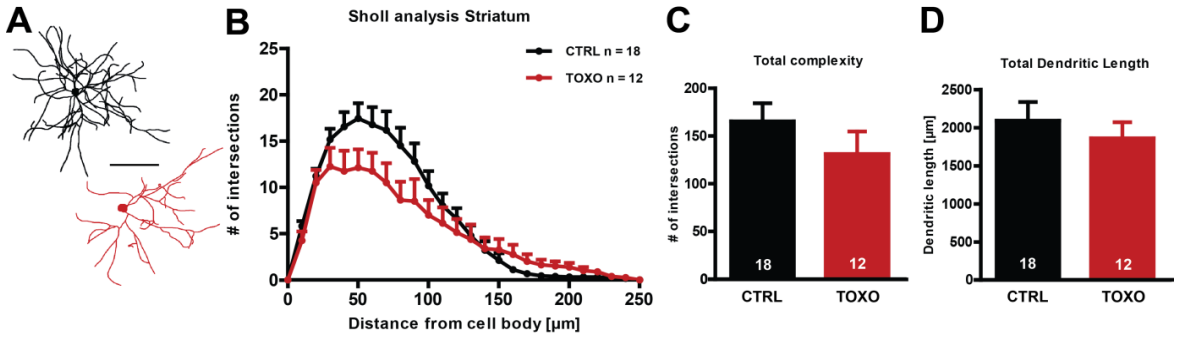

Figure 3.25 | Changes in dendritic complexity of medium spiny neurons in the striatum of mice chronically infected with *Toxoplasma gondii* - (A) Tracings of control and *T.gondii* infected medium spiny neurons (MSN) in the striatum (scale bar 100 µm). **(B)** The Sholl analysis of MSN. **(C)** Total dendritic complexity of MSN from control vs. *T.gondii* infected mice **(D)** Total dendritic length of *T.gondii* infected vs. control MSNs, Data presented as mean ± SEM, n = number of neurons

In addition to the hippocampus and striatum, pyramidal neurons of the cortex layer II/III were analyzed in mice chronically infected with *T.gondii*. Identification of the cortical layers was obtained via DAPI staining. In the appropriate layer, only neurons with a pyramidal shaped cell body and characteristic dendritic tree separated in several shorter basal dendrites and one primary apical dendrite with numerous branches reaching the brain surface were included. The dendritic complexity of the cortex layer II/III pyramidal cells was only slightly reduced in the apical part of the dendritic tree in *T.gondii* infected mice compared to control neurons (Fig 3.26A, 3.26B). The basal compartment showed a stronger decrease in intersections, which was significant for the more distal part between 110 and 140 µm from the cell body. Therefore, only the basal part showed a significant reduction in total dendritic length (Fig. 3.26C, basal, control: 1872.5 ± 168.0 µm, infected: 1357.4 ± 104.2 µm, p = 0.012) and total complexity (Fig. 3.26E, basal, control: 161.4 ± 15.1 intersections, infected: 124.3 ± 9.0 intersections, p = 0.044).

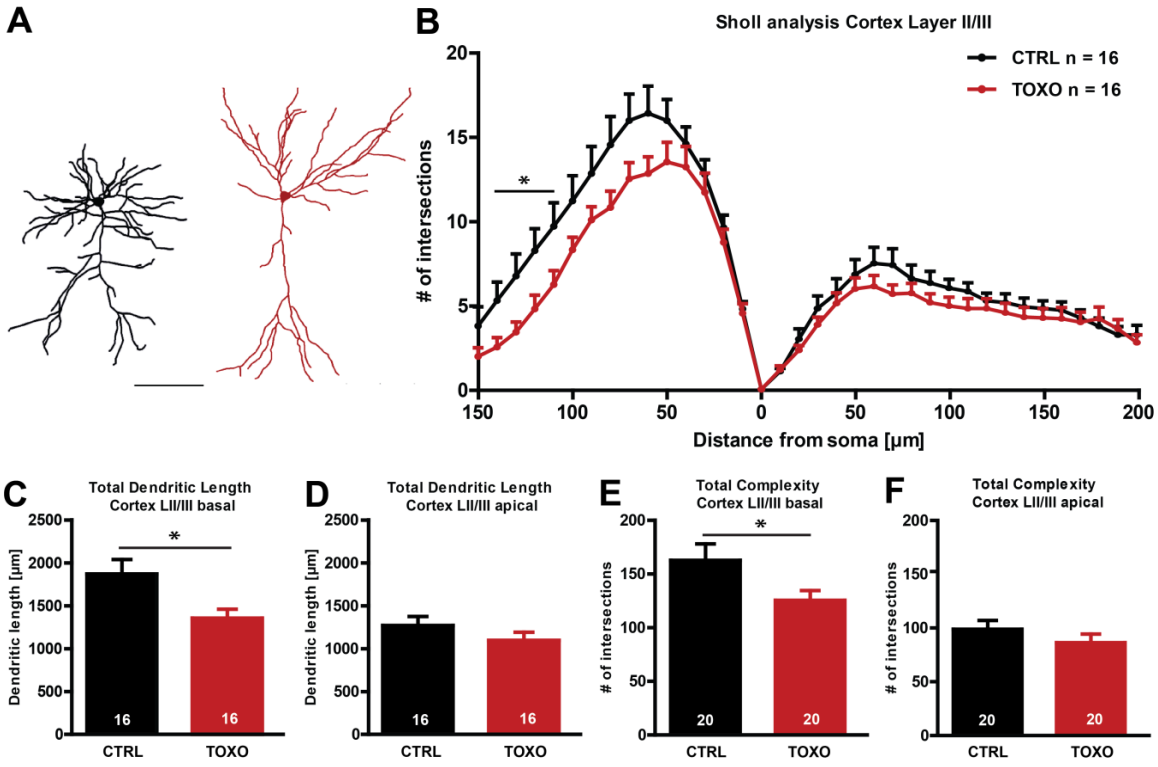

Figure 3.26: Influence of a chronic *Toxoplasma gondii* infection on dendritic complexity of cortex layer II/III pyramidal neurons – (A) Exemplified morphology of a cortex layer II/II neurons of control vs. *Toxoplasma* infected conditions (scale bar, 100 µm). **(B)** Dendritic complexity of cortical pyramidal neurons **(C)** Total complexity of infected vs. control cortex layer II and III neurons of the apical tree. **(D)** Total complexity of cortex layer II/III pyramidal neuron basal dendrites. **(E)** Total dendritic length of cortex layer II/III apical dendrites. **(F)** Total length of CA1 basal dendritic tree, Data presented as mean ± SEM. * = $p < 0.05$.

In the apical compartments only a very mild reduction in total dendritic length (Fig. 3.26D, basal, control: 1228.4 ± 102.8 µm, infected: 1059.7 ± 92.4 µm, p = 0.230) and total complexity (Fig. 3.26E, basal, control: 99.2 ± 8.2 intersections, infected: 86.5 ± 8.0 intersections, p = 0.276) was visible.

To summarize this line of evidence, even though the changes in dendritic architecture were not significant in the medium spiny neurons in the striatum, all evaluated cell types displayed a more or less string reduction in dendritic complexity 8 weeks after infection with *Toxoplasma gondii* in young adult mice.

Next, density and morphology of dendritic spines were analyzed in cortex layer II/III. Therefore, spines were counted on the basal dendrites as well as on mid-apical secondary dendrites. The number of dendritic spines per defined stretch of dendrite was clearly decreased in cortex layer II/III pyramidal neurons of *T.gondii* infected mice compared to the not-infected controls, reaching significance for both apical and basal dendrites (Fig. 3.27A, 3.27B, apical, control: 1.539 ± 0.047 spines/µm dendrite, infected: .1.159 ± 0.095 spines/µm, p = 0.001; Fig. 3.27C, 3.27D, basal, control: 1.474 ± 0.63 spines/µm dendrite, infected: 1.169 ± 0.116, p = 0.005).

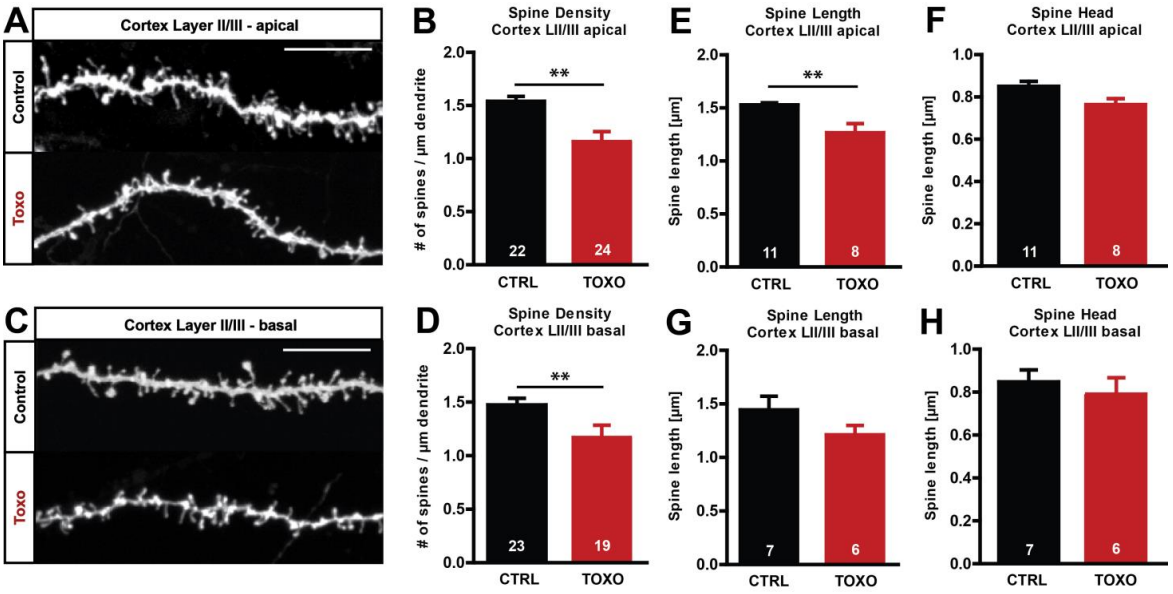

Figure 3.27: Spine density and morphology of cortex layer II/III pyramidal neurons of mice chronically infected with *Toxoplasma gondii* – (A, C) Confocal fluorescent images of dendrites from pyramidal neurons of the cortex layer II/III stained via DiOlistic technique (scale bar, 10 µm). **(B)** Spine density of cortex LII/III mid-apical dendrites upon *T.gondii* infection **(D)** The number of spines per µm of basal dendrite in *T.gondii* infected cortex LII/III cells vs. control. **(E, G)** Spine length of apical and basal spines from cortex layer II/III pyramidal neurons of mice chronically infected with *Toxoplasma gondii* vs. control **(F, H)** Spine width of apical and basal spines from cortex LII/III cells, ** = $p < 0.01$.

Besides the number of spines also the spine morphology as an indicator for the synaptic connectivity between neurons was analyzed by examining spine length and spine head width. While the spine length was significantly reduced on mid-apical dendrites of cortex layer II/III upon infection with *T.gondii* (Fig 3.27E, control: 1.530 ± 0.019 µm, infected: 1.266 ± 0.086 µm, $p = 0.0083$), basal dendrites showed only a slight decrease in spine length compared to control neurons (Fig 3.27G, control: 1.436 ± 0.126 µm, infected: 1.204 ± 0.087 µm, $p = 0.0995$). The spine head width was not significantly altered in apical or basal part of cortical neurons from infected mice (Fig 3.27F, apical, control: 0.850 ± 0.024 µm, infected: 0.764 ± 0.028 µm, $p = 0.2300$; Fig 3.27H basal, control: 0.848 ± 0.056 µm, infected: 0.790 ± 0.077 µm, $p = 0.4565$).

Taken together, young adult mice chronically infected with *Toxoplasma gondii* showed a reduction in the dendritic complexity in different brain areas and cell types. In cortex layer II/III also the spine density was decreased while the morphology of the remaining spines was not dramatically altered. Especially as the head width was similar to the one measured in control mice, the functional integrity of the synapses seems not to be affected.

4. DISCUSSION

Neuroinflammation is hypothesized to be an early event in the pathogenesis of neurodegenerative disease and systemic innate immune activation has been identified as risk factor for Alzheimer´s disease in humans. Whether a peripheral immune stimulation with different bacterial cell wall components in mice can induce a neurodegenerative phenotype and whether existing neurodegenerative pathology in an AD mouse model is worsened long after the acute immune stimulation has not been addressed yet.

In this work I investigated the long-term effects of a systemic immune activation with different endotoxic bacterial components on neuronal structure, function and learning behavior of mice. Different components as well as the influence of age were examined. Additionally, the APP/PS1 mouse model of Alzheimer´s disease was chosen to determine the influence of a peripheral immune stimulation on preexisting neurodegeneration.

In the first and second part of the thesis (chapter 3.1. and 3.2.) the presented data provide evidence for an age-dependent vulnerability towards an immune stimulation with LPS of *Salmonella typhimurium* and peptidoglycan/lipoteichoic acid of *Staphylococcus aureus*. While adult mice do not show changes in neuronal architecture, aged mice exhibit decreased dendritic complexity and spine density in neurons of the hippocampus and cortex. Furthermore, impairment in LTP and in the formation of spatial memory in the Morris water maze is discovered in aged WT mice. Aged mice show a higher microglia activation under basal conditions and further activation upon LPS stimulation which is not detectable in adult mice.

The treatment with *E.coli* LPS does not show these detrimental effects. However, in aged APP/PS1 mice, both *E.coli* and *S.typhimurium* LPS result in a reduction of dendritic branches and in spine density of hippocampal and cortical excitatory neurons. Likewise, synaptic plasticity is impaired with both kinds of LPS and upon PGN/LTA treatment. Interestingly, also adult APP/PS1 mice exhibit deleterious effects on neuronal architecture upon peripheral immune stimulation.

Furthermore, I could demonstrate that the impairment in LTP and neuronal structure after LPS *S.typhimurium* treatment can be rescued by the genetic ablation of the NLRP3 inflammasome which is required for the maturation of the proinflammatory cytokines IL-1β and IL-18.

The last part of the thesis (chapter 3.3.) describes the impact of chronic *Toxoplasma gondii* infection. Here, the data demonstrate that even young adult mice are sensible towards a CNS infection with *T.gondii* as they show reduction in dendritic complexity in various neuronal cell types. Furthermore, cortical neurons displayed a dramatic decrease in dendritic spine density and alterations in spine morphology.

4.1. Peripheral immune stimulation results in an age-dependent impairment in structural and functional synaptic plasticity

Sepsis and septic shock are characterized by an overwhelming systemic production of pro-inflammatory mediators as response to infection with different pathogens (Bone et al. 1992, Angus et al. 2001). Besides symptoms such as fever and hypotension also brain functions can be affected by a severe bacteraemia. During sepsis, up to 71% of the patients develop septic encephalopathy associated with attention and memory deficits, delirium and coma (Pine et al. 1983, Sprung et al. 1990, Wilson and Young 2003, Semmler et al. 2008).

In rodents, the intraperitoneal administration of lipopolysaccharide (LPS) is widely used to mimic severe bacterial infections and sepsis. In this model, the application of the endotoxic Gram negative bacterial cell wall component LPS is sufficient to induce high production of IL-1β and TNF-α in the periphery (Michie et al. 1988, Cannon et al. 1990) as well as in the brain parenchyma (Qin et al. 2007, Semmler et al. 2008). The literature provides adequate information about the usage of *E.coli* LPS to investigate effects of a peripheral immune activation on brain functions. Here, LPS concentrations range from 0.25 µg to 10 µg per g body weight for mice (Arai et al. 2001, Semmler et al. 2005, Qin et al. 2007, Richwine et al. 2008, Czapski et al. 2010, Lee et al. 2010). A lethal dose was described for 20 µg to 50 µg per g body weight (Jeong et al. 2009, Back et al. 2010). However, the distinct types of LPS and data on body weight loss, sickness behavior and mortality rate are not provided in most studies. Additionally, in the majority of cases analysis of different brain functions were executed only a few hours or days after the peripheral LPS application, therefore the survival of mice was not endangered even with higher doses. To examine the long-term effects of an immune stimulation with components of Gram negative bacteria, I established the peripheral applications of LPS from *E.coli* B8:0127 and *Salmonella enterica* serovar *typhimurium*. The long-term analysis of mice recovering from such an inflammatory insult, require lower doses of LPS than seen in most studies. Especially for the application of *Salmonella typhimurium* LPS not much is known about doses establishing a profound cytokine production in the periphery as well as in the CNS. In the present study, a dose of 0.4 µg/g body weight per mouse was established for *E.coli* and *S.typhimurium* LPS leading to a strong loss of body weight within the first days after immune stimulation with no fatalities in young adult and a mortality rate of around 20% in aged mice. As body weight loss of rodents can be correlated to pathogen burden and cytokine release during sepsis (Breuillé et al. 1993, Cooney et al. 1999), the chosen dosage was considered appropriate for the long-term study of a systemic immune activation.

Previous studies have addressed the acute consequences of a peripheral LPS administration including impairment of long-term potentiation in different hippocampal pathways. In the major output projection of the hippocampus, the CA1-subiculum pathway, LTP is impaired only 4 hours after peripheral LPS application (Commins et al. 2001). In the perforant path, which connects the entorhinal cortex and the dentate gyrus, maintenance of LTP is inhibited already 3 hours after LPS injections (Hennigan et al. 2007). Also within the Schaffer collaterals-CA1 synapses, mice show deficits in LTP 24 hours after peripheral immune stimulation (Strehl et al. 2014). These acute effects include not only impairment of neuronal plasticity *in vitro*, but also deficits in learning and memory tested *in vivo*. In the Morris water maze, LPS stimulated mice take longer to find the hidden platform on day 1 and 2 after injections in one study (Arai et al. 2001), while others show higher escape latencies on day 4 and day 8 of the training after a single LPS injection on day 1 (Shaw et al. 2001). Of note, all studies used adult mice or rats and different types of *E.coli* LPS. The impairment in neuronal signaling and learning behavior observed in LPS stimulated mice are associated with a massive production of pro-inflammatory cytokines not only in the periphery but also within the brain parenchyma. While the peak of cytokines in the brain such as IFN-γ, IL-1β, IL-6 and TNF-α appears around 6 hours after LPS injections (Biesmans et al. 2013), also several weeks after systemic infection or immune stimulation signs of neuroinflammation are still present (Qin et al. 2007, Bossù et al. 2012**,** Püntener et al. 2012, Valero et al. 2014). Even though the levels of pro-inflammatory cytokines were not quantified in this thesis, the data provided here show no long-term changes in neuroinflammation based on the microglia and astrocyte phenotype 3 months after systemic immune activation in adult mice.

Also no long-term changes in the neuronal architecture are shown after either *E.coli* or *S.typhimurium* LPS injection. The morphology and spine density of CA1 pyramidal neurons are not altered 3 months after LPS administration in 7 months old mice. Also neither the dendritic complexity nor the spine density of dentate gyrus granule cells is reduced in adult WT mice 3 months after peripheral immune stimulation with LPS of *E.coli* or *S.typhimurium*. This is in agreement with the few other studies investigating the effect of a peripheral immune stimulation on neuronal architecture. One study shows that the morphology of dentate gyrus granule cells is not altered several weeks after a single LPS administration and only mild changes in the memory formation during Morris water maze training are observed in adult mice (Valero et al. 2014). The intracerebroventricular injection of LPS has been shown to promote a reduction in dendritic complexity of CA1 pyramidal neurons in adult mice 24 hours after administration (Milatovic et al. 2010). However, 3 days after peripheral LPS injection the morphology of CA1 neurons is not affect in adult mice (Richwine et al. 2008). This suggests a stronger pro-inflammatory immune signaling in response to a local administration of LPS and that the peripheral

immune activation does not even lead to acute deleterious effects on neuronal morphology in adult mice.

In summary, the neuronal phenotype after peripheral immune stimulation is consistent with results of other studies and implies that no long-term detrimental consequences can be observed after a systemic immune activation in adult mice.

Several studies suggest that an acute peripheral inflammation causes stronger effects in aged animals. For example, CA1 neuronal complexity of apical dendrites is decreased in aged mice 3 days after peripheral immune activation with LPS, whereas CA1 neurons of young mice do not exhibit any alterations (Richwine et al. 2008). Similarly, while 3 months old mice do not show any changes in the late phase of long-term potentiation 4 days after infection with *E.coli*, aged mice 24 months of age exhibit significant lower theta burst induced L-LTP (Chapman et al. 2010). Also 7 days after infection with *E.coli* aged rats show impaired spatial memory formation in the Morris water maze, while there is no change between young infected and control rats. Interestingly, only hippocampus-dependent long-term memory formation is affected (Barrientos et al. 2006). In another model of peripheral immune activation, the administration of heat-killed *Mycobacterium butyricum* (complete Freund´s adjuvant) leads to a decrease in LTP 3 weeks after application in 12 months old rats but not in their 2 months old counterparts (Liu et al. 2012). Therefore, the acute effects occurring upon systemic inflammation caused by *E.coli* LPS have been reported to be stronger in aged rodents than in young. One focus of this study is whether this age-dependent vulnerability towards systemic inflammation is still visible after the initial sickness behavior was overcome. Three months after immune stimulation, the neuronal structure of hippocampal and cortical neurons in aged mice is only slightly reduced with *E.coli* LPS. Also both short-term and long-term synaptic plasticity in the hippocampus are not impaired. Solely the basal synaptic transmission is decreased after *E.coli* LPS administration. In line with this, also spatial memory formation in the Morris water maze was comparable to controls 3 months after *E.coli* LPS treatment. Taken together, even though *E.coli* LPS causes acute detrimental effects, I could not detect appreciable deleterious long-term consequences after LPS *E.coli* administration in aged, 16 months old mice.

The same experimental setup with LPS of *Salmonella typhimurium* on the other hand indeed leads to enduring changes in neuronal structure and synaptic plasticity in aged mice. Here, the dendritic complexity and spine density of cortical and hippocampal pyramidal neurons is reduced. This is accompanied by a significant lower LTP at the Schaffer collateral pathway. Basal synaptic transmission and presynaptic properties are not affected. Moreover, also in the Morris water maze, aged mice treated with LPS of *S.typhimurium* showed higher escape latencies due to a diminished use of hippocampus-dependent learning strategies. Unfortunately not much is known about the different modes

of action of *E.coli* and *S.typhimurium* LPS and studies are missing illuminating the influences on neuronal networks during the acute phase of inflammation. As described above for infections with *E.coli* or immune stimulation with *E.coli* LPS (Qin et al. 2007, Bossù et al. 2012, Valero et al. 2014), also infection with *Salmonella typhimurium* can induce long lasting neuroinflammation. Püntener and colleagues show a persistent production of IL-1β and IL-12 in the brain until three weeks after *S.typhimurium* infection (Püntener et al. 2012). However, a hint explaining the differences between the effects observed with *S. typhimurium* and *E.coli* LPS is given by an immunological study examining the role of different cytokine signaling cascades on the lethality linked to LPS types. While the deletion of TNF-α signaling leads to resistance against *E.coli* LPS induced lethality, the knockout mice still show sensitivity towards *S.typhimurium* LPS (Netea et al. 2001). On the other hand, mice with defective IL-1β and IL-18 signaling are completely protected against both types of LPS. These data propose a mainly TNF-α dependent induced inflammation via *E.coli* LPS and a mainly IL-1β and IL-18 dependent one with *S.typhimurium* LPS. Therefore, also studies discussing the effect of IL-1β and IL-18 on neuronal structure and function can be taken into account to understand the effect of *S.typhimurium* LPS treatment. Especially IL-1β came into focus in the field of neurodegeneration and systemic infection as master manipulator of neuroinflammation. In the healthy brain, the concentration of IL-1β is very low (Rothwell and Luheshi 2000). Upon insult, this cytokine is mostly produced by microglia but also astrocytes, neurons, infiltrating immune cells, oligodendrocytes and epithelial cells. While defective IL-1β signaling can impair synaptic plasticity and spatial learning, also a high concentration of IL-1β negatively affects neuronal signaling: Acute application of IL-1β prevents the induction of LTP in hippocampal slices (Ross et al. 2003). IL-1β application is sufficient to interfere with BDNF and neurotrophin-3 associated signaling transduction in cortical and hippocampal neurons (Soiampornkul et al. 2008) and with BDNF induced neuroplasticity in the hippocampus (Tong et al. 2008). Also hippocampus-dependent learning in the Morris water maze is completely prevented by systemic IL-1β application (Gibertini et al. 1995). It was further shown, that inhibition of IL-1 signaling circumvents damaging effects of systemic inflammation and that TNF-α signaling might not be required for neuroinflammation in certain scenarios. For instance, intrahippocampal administration of the IL-1 receptor antagonist IL-1RA prevents synaptic dysfunction and cognitive impairment in a mouse model of obesity (Erion et al. 2014). Also, blockade of circulating IL-1β was sufficient to rescue learning and memory deficits induced by a *Legionella pneumophila* infection (Gibertini et al. 1995).

Taken together these data make it tempting to speculate that the main difference between *E.coli* and *S.typhimurium* LPS indeed is a higher concentration of IL-1β with *S.typhimurium* LPS leading to a stronger inflammatory phenotype in the CNS, prolonged

activation of immune cells and a greater impact on neuronal signaling. However, this higher production of IL-1β which seems to be associated with the detrimental effects on neuronal morphology and function in aged mice is not sufficient to cause any long-term effects in adult, 4 months old mice in this study.

4.2. Peripheral immune stimulation with different LPS leads to an age-dependent activation of brain immune cells

While detrimental effects of a peripheral immune activation or infection on neuronal structure, synaptic plasticity and learning behavior are visible in aged rodents, younger individuals seem to be protected. The results presented in this thesis suggest a crucial role of the number and activation of microglia in aged, 16 months old mice. Already under baseline conditions, a higher activation of microglia, shown by a significantly lower number of primary processes was observed in aged mice. Interestingly, the number of microglia was not increased. Upon peripheral immune stimulation with either *E.coli* or *S.typhimurium* LPS an even stronger activation of microglia and macrophages is visible in the hippocampus of aged mice. Of note, *S.typhimurium* LPS led to an even more pronounced increase in microglia number and activation status. Unfortunately, it can only be speculated whether an initial increase of activation occurred in the acute phase of inflammation also in adult animals. However, there is no persistent activation of hippocampal microglia in adult mice. Although not tested in this study, the stronger activation of microglia seen in aged mice in this context is likely associated with a higher production of proinflammatory cytokines as demonstrated by Liu and colleagues (Liu et al. 2012).

Along with the data of this thesis, several other studies show differences in the CNS immune response of aged mice as well. Even despite the absence of a direct infection or inflammation to the CNS, the brain microglia have been shown to respond to a peripheral immune activation with the production of cytokines, chemokines and reactive nitrogen species similar to body macrophages and dendritic cells. Indeed, detecting peripheral inflammatory signals has been suggested to be an important feature of microglia (Nguyen et al. 2002). This inflammatory activation is normally transient and microglia go back to a resting state after the infection, injury or peripheral inflammation is overcome. This mechanism however, might be disturbed in the elderly. In fact, some markers of M1 microglia activation are up-regulated in mice and also in humans as consequence of normal aging. It has been found, that the expression of TLRs (Letiembre et al. 2007), MHC class II and CD11b (Morgan et al. 1999; Nicolle et al. 2001, Godbout et al. 2005) is enhanced in microglia of aged rodents. Also the astrocytic marker GFAP is up-regulated

(Godbout et al. 2005, Lee et al. 2000, Morgan et al. 1999). In response to an infection or a peripheral immune stimulus microglia and astrocytes of aged mice, 20 – 24 months of age, show a stronger and prolonged production of IL-1β and IL-6 and other proinflammatory mediators compared to young ones (Godbout et al., 2005; Barrientos et al., 2009a). And even more interestingly, this hyper reactive inflammatory response is restricted to the microglia/macrophages of the brain (Godbout et al., 2005; Barrientos et al., 2009a, 2015a).

Further studies show that the difference in microglia and astrocyte phenotype of young and aged mice mediates the deleterious actions of a systemic immune activation on neurons. While older, 12 months old rats exhibit high numbers of scavenger receptor $CD68^+$ and IL-$1\beta^+$ microglia 3 weeks after immune activation this phenotype could not be detected in 2 months old rats (Liu et al. 2012). Additionally, the impairment in LTP seen in that study was prevented upon microglia inhibition by systemic minocycline administration 10 days after the immune stimulation. Also injections of IL-1 receptor antagonist (IL-1RA) in the *cisterna magna* immediately prior to infection with *E.coli* abolished the significant lower theta burst induced L-LTP seen in aged mice, implying a critical role for cytokines such as IL-1β (Chapman et al. 2010). In aged rats, the production of IL-1β in response to *E.coli* infection was prolonged in comparison to younger animals. Interestingly, this effect was only observed in the hippocampus and led to disruption of hippocampus-dependent contextual fear conditioning (Barrientos et al. 2009) as long as IL-1β levels were elevated.

Taken together, the results of this study are in agreement with others showing that the proinflammatory status in the brain of aged mice seems to mediate the detrimental effects of a systemic inflammation.

Besides microglia and blood derived macrophages also astrocytes can contribute to an inflammatory environment in the brain. Astrocytes are the most abundant cell type in the CNS and alongside to their trophic support of neurons, they also are involved in protecting injured or infected areas of the brain by formation of a so called glial scar. Moreover, astrocytes are a prominent source of cytokines and chemokines. Especially after traumatic brain injury astrocytic production of proinflammatory mediators are associated with prolonged damage. After peripheral immune activation with *E.coli* LPS there is an increase in astrocytic NFκB activation with an activation peak 3 days after stimulation and a subsequent decline which was followed until day 16. Even though the astrocyte activation is still 1.5-fold increased and also apoptosis is still slightly elevated up to 2 weeks after stimulation, a further decrease to control conditions cannot be excluded (Fan et al. 2014). Other papers report an increase in astrocytes numbers and activation in a GFAP-reporter mouse with a peak at 6 hours after systemic LPS application declining to control conditions already after another 42 hours (Biesmans et al. 2013).

In the present study, I could not detect an increase in astrocyte numbers either in adult or in aged mice after peripheral immune stimulation. However, also here an upregulation in astrocytic activation markers shortly after the immune activation cannot be excluded. Interestingly, also upon ageing the basal number of astrocytes is not altered in the study presented here, making these cells less likely to be involved in an age-dependent vulnerability towards infection or systemic immune activation.

4.3. Long-term influences of a systemic immune activation on neuronal structure and signaling in the APP/PS1 mouse model of Alzheimer´s disease

AD is the most common cause of dementia in elderly people. During the disease progression, the death of neurons as well as the loss of synapses is strongly correlated with cognitive impairments. Pathological hallmarks of AD are the aggregation of amyloid-β peptide as byproduct of the amyloidogenic cleavage of the amyloid precursor protein into senile plaques and the abnormal intracellular aggregates of hyperphosphorylated forms of the microtubule-associated and stabilizing protein tau (Mandelkow and Mandelkow 1998). Several mouse models were designed featuring one or more pathological hallmarks already present in the young mouse.

In the present studies, I used the APP/PS1 mouse model reflecting the amyloid-portion of the AD pathology which is characterized by an increasing Aβ plaque load starting at about 6 months of age (Borchelt et al. 1997, Jankowsky et al. 2001) and resulting in a substantial plaque load in the hippocampus and cortex by 9 months (Jankowski et al. 2004) and a peak in plaque formation with 12 months of age (Garcia-Alloza et al. 2006). In addition, various studies show decreased numbers and altered morphology of dendritic spines in the hippocampus already in young adult APP/PS1 mice (Moolmann et al. 2004, Grutzendler et al. 2007, Kummer et al. 2011, Alonso-Nanclares et al. 2013, Heneka et al. 2013, Šišková et al. 2014). Further studies elucidate that an elevation in aggregated Aβ causes impairment in LTP (Nalbantoglu et al. 1997, Chapman et al. 1999, Kummer et al. 2011, Heneka et al. 2013). Deficits in hippocampus-dependent learning and memory start with 6 months of age and extent over the whole lifespan of the mice (Cao et al. 2007, Ding et al. 2008).

Along with this neurodegenerative phenotype, also neuroinflammation and changes in the CNS immune response are part of the AD pathology. It has been shown that in the brain of AD mouse models as well as in post mortem tissue of AD patients activated microglia, cytokines, chemokines and their receptors and astrogliosis is elevated (Cartier et al. 2005; Wyss-Coray 2006, Heneka and O´Banion 2007). Especially microglia surrounding Aβ plaques are positive for activation markers and pro-inflammatory mediators such as MHC

class II, Cox-2, MCP-1, TNF-a, IL-1β, and IL-6 (Akiyama et al. 2000, Glass et al. 2010). Thereby, the M1 activation of microglia mediated by TLR-, NLR- and RAGE-signaling further amplifies neurotoxic properties of Aβ deposits. Indeed, impairment in spatial learning and LTP of adult APP/PS1 mice is paralleled by increased expression of IL-1β (Gallagher et al. 2013, Kelly et al. 2013). Also, the administration of Aβ leads to LTP deficits and increased hippocampal IL-1β (Lyons et al., 2007). Furthermore, blockade of the IL-1 receptor improves hippocampus-dependent learning and memory in an animal model of AD (Kitazawa et al. 2011). And also the treatment of aged transgenic APP mice with minocycline to inactivate microglia rescued spatial learning (Fan et al., 2007).

But not only innate immunity of the brain contributes to AD pathology also systemic inflammation can drive neurodegeneration. Activation of the peripheral immune system caused by infection may be involved in the early stages of AD pathogenesis (Perry et al., 2007). And also simply the overproduction of inflammatory immune mediators as described for obesity and type 2 diabetes act as risk factors for AD (Granic et al. 2009, Jones et al. 2009). The peripheral immune stimulation with *E.coli* LPS also demonstrates a worsening of Aβ accumulation, tau pathology and even cognitive function in AD models (Qiao et al. 2001, Lee et al. 2010, Valero et al. 2014). Sheng and colleagues report higher numbers of activated microglia and astrocytes and higher levels of intracellular APP and Aβ in aged APP transgenic mice after 3 months of weekly LPS injections (Sheng et al. 2003).

The data described here show a reduction in dendritic complexity and spine density of cortical and hippocampal pyramidal neurons and granule cells of aged APP/PS1 mice 3 months after LPS *E.coli* or *S.typhimurium* treatment. Especially the phenotype seen in the dentate gyrus has not been observed in the aged WT mice. This is in agreement with a study by Valero and colleagues. Only 6 weeks after systemic LPS application, adult 3xTg AD mice show heavy impaired memory in the Morris water maze, decrease in synaptic markers and slight reduction in dendritic complexity of new born granule cells in the dentate gyrus (Valero et al. 2014). Of note, in the same study changes in granule cells complexity were not visible in WT controls.

Of course the study by Valero et al. (2014) emphasizes the differences between adult WT and AD mice. While I indeed could not find any differences in adult WT mice upon peripheral immune stimulation to the controls, adult APP/PS1 mice show decreased spine densities of the dentate gyrus granule cells 3 months after immune stimulation. Therefore, a higher sensitivity towards a systemic immune activation is also displayed here. Besides the changes in neuronal structure, also synaptic plasticity in aged APP/PS1 mice is altered. Here, the immune stimulation with either *E.coli* or *S.typhimurium* LPS leads to inhibition of LTP. This again is in contrast to the data on aged WT mice, which show no appreciable differences in neuronal signaling upon *E.coli* treatment. The differences

observed between WT and AD mice are likely mediated by a higher Aβ plaque load seen after peripheral immune activation (Qiao et al. 2001, Sheng et al. 2003, Lee et al. 2010). It is also tempting to speculate that the stronger production of inflammatory molecules in response to the peripheral insult may account for the differences in WT and AD mice. The primed status of microglia even in younger APP/PS1 might mediate this exaggerated response (Akiyama et al. 2000, Glass et al. 2010). Here, it is likely that, due to the pre-existing higher levels a threshold of pro-inflammatory mediators is even exceeded with the less potent *E.coli* LPS. However, also the involvement of peripheral immune cells cannot be excluded. Especially aged APP/PS1 mice show an enhanced pro-inflammatory profile of microglia and reduction of blood brain barrier integrity leading to enhanced immune cell recruitment into the CNS (Minogue et al. 2014). In this context, measuring the Aβ plaque load and the expression of inflammatory cytokines will be of extreme interest.

4.4. Long-term detrimental effects of a peripheral immune stimulation with LPS of *Salmonella typhimurium* are mediated by the NLRP3 inflammasome

The NOD-like receptor family, pyrin domain containing 3 (NLRP3) inflammasome is a multi protein complex catalyzing the maturation of the proinflammatory cytokines IL-1β and IL-18 in response to injury, infection or tissue damage. Components of the NLRP3 inflammasome are the cytoplasmic innate receptor NLRP3, the adaptor apoptosis-associated speck-like protein containing a CARD (ASC), and caspase-1. Both IL-1β and IL-18 are expressed as inactive precursor forms, pro-IL-1β and pro-IL-18 and require cleavage by activated caspase-1 for activation and secretion as mature cytokines. Besides in a scenario of infection or injury, also amyloid-β aggregates are able to activate the NLRP3 inflammasome (Halle et al. 2008). Direct brain injury or infection and also a peripheral immune stimulation with *E.coli* LPS can lead to high expression of all NLRP3 components (Zhang et al. 2014). And of course, the up-regulation of IL-1β and IL-18 in response to peripheral immune activation gives indirect evidence for the involvement of NLRP3 inflammasome in the several detrimental effects on neuronal function (Gibertini et al. 1995, Soiampornkul et al. 2008, Tong et al. 2008). It was further shown that NLRP3 deficiency can indeed prevent AD related pathology in the APP/PS1 model (Heneka et al. 2013). Here, reduced spine density in CA1 apical dendrites, impaired LTP and learning and memory deficits in the Morris water maze task were rescued in the APP/PS1/Nlrp3$^{-/-}$ mice. Furthermore, the phagocytic capacity of microglia was enhanced while the burden of amyloid β plaques was reduced. These data show a rescue of the Aβ mediated neurodegeneration in the absence of the NLRP3 inflammasome. In this thesis, I examined whether NLRP3 deficiency is also beneficial in the context of a systemic immune

activation and whether *Salmonella typhimurium* LPS leads to reduced neuronal complexity and plasticity in an inflammasome dependent manner. Surprisingly, the initial response to *S.typhimurium* LPS injection of the aged NLRP3 KO mice is not different from aged WT mice. NLRP3 KO mice show a similar body weight loss and an equivalent mortality rate of about 17% after immune stimulation with *S.typhimurium* LPS. Nevertheless, like the WT also the NLRP3 KO mice recovered and showed no sickness behavior or differences in body weight compared to control mice 3 months after immune stimulation. This initial sickness behavior of NLRP3 KO similar to WT mice suggests that other pro-inflammatory cytokines such as TNF-α mediate the peripheral immune activation and that inhibition of IL-1β and IL-18 signaling does not prevent LPS *S.typhimurium* induced lethality and immune activation as claimed by Netea and colleagues described above (Netea et al. 2001).

Nevertheless, the neuronal phenotype 3 months after immune stimulation indeed shows protection of NLRP3 KO mice against *S.typhimurium* LPS: The cortical as well as hippocampal excitatory neurons of NLRP3 KO show dendritic complexity similar to the control after the peripheral immune stimulation. In the CA1 basal compartment, even a slight increase is visible. Also the spine density in dentate gyrus and cortex layer II/III are comparable in NLRP3 KO controls and LPS stimulated mice. Solely the CA1 basal spine density is still decreased after peripheral immune activation. However, the absolute number of spines in the basal compartment is most likely not altered due to the increase in dendritic complexity.

In addition to the neuronal structure also the synaptic plasticity is restored in NLRP3 KO mice. There are no alterations in basal synaptic transmission, paired pulse facilitation and LTP 3 months after peripheral administration of *S.typhimurium* LPS. In a way the immune response and the observations made in the CNS of the aged, 16 months old NLRP3 KO mice resemble those of adult, 4 months old mice.

Although the activation of microglia and astrocytes as well as the production of pro-inflammatory cytokines was not quantified in this study, the data suggest that indeed higher IL-1β or IL-18 levels and stronger pro-inflammatory activation of microglia in aged WT mice is responsible for decreased neuronal dendritic complexity and LTP upon LPS *S.typhimurium* treatment. Even though at first glance, the neurodegenerative pathology of APP/PS1 mice seems quite different from the effects of a systemic immune activation only with a bacterial cell wall component, the data in this thesis partially support the hypothesis of a generalized detrimental function to IL-1β and IL-18 signaling in the context of neuroinflammation.

4.5. Long-term detrimental effects of a peripheral immune stimulation with PGN/LTA

Sepsis is a complex inflammatory response of the host's immune system to virulence factors like endotoxins. Until two decades ago, sepsis and septic shock as a multi-step inflammatory reaction was considered to be specific for Gram negative bacteria (Parrillo et al. 1990). Today we know, that most cases of sepsis are actually caused by Gram positive bacteria with the most prominent representatives *Stapylococcus aureus*, *Streptococcus pyogenes*, *Pseudomonas aeruginosa* and *Klebsiella spp.* (Martin et al. 2003). Especially *Staphylococcus aureus* came into focus in the context of nosocomial infections. However, studies with Gram positive bacteria or Gram positive bacterial endotoxins in the context of sepsis induced encephalopathy and neuroinflammation are still the exception.

Therefore, LPS is still the best described endotoxin and LPS injections serve as a model for systemic infections, sepsis and also neuroinflammation. Sepsis caused by Gram positive bacteria is mediated by the two major components of the gram-positive cell wall peptidoglycan (PGN) and lipoteichoic acid (LTA). In contrast to LPS, the recognition of LTA and PGN is mediated by TLR2, LBP, and CD14, whereas TLR-4 and MD-2 are not involved (Schröder et al. 2003). As major difference between TLR4 and TLR2 signaling, TLR2 binding leads to NFκB activation in the classical MyD88-dependent pathway and inhibits the TRIF-dependent signaling pathway (Akira and Takeda 2004).

Whether purified LTA and PGN can cause LPS-comparable immune response is still a matter of debate. On the one hand, it has been shown that both LTA and PGN are able to induce expression of IL-1, IL-6, TNFα and production of nitric oxide when given to macrophages *in vitro* and *in vivo* (Kengatharan et al 1996). In contrast, 10 µg/ml of LTA or PGN are sufficient to induce TNF-α production but fail to activate iNOS in mouse macrophages (Paul-Clark et al. 2006). A different study shows that GFAP, CD11b, MHC class II but not CD68 are highly expressed 2 days after intravenous administration of 20 µg/g LTA in the rat pineal gland (Jiang-Shieh et al. 2005). Furthermore, it has been hypothesized that only when acting together LTA and PGN can cause septic shock and organ toxicity already 6 hours after i.v. application in rats at doses of 10 µg/g and 3 µg/g, respectively (De Kimpe et al. 1995). Another study demonstrates that the magnitude of the inflammatory reaction towards Gram positive bacteria seems to be smaller than the LPS induced one (Abe et al. 2010). On the other hand, Hessle and colleagues found that Gram positive bacteria can induce expression of IL-1β, IL-6, IL-8 and TNF-α equally strong than Gram negative bacteria in human monocytes culture. However, the application of LTA and PGN alone failed to generate this strong response (Hessle et al. 2005). Another study could not find any signs of TLR2 activation with either LTA or PGN or in combination (LaFlamme et al. 2001). Systemic PGN has even been reported to

abolish the neuroinflammatory microglia phenotype induced by LPS (LaFlamme et al. 2003). Critical for the successful immune activation with PGN seems to be the purification method (Hanke and Kielian 2012). As PGN contains mainly sugars and amino acids which are also present or closely related to the ones found in mammals, possibly the structure of these cell wall component is of most relevance.

The presented body weight data here demonstrate that indeed PGN/LTA application does not provoke sickness behavior comparable to LPS in adult or aged WT mice. Also in the brain, 3 months after the peripheral application of PGN/LTA there is no change in the number or morphology of astrocytes and microglia. Yet, data on CNS immune cell activation are missing for time points during or shortly after immune stimulation. And still a pro-inflammatory activation status of microglia and astrocytes cannot be excluded, as besides the number and morphology of microglia no other immune relevant marker was quantified here. In addition to that, also the correlation between microglia morphology and activation status and function has recently been questioned (Kettenmann 2011; Tremblay and Sierra 2014) and a subtle but chronic production of pro-inflammatory cytokines might not be associated with altered microglia morphology in the presented scenario. Therefore, the question of whether PGN and LTA are able to induce LPS-comparable neuroinflammation is still unanswered.

Without doubt, in contrast to the wealth of experiments using LPS, not much is known about the influence of PGN/LTA or Gram positive bacteria mediated immune stimulation on neurons or glial cells of the CNS. More precisely, the influence of the application of Gram positive endotoxins on neuronal architecture or synaptic plasticity in rodents has not been addressed. Results from this study show that peripheral application of PGN/LTA does not cause long-term effects on neuronal morphology in adult mice. Neither in the cortex nor in the hippocampus a difference in dendritic complexity or spine density could be observed upon immune stimulation. In aged 19 months mice however, the neuronal phenotype 3 months after PGN/LTA treatment is comparable to the stimulation with LPS of *Salmonella typhimurium*. Especially in the cortex layer II/III, pyramidal neurons exhibit dramatic decrease in dendritic complexity and spine density. But also the apical CA1 dendrites and the basal CA1 spine density is negatively affected. In the dentate gyrus, the absolute number of synapses is probably not changed as dendritic complexity is increased while spine density is decreased.

LTP of the Schaffer collateral is mildly but significantly reduced upon PGN/LTA treatment. In contrast to the stimulation with *S.typhimurium* LPS there are no changes in the escape latency during the Morris water maze task. But indeed, also the use of hippocampus-dependent strategies is heavily impaired. Therefore, the only difference between a systemic immune activation with *S.typhimurium* LPS and PGN/LTA is the absence of an obvious immune activation of microglia in the latter.

Interestingly, also the APP/PS1 mice show a stronger sensitivity towards this unconventional immune stimulation. Here, in particular the CA1 apical compartment and the dentate gyrus granule cells show a stronger decrease in spine density than the aged WT mice. This is associated with a more intense impairment in LTP, although basal synaptic transmission is enhanced in comparison to control APP/PS1 mice. The impact on hippocampus-dependent learning and microglial activation was not examined in this study. Therefore, one can only speculate whether the AD mice show an immune activation in the brain different from WT mice after immune stimulation. Also the involvement of peripheral immune cells is possible. It was shown, that an enhanced pro-inflammatory profile of microglia of aged APP/PS1 mice along with disruption of blood brain barrier integrity promotes immune cell recruitment into the CNS diminishing neuroprotective and promoting neurodegenerative mechanisms (Minogue et al. 2014). Similar to the LPS model, also with PGN/LTA stimulation, even the adult APP/PS1 mice show slight alterations in neuronal morphology. Noteworthy, here again the spine density of the granule cells is remarkably decreased. But also in the adult APP/PS1 mice a quantification of the peripheral as well as the brain immune response will be necessary to understand the underlying mechanisms.

In summary, here for the first time age-dependent alterations in neuronal structure and signaling were reported for a model of Gram positive induced immune activation. The effects were intensified in the APP/PS1 mouse model for Alzheimer´s disease.

4.6. Chronic infection with *Toxoplasma gondii* causes changes in neuronal structure

The protozoan parasite *Toxoplasma gondii* (*T.gondii*) can infect a wide range of warm-blooded animals and based on seroprevalence data about 30 to 70% of the human population is infected showing a high geographical variety (Parlog et al. 2015). Infections with *T.gondii* can be asymptomatic as well as severe if it comes to eye and brain infections. Even after the acute phase, *T.gondii* remains within the host over its whole lifespan, thanks to adequate immune functions, usually unnoticed. In immunocompromised patients however, *T.gondii* infection can cause life-threatening encephalitis.

Today we know, that even in immune competent people *Toxoplasma gondii* causes subtle neurological and behavioral changes promoting mental disorders including depression and schizophrenia (Flegr 2007, Webster 2007). Also in rodents, infection with *T.gondii* leads to elaborated behavioral changes manifesting in a more curios and active behavior (Hay et al. 1985, Webster et al. 1994) and infected animals lose their innate fear of feline

odors (Berdoy et al. 2000). Even though some studies already suggest a contribution of low-level inflammation (Hermes et al. 2008), neurotransmitter imbalance (Gatkowska et al. 2012) or dopamine overproduction (Prandovszky et al. 2011), underlying mechanisms are still far from unraveled. In particular, the impact of chronic *Toxoplasma gondii* infection on neuronal architecture and signaling has not been explored yet.

In this study, the architecture of excitatory neurons of cortex layer II/III, the CA1 area and dentate gyrus of the hippocampus as well as of inhibitory medium spiny neurons of the striatum were examined 8 weeks after infection with *T.gondii*. In the hippocampus, CA1 pyramidal neurons and granule cells of the dentate gyrus show a significant reduction in dendritic complexity. Also the striatal medium spiny neurons exhibit a mild decrease in dendritic branches. In cortex layer II/III, pyramidal neurons display a significant reduction of intersections in the Sholl analysis of basal dendrites. The apical dendrites show only a slight reduction. Here, however additionally the spine density was dramatically reduced. It was further shown that the levels of synaptophysin and PSD95 are significantly reduced in cortex and hippocampus. But besides high numbers of astrocytes, activated microglia, T cells and scattered spots of apoptosis neurodegeneration was surprisingly low (Parlog 2015). Therefore, activation of brain resident as well as peripheral immune cells contributes to the decreased neuronal complexity without promoting neuronal death.

The distribution of *T.gondii* tissue cysts is usually very low in rodents and no preference for a specific brain area can be identified (Gulinello et al. 2010). In the same infection model as used for the analysis of neuronal morphology, likewise a random distribution of *T. gondii* cysts was observed with 6 to 10 parasite cysts within the cortex and 1 to 2 cysts within the hippocampus per 500 µm transversal brain slice (Parlog 2015). Even though this relatively low concentration of *T.gondii* tissue cysts was found in infected animals, a strong sickness behavior of the infected mice was noticeable 8 weeks after infection. This is line with other studies of C57Bl/6 mice chronically infected with *T.gondii*. In the genetically highly susceptible C57Bl/6 mice chronic type II ***T.gondii*** infections invariably cause lethal toxoplasmic encephalitis (Gigley et al. 2009). Therefore, it is not surprising that C57Bl/6 mice show other behavioral alterations besides the *T.gondii* specific loss of fear from cat odors. Gatkowska and colleagues report a decrease in locomotion, grooming and open field exploration associated with a progressive body weight loss in chronically *T.gondii* infected C57Bl/6 mice (Gatkowska et al. 2012). Interestingly, even though *T.gondii* tissue cysts are evenly distributed in brains of C57Bl/6 mice, the genetically resistant BALB/c mice show a twofold increase in tissue cysts in the amygdala (Vyas et al. 2007), which is important for memory of fear and emotional events and which might explain behavioral differences between the two mice strains. Unfortunately, data regarding body weight loss, food intake, exploration and locomotion activity are not provided in this study. But indeed, the phenotype observed in C57Bl/6 chronically infected with *T.gondii*

might rather resemble the *T.gondii* infection of immunocompromised patients than the latent unnoticed infection of healthy individuals. Therefore, changes in synaptic markers and neuronal structure shown in this thesis are more likely consequence of the chronic immune activation inevitably leading to death rather than a direct effect of the pathogen on single neurons.

The latent *T.gondii* infections of BALB/c mice would probably cause even smaller and less obvious changes within neuronal networks and provide a *T.gondii* specific mechanism besides the pro-inflammatory activation of brain resident immune cells. But most likely also there the immune response within the CNS and the recruitment of peripheral immune cells would play a pivotal role.

4.7. Conclusions and outlook

In this thesis, I could show that neuronal structure and function can be modified by the CNS infection with *T.gondii* as well as by the systemic innate immunity activated by different bacterial endotoxins. In contrast to the majority of studies in the field of neuroinflammation and neurodegeneration, here influences of an immune stimulation or infection were examined long after the acute phase of immune activation was over come. Thereby, it became obvious that a peripheral immune activation with different bacterial endotoxins failed to induce long-term changes in adult mice. However, direct CNS infection as displayed by the parasite *T.gondii* is sufficient to influence neurons also in young adult mice. Here, the chronic infection of C57Bl/6 with *T.gondii* leads to a cell type and brain region unspecific reduction in neuronal complexity. Changes in neuronal structure are most likely caused by the pro-inflammatory activation of microglia and astrocytes as well as peripheral immune cells as shown by Parlog 2015. As C57Bl/6 mice resemble a genetically sensitive mouse strain for chronic *T.gondii* infection, the data obtained here most likely give insight into the situation seen in immunocompromised patients developing toxoplasmic encephalitis. It would be very interesting to examine the effects of a chronic *T.gondii* infection in a genetically resistant model as the BALB/c mouse which could provide insight into the mechanisms underlying the latent infection as seen in a great proportion of the human population.

In contrast to the direct CNS infection, activation of the peripheral immune system alone shows detrimental effects on structure and function of hippocampal and cortical neurons only in aged, 16 months old WT mice. The reason for this might be a prolonged activation of microglia due to age-dependent priming of these brain macrophages. Furthermore, I could demonstrate that LPS of *E.coli* although it is the endotoxin used predominantly to establish neuroinflammation and investigate the connection between the peripheral immune system and CNS function, failed to induce appreciable long-term changes even in aged WT mice.

Immune stimulation with *Salmonella typhimurium* LPS however leads to decreased neuronal complexity and spine density accompanied with impairment in Schaffer collateral LTP and spatial learning in the Morris water maze. An even stronger activation of microglia as displayed here and a stronger production of IL-1β and IL-18 (Netea et al. 2001) might account for this phenomenon. This hypothesis could be partially confirmed by experiments with NLRP3 knockout animals. The genetic ablation of the NLRP3 inflammasome and therefore the maturation of IL-1β and IL-18 prevented reduction in dendritic complexity and spine density as well as it rescued the impairment in LTP upon immune stimulation with *S.typhimurium* LPS in aged mice. However, further experiments are necessary to verify the important role of IL-1β in the described scenario. As obvious

step, it is needed to quantify the activation of microglia and astrocytes during the time course of immune stimulation. In addition, a more detailed description of the activation phenotype of the CNS immune cells is necessary to draw conclusions about their actual function. Immune activation markers as CD11b, CD68, MHC class II, Cox-2, MCP-1, TNF-a, IL-1β, IL-6, IL-18 are only some to mention here. And of course, the upregulation of NLRP3 inflammasome components as caspase-1, NLRP3 and ASC has to be shown.

As the immune activation paradigm used in this thesis resembles the situation of sepsis-recovery, further long-term studies with prolonged but low doses of endotoxins could shed light on the mechanisms seen in patients with type 2 diabetes, severe obesity or atherosclerosis. The influence seen after chronic overproduction of proinflammatory mediators without life-threatening upregulation of the peripheral immune system could display a completely different danger for the CNS. In line with this, for a convincing role of solely the peripheral immune system, the integrity of the blood brain barrier in all genotypes and age groups needs proof.

One important finding during my investigations was that also the immune stimulation with endotoxins of the Gram positive bacterial cell wall can lead to a neurodegenerative phenotype in aged WT mice. So far, neither the neuronal structure nor synaptic plasticity and hippocampus-dependent learning were investigated after peripheral application of PGN and LTA from *Staphylococcus aureus*. As the majority of sepsis cases are caused by Gram positive bacteria and as *S.aureus* gained notoriety in the context of nosocomial infections, the development of a suitable model for these diseases is more than overdue. In this study, I could demonstrate that the outcome of a peripheral immune activation with PGN/LTA shows remarkable similarity with the one of *S.typhimurium* LPS. First, it has to be confirmed, that PGN/LTA leads to peripheral immune activation and actually can cause neuroinflammation as studies are not in agreement concerning this question so far. Further, similarities in the mode of action between *Salmonella typhimurium* LPS and PGN/LTA of *Staphylococcus aureus* might provide information about how sepsis, severe bacteraemia, septic shock, type 2 diabetes, obesity or periodontitis can all promote neurodegeneration.

5. REFERENCES

Abbott NJ, Rönnbäck L, Hansson E, Astrocyte-endothelial interactions at the blood-brain barrier, Nat Rev Neurosci. 2006; 7(1): 41 - 53

Abe R, Oda S, Sadahiro T, Nakamura M, Hirayama Y, Tateishi Y, Shinozaki K, Hirasawa H. Gram-negative bacteremia induces greater magnitude of inflammatory response than Gram-positive bacteremia. Crit Care. 2010; 14:R27

Abraham WC, How long will long-term potentiation last? Philos. Trans. R. Soc. Lond. B Biol. Sci. 2003; 358: 735 – 744

Akira S, Takeda K, Toll-like receptor signaling, *Nat Rev Immunol* 2004; 4: 499 – 511

Akira S, Uematsu S, Takeuchi O, Pathogen recognition and innate immunity, Cell. 2006; 124(4): 783 - 801

Akiyama H, Barger S, Barnum S, Bradt B, Bauer J, Cole GM, Cooper NR, Eikelenboom P, Emmerling M, Fiebich BL, Finch CE, Frautschy S, Griffin WS, Hampel H, Hull M, Landreth G, Lue L, Mrak R, Mackenzie IR, McGeer PL, O'Banion MK, Pachter J, Pasinetti G, Plata-Salaman C, Rogers J, Rydel R, Shen Y, Streit W, Strohmeyer R, Tooyoma I, Van Muiswinkel FL, Veerhuis R, Walker D, Webster S, Wegrzyniak B, Wenk G, Wyss-Coray T.Inflammation and Alzheimer's disease, Neurobiol. Aging. 2000; 21: 383 – 421

Alonso-Nanclares L, Merino-Serrais P, Gonzalez S, DeFelipe J, Synaptic changes in the dentate gyrus of APP/PS1 transgenic mice revealed by electron microscopy, J Neuropathol Exp Neurol. 2013; 72(5): 386 - 95

Alvarez P, Zola-Morgan S, Squire LR, The animal model of human amnesia: long-term memory impaired and short-term memory intact, Proc Natl Acad Sci U S A. 1994; 91(12): 5637 - 41

Alzheimer A, Stelzmann RA, Schnitzlein HN, Murtagh FR, An English translation of Alzheimer's 1907 paper, "Über eine eigenartige Erkankung der Hirnrinde" Clin Anat. 1995; 8: 429 – 31

Amor S, Peferoen LA, Vogel DY, Breur M, van der Valk P, Baker D, van Noort JM, Inflammation in neurodegenerative diseases: an update, Immunology. 2014; 142(2): 151 - 66

Anderson KV and Nüsslein-Volhard C Dorsal-group genes of Drosophila, In Gametogenesis and the Early Embryo, J. Gall, ed. (New York: Alan R. Liss, Inc.), 1986: 177 - 194

Angus DC, Linde-Zwirble WT, Lidicker J, Clermont G, Carcillo J and Pinsky MR, Epidemiology of severe sepsis in the United States: analysis of incidence, outcome, and associated costs of care, Critical Care Medicine, 2001; 29(7): 1303 – 1310

Arai A, Black J, Lynch G, Origins of the variations in long-term potentiation between synapses in the basal versus apical dendrites of hippocampal neurons, Hippocampus 4 1994*:* 1–9

Arai K, Matsuki N, Ikegaya Y, Nishiyama N, Deterioration of spatial learning performances in lipopolysaccharide-treated mice, Jpn J Pharmacol 2001; 87:195 – 201

Astiz M, Saha D, Lustabader D, Monocyte response to bacterial toxins, expression of surface receptors and release of anti-inflammatory cytokines during sepsis. J Lab Clin Med 1996; 128: 584 – 600

Avital A, Goshen I, Kamsler A, Segal M, Iverfeldt K, Richter-Levin G, Yirmiya R, Impaired interleukin-1 signaling is associated with deficits in hippocampal memory processes and neural plasticity, Hippocampus. 2003; 13(7): 826 – 34

Back MR, Sarac TP, Moldawer LL, Welborn MB 3rd, Seeger JM, Huber TS, Laparotomy prevents lethal endotoxemia in a murine sequential insult model by an IL-10-dependent mechanism, Shock. 2000; 14(2): 157 - 162

Barrientos RM, Higgins EA, Biedenkapp JC, Sprunger DB, Wright-Hardesty KJ, Watkins LR, Rudy JW, Maier SF, Peripheral infection and aging interact to impair hippocampal memory consolidation, Neurobiol Aging. 2006; 27(5): 723 - 32

Barrientos RM, Frank MG, Hein AM, Higgins EA, Watkins LR, Rudy JW, Maier SF, Time course of hippocampal IL-1 beta and memory consolidation impairments in aging rats following peripheral infection. Brain Behav Immun 23 2009a: 46–54

Barrientos RM, Thompson VM, Arnold TH, Frank MG, Watkins LR, Maier SF, The role of hepatic and splenic macrophages in E. coli-induced memory impairments in aged rats, Brain Behav Immun 2015a; 43: 60 – 67

Beach TG, Walker R, McGeer EG, Patterns of gliosis in Alzheimer's disease and aging cerebrum, Glia 1989; 2(6): 420 – 36

Bear MF, Malenka RC, Synaptic plasticity: LTP and LTD, Curr Opin Neurobiol. 1994; 4(3): 389 - 99

Bellinger FP, Madamba S, Siggins GR, Interleukin-1β inhibits synaptic strength and long-term potentiation in the rat CA1 hippocampus. Brain Res 1993; 628: 227 – 234

Berdoy M, Webster JP, Macdonald DW, Fatal attraction in rats infected with *Toxoplasma gondii.* Proc. Biol. Sci. 2000; 267: 1591 – 1594

Bertram L, Tanzi RE, The genetic epidemiology of neurodegenerative disease, J Clin Invest. 2005; 115(6): 1449 – 1457

Biesmans S, Meert TF, Bouwknecht JA, Acton PD, Davoodi N, De Haes P, Kuijlaars J, Langlois X, Matthews LJ, Ver Donck L, Hellings N, Nuydens R, Systemic immune activation leads to neuroinflammation and sickness behavior in mice, Mediators Inflamm. 2013; 2013: 271359

Blackwell TS, Christman JW, Sepsis and cytokines: current status, Br J Anaesth. 1996; 77(1): 110 - 117

Blanchard V, Moussaoui S, Czech C, Touchet N, Bonici B, Planche M, Canton T, Jedidi I, Gohin M, Wirths O, Bayer TA, Langui D, Duyckaerts C, Tremp G, Pradier L, Time sequence of maturation of dystrophic neurites associated with Aβ deposits in APP/PS1 transgenic mice," Experimental Neurology, 2003; 184(1): 247 – 263

Bliss TV, Collingridge GL, A synaptic model of memory: long-term potentiation in the hippocampus, Nature. 1993; 361(6407): 31 - 39

Bliss TV, Gardner-Medwin AR, Long-lasting potentiation of synaptic transmission in the dentate area of the unanaestetized rabbit following stimulation of the perforant path, J Physiol. 1973; 232(2): 357 - 374

Bliss TVP, Lømo T, Long-lasting potentiation of synaptic transmission in the dentate area of the anaesthetized rabbit following stimulation of the perforant path**,** J Physiol. 1973; 232(2): 331 – 356

Block ML, Zecca L, Hong JS, Microglia-mediated neurotoxicity: uncovering the molecular mechanisms. Nat Rev Neurosci 2007; 8(1): 57 – 69

Bogdan C, Nathan C, Modulation of macrophage function by transforming growth factor b, interleukin-4, and interleukin-10. Ann N Y Acad Sci 1993; 685:713 – 739

Bone RC, Balk RA, Cerra FB, Definitions for sepsis and organ failure and guidelines for the use of innovative therapies in sepsis, The ACCP/SCCM Consensus Conference Committee, American College of Chest Physicians/Society of Critical Care Medicine, Chest, 1992; 101(6): 1644 – 1655

Boothroyd JC, E Grigg ME, Population biology of Toxoplasma gondii and its relevance to human infection: do different strains cause different disease? Current Opinion in Microbiology 2002; 5: 438 – 442

Borchelt DR, Ratovitski T, van Lare J, Lee MK, Gonzales V, Jenkins NA, Copeland NG, Price DL, Sisodia SS, Accelerated amyloid deposition in the brains of transgenic mice coexpressing mutant presenilin 1 and amyloid precursor proteins, Neuron 1997; 19(4): 939 – 945

Bossù P, Cutuli D, **Palladino I**, **Caporali P**, **Angelucci F**, **Laricchiuta D**, **Gelfo F**, **De Bartolo P**, **Caltagirone C, Petrosini L,** A single intraperitoneal injection of endotoxin in rats induces long-lasting modifications in behavior and brain protein levels of TNF-α and IL-18, **Journal of Neuroinflammation** 2012; 9:101

Bourne J, Harris KM, Do thin spines learn to be mushroom spines that remember? Current Opinion in Neurobiology
2007; 17: 1 – 6

Bowie A, O'Neill LA The interleukin-1 receptor/Toll-like receptor superfamily: signal generators for pro-inflammatory interleukins and microbial products. Journal of Leukocyte Biology 2000; 67(4): 508 - 514

Braak H, Braak E, Demonstration of amyloid deposits and neurofibrillary changes in whole brain sections, Brain Pathol. 1991; 1(3): 213 - 216

Braak H, Braak E, [Morphological changes in the human cerebral cortex in dementia], J Hirnforsch. 1991; 32(3): 277 - 282

Breuillé D, Farge MC, Rosé F, Arnal M, Attaix D, Obled C, Pentoxifylline decreases body weight loss and muscle protein wasting characteristics of sepsis, Am J Physiol. 1993 Oct;265(4 Pt 1): E660 - 6

Bsibsi M, Nomden A, van Noort JM, Baron W, Toll-like receptors 2 and 3 agonists differentially affect oligodendrocyte survival, differentiation, and myelin membrane formation, J Neurosci Res. 2012; 90(2): 388 - 98

Cannon JG, Tompkins RG, Gelfand J, Michie HR, Stanford GG and van der Meer JW, **Circulating interleukin-1 and tumour necrosis factor in septic shock and endotoxin fever, The Journal of Infectious Diseases 02/1990; 161(1): 79 - 84.**

Cao D, Lu H, Lewis TL, Li L, Intake of sucrose-sweetened water induces insulin resistance and exacerbates memory deficits and amyloidosis in a transgenic mouse model of Alzheimer disease. J. Biol. Chem. 2007; 282: 36275 – 36282

Carson MJ, Thrash CJ, Walter B, The cellular response in neuroinflammation: The role of leukocytes, microglia and astrocytes in neuronal death and survival, Clin Neurosci Res. 2006; 6(5): 237 – 245

Cartier L, Hartley O, Dubois-Dauphin M, Krause KH, Chemokine receptors in the central nervous system: role in brain inflammation and neurodegenerative diseases, Brain Res Brain Res Rev. 2005; 48(1): 16 - 42

Cerajewska TL, Davies M, West NX, Periodontitis: a potential risk factor for Alzheimer's disease, British Dental Journal 2015; 218: 29 - 34

Chapman PF, White GL, Jones MW, Cooper-Blacketer D, Marshall VJ, Irizarry M, Younkin L, Good MA, Bliss TV, Hyman BT, Younkin SG, Hsiao KK, Impaired synaptic plasticity and learning in aged amyloid precursor protein transgenic mice, Nat Neurosci. 1999; 2(3): 271 – 276

Chapman TR, Barrientos RM, Ahrendsen JT, Maier SF, Patterson SL, Synaptic correlates of increased cognitive vulnerability with aging: peripheral immune challenge and aging interact to disrupt theta-burst late-phase long-term potentiation in hippocampal area CA1, J Neurosci. 2010; 30(22): 7598 - 603

Chen J, Buchanan JB, Sparkman NL, Godbout JP, Freund GG, Johnson RW, Neuroinflammation and disruption in working memory in aged mice after acute stimulation of the peripheral innate immune system. Brain Behav Immun. 2008; 22(3): 301-11

Chishti MA, Yang DS, Janus C, Phinney AL, Horne P, Pearson J, Strome R, Zuker N, Loukides J, French J, Turner S, Lozza G, Grilli M, Kunicki S, Morissette C, Paquette J, Gervais F, Bergeron C, Fraser PE, Carlson GA, George-Hyslop PS, Westaway D, Early-onset amyloid deposition and cognitive deficits in transgenic mice expressing a double mutant form of amyloid precursor protein 695," The Journal of Biological Chemistry 2001; 276(24): 21562 – 21570

Chung IY, Benveniste EN, Tumor necrosis factor-alpha production by astrocytes. Induction by lipopolysaccharide, IFN-gamma, and IL-1 beta, J Immunol. 1990; 144(8): 2999 - 3007

Clarke LE, Barres BA, Emerging roles of astrocytes in neural circuit development, Nat.Rev.Neurosci. 2013; 14(5): 311 - 321

Collingridge GL, The induction of N-methyl-D-aspartate receptor-dependent long-term po-tentiation, Philos Trans R Soc Lond B Biol Sci. 2003; 358(1432): 635 – 641

Collingridge GL, Isaac JT, Wang YT, Receptor trafficking and synaptic plasticity, Nat Rev Neurosci. 2004; 5(12): 952 - 62

Commins S, O'Neill LA, O'Mara SM, The effects of the bacterial endotoxin lipopolysaccharide on synaptic transmission and plasticity in the CA1-subiculum pathway in vivo, Neuroscience 2001; 102:273–280.

Cooney R, Kimball SR, Eckman R, Maish G 3rd, Shumate M, Vary TC, TNF-binding protein ameliorates inhibition of skeletal muscle protein synthesis during sepsis, Am J Physiol. 1999; 276(4 Pt 1): E611-9

Cunningham AJ, Murray CA, O'Neill LA, Lynch MA, O'Connor JJ, Interleukin-1 beta (IL-1 beta) and tumour necrosis factor (TNF) inhibit long-term potentiation in the rat dentate gyrus in vitro, Neurosci Lett. 1996; 203(1): 17-20

Czapski GA, Gajkowska B, Strosznajder JB, Systemic administration of lipopolysaccharide induces molecular and morphological alterations in the hippocampus, Brain Res. 2010; 1356: 85 - 94

Debanne D, Guérineau NC, Gähwiler BH, Thompson SM, Paired-pulse facilitation and depression at unitary synapses in rat hippocampus: quantal fluctuation affects subsequent release, J Physiol. 1996; 491(Pt 1): 163 – 176

De Kimpe SJ, M Kengatharan M, Thiemermann C and Vane JR, The cell wall components peptidoglycan and lipoteichoic acid from Staphylococcus aureus act in synergy to cause shock and multiple organ failure, Proc Natl Acad Sci U S A. 1995; 92(22): 10359 – 10363

del Río-Hortega P, Microglia, Cytology and Pathology of the Nervous System 2 1932: 482 - 534

del Río-Hortega P, Estudios sobre la neuroglia. La microglía y su transformación en células en bastoncito y cuerpos gránulo-adiposos: [Madrid].

Deng W, Aimone JB, Gage FH, New neurons and new memories: how does adult hippocampal neurogenesis affect learning and memory? Nature Reviews Neuroscience 2010; 11: 339 - 350

Devanand DP, Jacobs DM, Tang MX, Del Castillo-Castaneda C, Sano M, Marder K, Bell K, Bylsma FW, Brandt J, Albert M, Stern Y, The course of psychopathologic features in mild to moderate Alzheimer disease, Arch Gen Psychiatry. 1997 54(3): 257 - 63

DiCarlo G, Wilcock D, Henderson D, Gordon M, Morgan D, Intrahippocampal LPS injections reduce Abeta load in APP+PS1 transgenic mice, Neurobiol Aging. 2001; 22(6): 1007 - 12

Di Filippo M, Chiasserini D, Gardoni F, Viviani B, Tozzi A, Giampà C, Costa C, Tantucci M, Zianni E, Boraso M, Siliquini S, de Iure A, Ghiglieri V, Colcelli E, Baker D, Sarchielli P, Fusco FR, Di Luca M, Calabresi P, Effects of central and peripheral inflammation on hippocampal synaptic plasticity, Neurobiology of Disease 52; 2013: 229 – 236

Dinarello CA Interleukin-1 and Interleukin-1 Antagonism, Blood,1991; 77(8): 1627 - 1652

Ding Y, Qiao A, Wang Z, Goodwin JS, Lee ES, Block ML, Retinoic acid attenuates beta-amyloid deposition and rescues memory deficits in an Alzheimer's disease transgenic mouse model. J. Neurosci. 2008; 28: 11622 – 11634

Dubey JP, Miller NL, Frenkel JK, Toxoplasma gondii life cycle in cats, J Am Vet Med Assoc. 1970; 157(11): 1767 - 70

Dudek SM, Bear MF, Homosynaptic long-term depression in area CA1 of hippocampus and effects of N-methyl-D-aspartate receptor blockade, Proc Natl Acad Sci U S A. 1992; 89(10): 4363 - 4367

Eichenbaum H, Hippocampus: cognitive processes and neural representations that underlie declarative memory, Neuron. 2004; 44(1): 109 - 120

Eikelenboom P, van Exel E, Hoozemans JJM, Veerhuis R, Rozemuller AJM, van Gool WA, Neuroinflammation – An Early Event in Both the History and Pathogenesis of Alzheimer's Disease, Neurodegenerative Disease 2010; 7: 38 – 41

Elkabes S, DiCicco-Bloom EM, Black IB, Brain Microglia/Macrophages Express Neurotrophins that Selectively Regulate Microglial Proliferation and Function, The Journal of Neuroscience 1996, 76(8): 2508-2521

Engelhardt B, Molecular mechanisms involved in T cell migration across the blood-brain barrier, J Neural Transm 2006; 113(4): 477 - 85

Engelhardt B, Ransohoff RM, Capture, crawl, cross: the T cell code to breach the blood-brain barriers, Trends Immunol. 2012; 33(12): 579 - 589

Erion JR, Wosiski-Kuhn M, Dey A, Hao S, Davis CL, Pollock NK, Stranahan AM, Obesity elicits interleukin 1-mediated deficits in hippocampal synaptic plasticity, J Neurosci. 2014; 34(7): 2618 - 31

Fan R, Xu F, Previti ML, Davis J, Grande AM, Robinson JK, Van Nostrand WE, Minocycline reduces microglial activation and improves behavioral deficits in a transgenic model of cerebral microvascular amyloid, J Neurosci. 2007; 27(12): 3057 - 3063

Fan L, Wang T, Chang L, Song Y, Wu Y, Ma D, Systemic inflammation induces a profound long term brain cell injury in rats, Acta Neurobiol Exp (Wars) 2014; 74(3): 298 - 306

Ferguson DJ, Hutchison WM, The host-parasite relationship of Toxoplasma gondii in the brains of chronically infected mice, Virchows Arch A Pathol Anat Histopathol, 1987; 411(1): 39 - 43

Feustel SM, Meissner M, Liesenfeld O, ***Toxoplasma gondii*** and the blood-brain barrier, Virulence 2012; 3(2): 182 – 192

Fischer HG, Nitzgen B, Reichmann G, Gross U, Hadding U, Host cells of *Toxoplasma gondii* encystation in infected primary culture from mouse brain, Parasitol Res. 1997; 83(7) : 637 - 641

Fischer O, Miliare Nekrosen mit drusigen Wucherungen der Neurofibrillen, eine regelmässige Veränderung der Hirnrinde bei seniler Demenz. Monatsschr Psychiatr Neurol 1907; 22: 361 – 372

Flegr J, Effects of toxoplasma on human behavior, Schizophr Bull. 2007; 33(3): 757 - 760

Flores EA, Bistrian BR, Pomposelli JJ, Dinarello CA, Blackburn GL, Istfan NW, **Infusion of tumor necrosis factor/cachectin promotes muscle catabolism in the rat, A synergistic effect with interleukin 1, J Clin Invest. 1989; 83(5): 1614 - 1622**

Frenkel JK, ***Toxoplasma*** in and around us. BioScience. 1973; 23: 343 – 352

Frey U, Krug M, Reymann KG, Matthies H, Anisomycin, an inhibitor of protein synthesis, blocks late phases of LTP phenomena in the hippocampal CA1 region in vitro, Brain Res. 1988; 452(1-2): 57 - 65

Fujita Y, Sakata H, Electrophysiological properties of CA1 and CA2 apical dendrites of rabbit hippocampus, J Neurophysiol. 1962; 25: 209 - 222

Gallagher JJ, Minogue AM, Lynch MA, Impaired performance of female APP/PS1 mice in the Morris water maze is coupled with increased Aβ accumulation and microglial activation, Neurodegener Dis. 2013; 11(1): 33 – 41

Games D, Adams D, Alessandrini R, Barbour R, Borthelette P, Blackwell C, Carr T, Clemens J, Donaldson T, Gillespie F, Guido T, Hagopian S, Johnson-Wood K, Khan K, Lee M, Leibowitz P, Lieberburg I, Sheila Little S, Eliezer Masliah E, Lisa McConlogue L, Martin Montoya-Zavala M, Lennart Mucke L, Paganini L, Penniman E, Power M, Schenk D, Seubert P, Snyder B, Soriano F, Tan H, Vitale J, Wadsworth S, Wolozin B, Zhao J, Alzheimer-type neuropathology in transgenic mice overexpressing V717F β-amyloid precursor protein, Nature 1995; 373(6514): 523 – 527

Garcia-Alloza M, Robbins EM, Zhang-Nunes SX, Purcell SM, Betensky RA, Raju S, Prada C, Greenberg SM, Bacskai BJ, Frosch MP, Characterization of amyloid deposition in the APPswe/PS1dE9 mouse model of Alzheimer disease, Neurobiol Dis. 2006; 24(3): 516 - 24

Garthe A, Behr J and Kempermann G, Adult-generated hippocampal neurons allow the flexible use of spatially precise learning strategies. PLoSONE 2009*;* 4: 54 - 64

Garthe A and Kempermann G, An old test for new neurons: refining the Morris water maze to study the functional relevance of adult hippocampal neurogenesis. Front.Neurosci. 7 2013: 63

Gatkowska J, Wieczorek M, Dziadek B, Dzitko K, Dlugonska H, Behavioral changes in mice caused by Toxoplasma gondii invasion of brain, Parasitol Res 2012; 111: 53 – 58

Gibertini M, Newton C, Friedman H, Klein TW, Spatial learning impairment in mice infected with Legionella pneumophila or administered exogenous interleukin-1-beta, Brain Behav Immun. 1995; 9(2): 113 - 128

Gigley JP, Fox BA, Bzik DJ, Long-Term Immunity to Lethal Acute or Chronic Type II ***Toxoplasma gondii*** Infection Is Effectively Induced in Genetically Susceptible C57BL/6 Mice by Immunization with an Attenuated Type I Vaccine Strain, Infect Immun. 2009; 77(12): 5380 – 5388

Glass CK, Saijo K, Winner B, Marchetto MC, Gage FH, Mechanisms Underlying Inflammation in Neurodegeneration, Cell. 2010; 140(6): 918 – 934

Glenner GG, Wong CW, Alzheimer's disease: initial report of the purification and characterization of a novel cerebrovascular amyloid protein, Biochem Biophys Res Commun. 1984; 120(3): 885 - 90

Godbout JP, Chen J, Abraham J, Richwine AF, Berg BM, Kelley KW, et al. Exaggerated neuroinflammation and sickness behavior in aged mice after activation of the peripheral innate immune system. FASEBJ. 19 2005; 1329 – 1331

Gong CX, Iqbal K, Hyperphosphorylation of microtubule-associated protein tau: a promising therapeutic target for Alzheimer disease, Curr Med Chem. 2008; 15(23): 2321 - 2328

Granic I, Dolga AM, Nijholt IM, van Dijk G, Eise ULM, Inflammation and NF-κB in Alzheimer's Disease and Diabetes, Journal of Alzheimer's Disease 2009; 16: 809 – 821

Grueninger F, Bohrmann B, Czech C, Ballard TM, Frey JR, Weidensteiner C, von Kienlin M, Ozmen L, Phosphorylation of Tau at S422 is enhanced by Aβ in TauPS2APP triple transgenic mice," Neurobiology of Disease 2009; 37(2): 294 – 306

Grutzendler J, Helmin K, Tsai J, Gan WB, Various dendritic abnormalities are associated with fibrillar amyloid deposits in Alzheimer's disease, Ann N Y Acad Sci. 2007; 1097: 30-9

Gulinello M, Acquarone M, Kim JH, Spray DC, Barbosa HS, Sellers R, Tanowitz HB, Weiss LM, Acquired infection with Toxoplasma gondii in adult mice results in sensorimotor deficits but normal cognitive behavior despite widespread brain pathology. *Microbes Infect* 2010; 12: 528 – 537

Hailman E, Lichenstein HS, Wurfel MM, Miller DS, Johnson DA, Kelley M, Busse LA, Zukowski MM, Wright SD Lipopolysaccharide (LPS)-binding protein accelerates the binding of LPS to CD14. J Exp Med. 1994; 179(1): 269 - 277

Haley JE, Schaible E, Pavlidis P, Murdock A, Madison DV, Basal and apical synapses of CA1 pyramidal cells employ different LTP induction mechanisms, Learn Mem 3 1996*:* 289 – 295

Halle A, Hornung V, Petzold GC, Stewart CR, Monks BG, Reinheckel T, Fitzgerald KA, Latz E, Moore KJ, Golenbock DT, The NALP3 inflammasome is involved in the innate immune response to amyloid-beta, Nat Immunol. 2008; 9(8): 857 - 865

Hanke ML, Kielian T, Deciphering mechanisms of staphylococcal biofilm evasion of host immunity Front Cell Infect Microbiol. 2012; 2: 62

Hankenson FC, Ruskoski N, van Saun M, Ying GS, Oh J, Fraser NW, Weight loss and reduced body temperature determine humane endpoints in a mouse model of ocular herpesvirus infection, J Am Assoc Lab Anim Sci. 2013; 52(3): 277 - 85

Hansson GK, Hermansson A, The immune system in atherosclerosis. Nature Immunol. 2011; 12: 204 – 212

Harris KM, Stevens JK, Dendritic spines of CA1 pyramidal cells in the rat hippocampus: serial electron microscopy with reference to their biophysical characteristics. J Neurosci. 1989; 9: 2982 – 2997

Hashimoto C, Hudson KL and Anderson KV TheToll gene of Drosophila, required for dorso–ventral embryonic polarity appears to encode a transmembrane protein. Cell 1988; 52: 269 – 279

Hay J, Aitken PP, Arnott MA, The influence of congenital *Toxoplasma* infection on the spontaneous running activity of mice. Z. Parasitenkd. 1985; 71: 459 – 462

Hayashi Y, Majewska AK, Dendritic spine geometry: functional implication and regulation, Neuron. 2005; 46(4): 529 – 532

Hein AM, Stasko MR, Matousek SB, Scott-McKean JJ, Maier SF, Olschowka JA, Costa ACS, O'Banion MK, Sustained hippocampal IL-1β overexpression impairs contextual and spatial memory in transgenic mice, Brain Behav Immun. 2010; 24(2): 243

Heneka MT, Carson MJ, El Khoury J, Landreth GE, Brosseron F, Feinstein DL, Jacobs AH, Wyss-Coray T, Vitorica J, Ransohoff RM, Herrup K, Frautschy SA, Finsen B, Brown GC, Verkhratsky A, Yamanaka K, Koistinaho J, Latz E, Halle A, Petzold GC, Town T, Morgan D, Shinohara ML, Perry VH, Holmes C, Bazan NG, Brooks DJ, Hunot S, Joseph B, Deigendesch N, Garaschuk O, Boddeke E, Dinarello CA, Breitner JC, Cole GM, Golenbock DT, Kummer MP, Neuroinflammation in Alzheimer's disease, Lancet Neurol. 2015; 14(4): 388 - 405

Heneka MT, Kummer MP, Stutz A, Delekate A, Schwartz S, Vieira-Saecker A, Griep A, Axt D, Remus A, Tzeng T-C, Gelpi E, Halle A, Korte M, Latz E and Golenbock DT, NLRP3 is activated in Alzheimer's disease and contributes to pathology in APP/PS1 mice, Nature 2013; 493(7434): 674 - 678

Heneka MT, O'Banion MK, Inflammatory processes in Alzheimer's disease, J Neuroimmunol. 2007; 184(1–2): 69 – 91

Hennigan A, Trotter C, Kelly AM, Lipopolysaccharide impairs longterm potentiation and recognition memory and increases p75NTR expression in the rat dentate gyrus. Brain Res 2007; 1130: 158 – 166

Hermes G, Ajioka JW, Kelly KA, Mui E, Roberts F, Kasza K, Mayr T, Kirisits MJ, Wollmann R, Ferguson DJ, Roberts CW, Hwang JH, Trendler T, Kennan RP, Suzuki Y, Reardon C, Hickey WF, Chen L, McLeod R, Neurological and behavioral abnormalities, ventricular dilatation, altered cellular functions, inflammation, and neuronal injury in brains of mice due to common, persistent, parasitic infection, J Neuroinflammation 2008; 5: 48

Hessle CC, Andersson B, Wold AE, Gram-positive and Gram-negative bacteria elicit different patterns of pro-inflammatory cytokines in human monocytes, Cytokine. 2005; 30(6): 311 - 318

Hoffmann O, Mahrhofer C, Rueter N, Freyer D, Bert B, Fink H and Weber JR, Pneumococcal Cell Wall-Induced Meningitis Impairs Adult Hippocampal Neurogenesis, Infect. Immun. September 2007; 75(9): 4289 - 4297

Holmes C, Cunningham C, Zotova E, Woolford J, Dean C, Kerr S, Culliford D, Perry VH, Systemic inflammation and disease progression in Alzheimer disease, Neurology. 2009; 73(10): 768 - 74

Holtmaat A, Svoboda K, Experience-dependent structural synaptic plasticity in the mammalian brain, Nat Rev Neurosci. 2009; 10(9): 647 - 658

Horst SA, Hoerr V, Beineke A, Kreis C, Tuchscherr L, Kalinka J, Lehne S, Schleicher I, Köhler G, Fuchs T, Raschke MJ, Rohde M, Peters G, Faber C, Löffler B, Medina E, **A Novel Mouse Model of** *Staphylococcus aureus* **Chronic Osteomyelitis That Closely Mimics the Human Infection: An Integrated View of Disease Pathogenesis, The American Journal of Pathology 2012; 181(4): 1206 – 1214**

Hsiao K, Chapman P, Nilsen S, Eckman C, Harigaya Y, Younkin S, Yang F, Cole G, Correlative memory deficits, Aβ elevation, and amyloid plaques in transgenic mice, Science 1996; 274(5284): 99 – 102

Hunter CA, Remington JS, Immunopathogenesis of toxoplasmic encephalitis. J Infect Dis. 1994; 170: 1057 – 67

Itagaki S, McGeer PL, Akiyama H, Zhu S, Selkoe D, Relationship of microglia and astrocytes to amyloid deposits of Alzheimer disease, J Neuroimmunol. 1989; 24(3): 173 – 82

Jankowsky JL, Slunt HH, Ratovitski T, Jenkins NA, Copeland NG, Borchelt DR, Co-expression of multiple transgenes in mouse CNS: a comparison of strategies, Biomol Eng. 2001; 17(6):157-65

Jankowsky JL, Fadale DJ, Anderson J, Xu GM, Gonzales V, Jenkins NA, Copeland NG, Lee MK, Younkin LH, Wagner SL, Younkin SG, Borchelt DR, Mutant presenilins specifically elevate the levels of the 42 residue beta-amyloid peptide in vivo: evidence for augmentation of a 42-specific gamma secretase, Hum Mol Genet. 2004; 13(2): 159 - 170

Jeong YI, Jung ID, Lee CM, Chang JH, Chun SH, Noh KT, Jeong SK, Shin YK, Lee WS, Kang MS, Lee SY, Lee JD, Park YM, The novel role of platelet-activating factor in protecting mice against lipopolysaccharide-induced endotoxic shock, PLoS One. 2009; 4(8): e6503

Jiang Y, Wei N, Zhu J, Lu T, Chen Z, Xu G, Liu X, Effects of brain-derived neurotrophic factor on local inflammation in experimental stroke of rat, Mediators Inflamm. 2010; 2010: 372423

Jiang-Shieh YF, Wu CH, Chien HF, Wei IH, Chang ML, Shieh JY, Wen CY, Reactive changes of interstitial glia and pinealocytes in the rat pineal gland challenged with cell wall components from gram-positive and -negative bacteria, J Pineal Res. 2005; 38(1): 17 - 26

Jo JH, Park EJ, Lee JK, Jung MW, Lee CJ, Lipopolysaccharide inhibits induction of long-term potentiation and depression in the rat hippocampal CA1 area, Eur J Pharmacol 2001; 422: 69 –76

Jones A, Kulozik P, Ostertag A, Herzig S, Common pathological processes and transcriptional pathways in Alzheimer's disease and type 2 diabetes, J. Alzheimers Dis. 2009; 16: 787 – 808

Kawanokuchi J, Mizuno T, Takeuchi H, Kato H, Wang J, Mitsuma N, Suzumura A, Production of interferon-γ by microglia. Mult Scler 2006; 12: 558 – 564

Kelly RJ, Minogue AM, Lyons A, Jones RS, Browne TC, Costello DA, Denieffe S, O'Sullivan C, Connor TJ, Lynch MA, Glial Activation in A beta PP/PS1 Mice is Associated with Infiltration of IFN gamma-Producing Cells, Journal of Alzheimers Disease. 2013; 37: 63 - 75

Kengatharan KM, De Kimpe SJ, Thiemermann C, Role of nitric oxide in the circulatory failure and organ injury in a rodent model of gram-positive shock, Br J Pharmacol. 1996; 119(7): 1411 - 1421

Kerschensteiner M, Gallmeier E, Behrens L, Leal VV, Misgeld T, Klinkert WE, Kolbeck R, Hoppe E, Oropeza-Wekerle RL, Bartke I, Stadelmann C, Lassmann H, Wekerle H, Hohlfeld R, Activated human T

cells, B cells, and monocytes produce brain-derived neurotrophic factor in vitro and in inflammatory brain lesions: a neuroprotective role of inflammation? J Exp Med. 1999; 189(5): 865 – 870

Kettenmann H, Hanisch UK, Noda M, Verkhratsky A, Physiology of Microglia, Physiological Reviews, 2011; 91(2): 461 - 553

Kim JJ, Diamond DM, The stressed hippocampus, synaptic plasticity and lost memories, Nature Reviews Neuroscience 2002; 3: 453 - 462

Kinsbourne M, Wood F, Short-term memory and the amnesic syndrome, Short-Term Memory. D. Deutsch and J.A. Deutsch, Academic Press, New York 1975: 257 – 291

Kitazawa M, Cheng D, Tsukamoto MR, Koike MA, Wes PD, Vasilevko V, Cribbs DH, LaFerla FM, Blocking IL-1 signaling rescues cognition, attenuates tau pathology, and restores neuronal β-catenin pathway function in an Alzheimer's disease model, J Immunol. 2011; 187(12): 6539 - 6549

Kreutzberg GW, Microglia: a sensor for pathological events in the CNS, Trends Neurosci. 1996; 19, 312 – 318

Kramar EA, Lynch G, Developmental and regional differences in the consolidation of long-term potentiation, Neuroscience 118 2003*:* 387 – 398

Krueger JM, Fang J, Taishi P, Chen Z, Kushikata T, Gardi J, Sleep. A physiologic role for IL-1 beta and TNF-alpha, Ann. NY Acad. Sci. 1998; 856: 148 – 159

Kummer MP, Hermes M, Delekarte A, Hammerschmidt T, Kumar S, Terwel, D, Walter J, Pape H-C, König S, Roeber S, Jessen F, Klockgether T, Korte M and Heneka MT, Nitration of Tyrosine 10 Critically Enhances Amyloid β Aggregation and Plaque Formation, Neuron 2011; 71: 833–844

Lachenmaier SM, Deli MA, Meissner M, Liesenfeld O, Intracellular transport of *Toxoplasma gondii* through the blood-brain barrier, J Neuroimmunol. 2011; 232(1-2): 119 - 30

Laflamme N, Soucy G, Rivest S, Circulating cell wall components derived from gram-negative, not gram-positive, bacteria cause a profound induction of the gene-encoding Toll-like receptor 2 in the CNS, J Neurochem. 2001; 79(3): 648 - 657

Laflamme N, Echchannaoui H, Landmann R, Rivest S, Cooperation between toll-like receptor 2 and 4 in the brain of mice challenged with cell wall components derived from gram-negative and gram-positive bacteria, Eur J Immunol. 2003; 33(4): 1127 - 1138

Lawson LJ, Perry VH, Dri P, Gordon S, Heterogeneity in the distribution and morphology of microglia in the normal adult mouse brain. Neuroscience 39 1990, 151–170

Lee CK, Weindruch R, Prolla TA, Gene-expression profile of the ageing brain in mice, Nat Genet. 2000; 25(3): 294 -297

Lee DC, Rizer J, Selenica ML, Reid P, Kraft C, Johnson A, Blair L, Gordon MN, Dickey CA, Morgan D, LPS- induced inflammation exacerbates phospho-tau pathology in rTg4510 mice, J Neuroinflammation. 2010; 7: 56

Letiembre M, Hao W, Liu Y, Walter S, Mihaljevic I, Rivest S, Hartmann T, Fassbender K, Innate immune receptor expression in normal brain aging, Neuroscience. 2007; 146(1): 248-54

Lin B, Kramar EA, Bi X, Brucher FA, Gall CM, Lynch G, Theta stimulation polymerizes actin in dendritic spines of hippocampus, J Neurosci 2005; 25: 2062 - 2069

Ling PR, Schwartz JH, Bistrian BR, Mechanisms of host wasting induced by administration of cytokines in rats, Am J Physiol. 1997; 272(3 Pt 1): E333 - 9

Liu X, Wu Z, Hayashi Y, Nakanishi H, Age-dependent neuroinflammatory responses and deficits in long-term potentiation in the hippocampus during systemic inflammation, Neuroscience. 2012; 216:133 - 42

Lord A, Kalimo H, Eckman C, Zhang X-Q, Lannfelt L, Nilsson LNG, The Arctic Alzheimer mutation facilitates early intraneuronal Aβ aggregation and senile plaque formation in transgenic mice, Neurobiology of Aging 2006; 27(1): 67 – 77

Luchsinger JA, Gustafson DR, Adiposity, type 2 diabetes, and Alzheimer's disease, J. Alzheimers Dis. 2009; 16: 693 – 704

Lyons RE, McLeod R, Roberts CW, *Toxoplasma gondii* tachyzoite-bradyzoite interconversion, Trends Parasitol. 2002; 18(5): 198 - 201

Lyons A, Griffin RJ, Costelloe CE, Clarke RM, Lynch MA, IL-4 attenuates the neuroinflammation induced by amyloid-beta *in vivo* and *in vitro*, J Neurochem. 2007; 101(3): 771 – 81

Maggio N, Shavit-Stein E, Dori A, Blatt I, Chapman J, Prolonged systemic inflammation persistently modifies synaptic plasticity in the hippocampus: modulation by the stress hormones, Front Mol Neurosci. 2013; 6: 46

Malenka RC, Bear MF, LTP and LTD: an embarrassment of riches, Neuron. 2004; 44(1): 5 - 21

Malenka RC, Nicoll RA, Long-term potentiation--a decade of progress? Science. 1999; 285(5435): 1870 - 1874

Mandelkow EM, Mandelkow E, Tau in Alzheimer's disease, Trends Cell Biol. 1998; 8(11): 425 – 7

Marin I, Kipnis J, Learning and memory ... and the immune system, Learn Mem. 2013; 20(10): 601 – 606

Martin GS, Mannino GM, Eaton S and Moss M, The epidemiology of sepsis in the United States from 1979 through 2000**,** The New England Journal of Medicine, 2003; 348(16): 1546 – 1554

Martin GS, Sepsis, severe sepsis and septic shock: changes in incidence, pathogens and outcomes, Expert Rev Anti Infect Ther. 2012; 10(6): 701-6

Martinez FO, Sica A, Mantovani A, Locati M, Macrophage activation and polarization; Front Biosci. 2008; 13: 453–461

Matsumoto Y, Yamaguchi T, Watanabe S, Yamamoto T, Involvement of arachidonic acid cascade in working memory impairment induced by interleukin-1 β, Neuropharmacology 2004; 46: 1195 – 1200

Matsuoka Y, Lamirande EW, Subbarao K, The mouse model for influenza, Curr Protoc Microbiol 2009 Chapter 15: Unit 15G.3

McKimmie CS, Fazakerley JK, In response to pathogens, Glial cells dynamically and differentially regulate Toll-like receptor gene expression, Journal of Neuroimmunology 2005; 169(1-2): 116 – 125

Michaud JP, Hallé M, Lampron A, Thériault P, Préfontaine P, Filali M, Tribout-Jover P, Lanteigne AM, Jodoin R, Cluff C, Brichard V, Palmantier R, Pilorget A, Larocque D, Rivest S, Toll-like receptor 4

stimulation with the detoxified ligand monophosphoryl lipid A improves Alzheimer's disease-related pathology, Proc Natl Acad Sci U S A. 2013; 110(5): 1941- 1946

Michie HR, Manogue KR, Spriggs DR, Revhaug A, O'Dwyer S, Dinarello CA, Cerami A, Wolff SM and Wilmore DW, Detection of Circulating Tumor Necrosis Factor after Endotoxin Administration, N Engl J Med 1988; 318:1481-1486

Milatovic D, Montine TJ, Zaja-Milatovic S, Madison JL, Bowman AB and Aschner M, Morphometric Analysis in Neurodegenerative Disorders, Curr Protoc Toxicol. 2010; 12 (16): 1–14

Min SS, Quan HY, Ma J, Han JS, Jeon BH, Seol GH, Chronic brain inflammation impairs two forms of long-term potentiation in the rat hippocampal CA1 area, Neurosci Lett. 2009; 456(1): 20-4

Minogue AM, Jones RS, Kelly RJ, McDonald CL, Connor TJ, Lynch MA, Age-associated dysregulation of microglial activation is coupled with enhanced blood-brain barrier permeability and pathology in APP/PS1 mice, Neurobiol Aging. 2014; 35(6): 1442 - 1452

Moechars D, Dewachter I, Lorent K, Reversé D, Baekelandt V, Naidu A, Tesseur I, Spittaels K, Haute CV, Checler F, Godaux E, Cordell B, Van Leuven F, Early phenotypic changes in transgenic mice that overexpress different mutants of amyloid precursor protein in brain, The Journal of Biological Chemistry 1999; 274(10): 6483 - 6492

Mogensen TH, Pathogen Recognition and Inflammatory Signaling in Innate Immune Defenses, Clin Microbiol Rev. 2009; 22(2): 240 – 273

Montoya JG, Liesenfeld O, Toxoplasmosis, Lancet, 2004; 363(9425): 1965 - 76

Montoya JG, Remington JS, Management of Toxoplasma gondii infection during pregnancy. Clin Infect Dis. 2008; 47: 554 – 66

Moolman DL, Vitolo OV, Vonsattel JP, Shelanski ML, Dendrite and dendritic spine alterations in Alzheimer models, J Neurocytol. 2004; 33(3): 377-87

Moore AH, Wu M, Shaftel SS, Graham KA, O'Banion MK, Sustained expression of interleukin-1β in mouse hippocampus impairs spatial memory. Neuroscience 2009; 164*:* 1484–1495

Morgan TE , Xie Z, Goldsmith S, Yoshida T, Lanzrein AS, Stone D, Rozovsky I, Perry G, Smith MA, Finch CE, The mosaic of brain glial hyperactivity during normal ageing and its attenuation by food restriction, Neuroscience 1999; 89(3): 687–699

Morris RG, Garrud P, Rawlins JN, O'Keefe J, Place navigation impaired in rats with hippocampal lesions, Nature. 1982; 297(5868): 681-3.

Morris R, Developments of a water-maze procedure for studying spatial learning in the rat, J Neurosci Methods. 1984; 11(1): 47-60

Munder M, Eichmann K, Moran JM, Centeno F, Soler G, Modolell M, Th1/Th2-regulated expression of arginase isoforms in murine macrophages and dendritic cells, J Immunol 1999; 163: 3771 - 3777

Murabe Y, Sano Y, Morphological studies on neuroglia. V. Microglial cells in the cerebral cortex of the rat, with special reference to their possible involvement in synaptic function, Cell Tissue Res. 1982; 223(3): 493 - 506

Murabe Y, Sano Y, Morphological studies on neuroglia. VI. Postnatal development of microglial cells, Cell Tissue Res. 1982; 225(3): 469 - 485

Murray AC and Lynch MA, **Evidence That Increased Hippocampal Expression of the Cytokine Interleukin-1β Is a Common Trigger for Age- and Stress-Induced Impairments in Long-Term Potentiation,**
The Journal of Neuroscience, 1998; 18(8): 2974 - 2981

Nalbantoglu J, Tirado-Santiago G, Lahsaïni A, Poirier J, Goncalves O, Verge G, Momoli F, Welner SA, Massicotte G, Julien JP, Shapiro ML, Impaired learning and LTP in mice expressing the carboxy terminus of the Alzheimer amyloid precursor protein, Nature. 1997; 387(6632): 500 - 505

Netea MG, Kullberg BJ, Joosten LA, Sprong T, Verschueren I, Boerman OC, Amiot F, van den Berg WB, Van der Meer JW, Lethal Escherichia coli and Salmonella typhimurium endotoxemia is mediated through different pathways, Eur J Immunol. 2001; 31(9): 2529 - 38

Nguyen MD, Julien JP and Rivest S, **Innate Immunity: The Missing Link In Neuroprotection and Neurodegeneration? Nature Reviews Neuroscience 2002; 3, 216 - 227**

Nicolle MM, Gonzalez J, Sugaya K, Baskerville KA, Bryan D, Lund K, Gallagher M, McKinney M, Signatures of hippocampal oxidative stress in aged spatial learning-impaired rodents, Neuroscience 2001; 107(3): 415 - 31

Nimmerjahn A, Kirchhoff F, Helmchen F, Resting microglial cells are highly dynamic surveillants of brain parenchyma in vivo, Science. 2005; 308(5726): 1314 - 1318

Oddo S, Caccamo A, Shepherd JD, Murphy MP, Golde TE, Kayed R, Metherate R, Mattson MP, Akbari Y, LaFerla FM, Triple-transgenic model of Alzheimer's disease with plaques and tangles: intracellular Aβ and synaptic dysfunction, Neuron 2003; 39(3): 409 – 421

Olefsky JM, Glass CK, **Macrophages, inflammation, and insulin resistance. Annu. Rev. Physiol. 2010; 72, 219 – 246**

O'Keefe J, Nadel L, Precis of O'Keefe and Nadel's the hippocampus as a cognitive map, Behav. Brain Sci. 1979; 2: 487 – 533

O'Keefe GM, Nguyen VT, Benveniste EN, Regulation and function of class II major histocompatibility complex, CD40, and B7 expression in macrophages and microglia: implications in neurological diseases. J. Neurovirol. 2002; **8**, 496 – 512

O'Neill LAJ, Golenbock D, Bowie AG, **The history of Toll-like receptors — redefining innate immunity, Nature Reviews Immunology 2013; 13, 453–460**

Ota Y, Zanetti AT, Hallock RM, The Role of Astrocytes in the Regulation of Synaptic Plasticity and Memory Formation, Neural Plast. 2013; 185463

Ousman SS, Kubes P, **Immune surveillance in the central nervous system, Nature Neuroscience 2012; 15: 1096 – 1101**

Ouyang Y, Wong M, Capani F, Rensing N, Lee C-S, Liu Q, Neusch C, Martone ME, Wu JY, Yamada K, Ellisman MH, Choi DW, Transient decrease in F-actin may be necessary for translocation of proteins into dendritic spines, Eur J Neurosci 2005; 22: 2995 - 3005

Ozinsky A, Underhill DM, Fontenot JD, Hajjar AM, Smith KD, Wilson CB, Schroeder L, and Aderem A The repertoire for pattern recognition of pathogens by the innate immune system is defined by cooperation between Toll-like receptors. Proc Natl Acad Sci U S A. 2000; 97(25): 13766 – 13771

Paolicelli RC, Bolasco G, Pagani F, Maggi L, Scianni M, Panzanelli P, Giustetto M, Alves Ferreira T, Guiducci E, Dumas L, Ragozzino D, Gross CT, Synaptic pruning by microglia is necessary for normal brain development. Science 2011; 333: 1456 – 1458

Parlog A, Neuronal alterations in chronic cerebral *Toxoplasma gondii* infection, Dissertation 2015

Parrillo JE, Parker MM, Natanson C, Suffredini AF, Danner RL, Cunnion RE, Ognibene FP, Septic shock in humans. Advances in the understanding of pathogenesis, cardiovascular dysfunction, and therapy, Ann Intern Med. 1990; 113(3): 227 - 242

Pavesio CE, Lightman S, *Toxoplasma gondii* and ocular toxoplasmosis: pathogenesis, Br J Ophthalmol. 1996; 80: 1099 – 1107

Peferoen L, Kipp M, Valk P, Noort JM, Amor S, Oligodendrocyte-microglia cross-talk in the central nervous system, Immunology. 2014; 141(3): 302 – 313

Perea G, Navarrete M, Araque A, Tripartite synapses: astrocytes process and control synaptic information, Trends Neurosci. 2009; 32(8): 421 - 431

Perry VH, Gordon S, Macrophages and the nervous system. Int. Rev. Cytol. 1991; 125, 203–244

Perry VH, Cunningham C, Holmes C, Systemic infections and inflammation affect chronic neurodegeneration, Nat Rev Immunol. 2007; 7(2): 161 - 167

Perry VH, Nicoll JA, Holmes C, Microglia in neurodegenerative disease, Nat Rev Neurol. 2010; 6(4): 193 - 201

Pine RW, Wertz MJ, Lennard ES, Dellinger EP, Carrico CJ, Minshew BH, Determinants of organ malfunction or death in patients with intra-abdominal sepsis - A discriminant analysis, Arch Surg 1983; 118:242–249

Prandovszky E, Gaskell E, Martin H, Dubey JP, Webster JP, McConkey GA, The neurotropic parasite *Toxoplasma gondii* increases dopamine metabolism, PLoS One 2011; 6: e23866

Prencipe G, Minnone G, Strippoli R, De Pasquale L, Petrini S, Caiello I, Manni L, De Benedetti F, Bracci-Laudiero L, Nerve growth factor downregulates inflammatory response in human monocytes through TrkA, J Immunol. 2014; 192(7): 3345 – 3354

Price JL, Morris JC, Tangles and plaques in nondemented aging and "preclinical" Alzheimer's disease, Ann Neurol. 1999; 45(3): 358 – 68

Pugh CR, Kumagawa K, Fleshner M, Watkins LR, Maier SF, Rudy JW, Selective effects of peripheral lipopolysaccharide administration on contextual and auditory-cue fear conditioning, Brain Behav Immun. 1998; 12: 212–229

Püntener U, Booth SG, Perry VH, Teeling JL, Long-term impact of systemic bacterial infection on the cerebral vasculature and microglia. J Neuroinflammation. 2012; 9:146

Qiao X, Cummins DJ, Paul SM, Neuroinflammation-induced acceleration of amyloid deposition in the APPV717F transgenic mouse, Eur. J. Neurosci. 2001; 14: 474 − 482

Qin L, Wu X, Block ML, Liu Y, Breese GR, Hong JS, Knapp DJ, Crews FT, Systemic LPS causes chronic neuroinflammation and progressive neurodegeneration, Glia. 2007; 55(5): 453 - 462

Qiu C, Kivipelto M, von Strauss E, Epidemiology of Alzheimer's disease: occurrence, determinants, and strategies toward intervention, Dialogues Clin Neurosci. 2009; 11(2): 111 – 128

Ransohoff RM, Cardona AE, The myeloid cells of the central nervous system parenchyma, Nature 2010; 468: 253 – 262

Ribé EM, Pérez M, Puig B, Gich I, Lim F, Cuadrado M, Sesma T, Catena S, Sánchez B, Nieto M, Gómez-Ramos P, Morán MA, Cabodevilla F, Samaranch L, Ortiz L, Pérez A, Ferrer I, Avila J, Gómez-Isla T, Accelerated amyloid deposition, neurofibrillary degeneration and neuronal loss in double mutant APP/tau transgenic mice," Neurobiology of Disease 2005; 20(3): 814 – 822

Richards JG, Higgins GA, Ouagazzal AM, Ozmen L, Kew JN, Bohrmann B, Malherbe P, Brockhaus M, Loetscher H, Czech C, Huber G, Bluethmann H, Jacobsen H, Kemp JA, PS2APP transgenic mice, coexpressing hPS2mut and hAPPswe, show age-related cognitive deficits associated with discrete brain amyloid deposition and inflammation," Journal of Neuroscience 2003; 23(26): 8989 – 9003

Richwine AF, Parkin AO, Buchanan JB, Chen J, Markham JA, Juraska JM, Johnson RW, Architectural changes to CA1 pyramidal neurons in adult and aged mice after peripheral immune stimulation, Psychoneuroendocrinology. 2008; 33(10): 1369 - 1377

Rosenberger CM, Scott MG, Gold MR, Hancock RE, Finlay BB, Salmonella typhimurium infection and lipopolysaccharide stimulation induce similar changes in macrophage gene expression, J Immunol. 2000; 164(11): 5894 - 5904

Ross FM, Allan SM, Rothwell NJ, Verkhratsky A, A dual role for interleukin-1 in LTP in mouse hippocampal slices, J Neuroimmunol. 2003; 144(1-2): 61 – 7

Rothwell NJ, Luheshi GN, Interleukin 1 in the brain: biology, pathology and therapeutic target, Trends Neurosci. 2000; 23(12): 618 - 625

Saijo K, Glass CK, Microglial cell origin and phenotypes in health and disease, Nat Rev Immunol. 2011; 11(11): 775 - 787

Sajikumar S, **Korte** M, Different compartments of apical CA1 dendrites have different plasticity thresholds for expressing synaptic tagging and capture, Learn Mem. 2011; 18(5): 327-31

Sholl DA, Dendritic organization in the neurons of the visual and motor cortices of the cat, J Anat 1953; 87: 387 - 406

Schneider H, Pitossi F, Balschun D, Wagner A, Del Rey A, Besedovsky HO, A neuromodulatory role of interleukin-1beta in the hippocampus. Proc. Natl. Acad. Sci. USA 1998*;* 95: 7778 – 7783

Schröder NW, Morath S, Alexander C, Hamann L, Hartung T, Zähringer U, Göbel UB, Weber JR, Schumann RR, Lipoteichoic acid (LTA) of Streptococcus pneumoniae and Staphylococcus aureus activates immune cells via Toll-like receptor (TLR)-2, lipopolysaccharide-binding protein (LBP), and CD14, whereas TLR-4 and MD-2 are not involved, J Biol Chem. 2003; 278(18): 15587 - 15594

Schumann RR, Leong SR, Flaggs GW, Gray PW, Wright SD, Mathison JC, Tobias PS, Ulevitch RJ Structure and function of lipopolysaccharide binding protein. Science. 1990; 249(4975): 1429 - 31

Scoville WB, Milner B, Loss of recent memory after bilateral hippocampal lesions, J Neurol Neurosurg Psychiatry. 1957; 20(1): 11 - 21

Semmler A, Okulla T, Sastre M, Dumitrescu-Ozimek L, Heneka MT, Systemic inflammation induces apoptosis with variable vulnerability of different brain regions, J Chem Neuroanat. 2005; 30(2-3): 144 -157

Semmler A, Hermann S, Mormann F, Weberpals M, Paxian SA, Okulla T, Schäfers M, Kummer MP, Klockgether T, Heneka MT, Sepsis causes neuroinflammation and concomitant decrease of cerebral metabolism, J Neuroinflammation. 2008; 5: 38

Shaw KN, Commins S, O'Mara SM, Lipopolysaccharide causes deficits in spatial learning in the water maze but not in BDNF expression in the rat dentate gyrus, Behav Brain Res 2001; 124: 47 – 54

Sheng JG, Bora SH, Xu G, Borchelt DR, Price DL, Koliatsos VE, Lipopolysaccharide-induced-neuroinflammation increases intracellular accumulation of amyloid precursor protein and amyloid beta peptide in APPswe transgenic mice, Neurobiol Dis. 2003; 14(1): 133 - 145

Shirai Y, On the transplantation of the rat sarcoma in adult heterogeneous animals. Jap Med World. 1921; 1: 14 – 15

Silva B, Sousa L, Miranda A, Vasconcelos A, Reis H, Barcelos L, Arantes R, Teixeira A, Rachid MA, Memory deficit associated with increased brain proinflammatory cytokine levels and neurodegeneration in acute ischemic stroke, Arq Neuropsiquiatr. 2015; 73(8): 655-9

Simard M, Nedergaard M, The neurobiology of glia in the context of water and ion homeostasis, Neuroscience 2004; 129(4): 877 – 896

Šišková Z, Justus D, Kaneko H, Friedrichs D, Henneberg N, Beutel T, Pitsch J, Schoch S, Becker A, von der Kammer H, Remy S, Dendritic structural degeneration is functionally linked to cellular hyperexcitability in a mouse model of Alzheimer's disease, Neuron. 2014; 84(5): 1023-33

Slifko TR, Smith HV and Rose JB Emerging parasite zoonoses associated with water and food, International Journal for Parasitology, 2000; 30(12-13): 1379 –1393

Sofroniew MS, Vinters HV, Astrocytes: biology and pathology, Acta Neuropathol 2010; 119: 7 – 35

Soiampornkul R, Tong L, Thangnipon W, Balazs R, Cotman CW, Interleukin-1beta interferes with signal transduction induced by neurotrophin-3 in cortical neurons, Brain Res. 2008; 1188: 189 - 197

Sparkman NL, Kohman RA, Scott VJ, Boehm GW, Bacterial endotoxin-induced behavioral alterations in two variations of the Morris water maze, Physiol Behav 2005; 86: 244 – 251

Sprung CL, Peduzzi PN, Shatney CH, Schein RM, Wilson MF, Sheagren JN, Hinshaw LB, Impact of encephalopathy on mortality in the sepsis syndrome, Crit Care Med 1990; 18: 801 – 806

Stein M, Keshav S, Harris N, Gordon S, Interleukin 4 potently enhances murine macrophage mannose receptor activity: a marker of alternative immunologic macrophage activation. J Exp Med 1992; 176: 287 – 292

Strehl A, Lenz M, Itsekson-Hayosh Z, Becker D, Chapman J, Deller T, Maggio N, Vlachos A, Systemic inflammation is associated with a reduction in Synaptopodin expression in the mouse hippocampus, Exp Neurol. 2014; 261: 230 - 235

Sturchler-Pierrat C, Abramowski D, Duke M, Wiederhold KH, Mistl C, Rothacher S, Ledermann B, Bürki K, Frey P, Paganetti PA, Waridel C, Calhoun ME, Jucker M, Probst A, Staufenbiel M, Sommer B, Two amyloid precursor protein transgenic mouse models with Alzheimer disease-like pathology, Proceedings of the National Academy of Sciences of the United States of America 1997; 94(24): 13287 – 13292

Takeda K, Kaisho T and Akira S Toll-like receptors, Annual Review of Immunology 2003; 21: 335 - 376

Takumi Y, Ramirez-Leon V, Laake P, Rinvik E, Ottersen OP, Different modes of expression of AMPA and NMDA receptors in hippocampal synapses. Nat Neurosci. 1999; 2: 618 – 624

Tarawneh R, Holtzman DM, **The Clinical Problem of Symptomatic Alzheimer Disease and Mild Cognitive Impairment, Cold Spring Harb Perspect Med. 2012; 2(5): a006148**

Tateda K, Matsumoto T, Miyazaki S and Yamaguchi K Lipopolysaccharide-induced lethality and cytokine production in aged mice, Infect Immun. 1996; 64(3): 769-74.

Tenter AM, Heckeroth AR and Weiss LM Toxoplasma gondii: from animals to humans, International Journal for Parasitology, 2000; 30(12-13): 1217 – 1258

Tong L, Balazs R, Soiampornkul R, Thangnipon W, Cotman CW, Interleukin-1 beta impairs brain derived neurotrophic factor-induced signal transduction, Neurobiol Aging. 2008; 29(9): 1380 - 1393

Tong L, Prieto GA, Kramár EA, Smith ED, Cribbs DH, Lynch G, Cotman CW, BDNF-dependent synaptic plasticity is suppressed by IL-1β via p38 MAPK, J Neurosci. 2012; 32(49): 17714 – 17724

Tremblay ME, Majewska AK, A role for microglia in synaptic plasticity? Commun Integr Biol 2011; 4: 220 – 222

Tremblay M-E, Amanda Sierra A, Microglia in Health and Disease, Springer, 2014 - 486 pages

Trudler D, Farfara D, Frenkel D, Toll-Like Receptors Expression and Signaling in Glia Cells in Neuro-Amyloidogenic Diseases: Towards Future Therapeutic Application, Mediators of Inflammation 2010; (2010): 497987

Turnbull IR, Gilfillan S, Cella M, Aoshi T, Miller M, Piccio L, Hernandez M, Colonna M, **Cutting edge: TREM-2 attenuates macrophage activation, J Immunol. 2006; 177(6): 3520 - 3524**

Valero J, Mastrella G, Neiva I, Sánchez S, Malva JO, Long-term effects of an acute and systemic administration of LPS on adult neurogenesis and spatial memory, Front Neurosci. 2014; 8: 83

Van Broeck B, Vanhoutte G, Pirici D, Van Dam D, Wils H, Cuijt I, Vennekens K, Zabielski M, Michalik A, Theuns J, De Deyn PP, Van der Linden A, Van Broeckhoven C, Kumar-Singh S, Intraneuronal amyloid β and reduced brain volume in a novel APP T714I mouse model for Alzheimer's disease, Neurobiology of Aging 2008; 29(2): 241 – 252

Van Harreveld A, Fifkova E, Swelling of dendritic spines in the fascia dentata after stimulation of the perforant fibers as a mechanism of post-tetanic potentiation, Exp Neurol. 1975; 49(3): 736 - 749

van Heeckeren AM, Tscheikuna J, Walenga RW, Konstan MW, Davis PB, Erokwu B, Haxhiu MA, Ferkol TW, Effect of Pseudomonas infection on weight loss, lung mechanics, and cytokines in mice, Am J Respir Crit Care Med. 2000; 161(1): 271 - 279

Vereker E, Campbell V, Roche E, McEntee E and Lynch MA, Lipopolysaccharide Inhibits Long Term Potentiation in the Rat Dentate Gyrus by Activating Caspase-1, The Journal of Biological Chemistry 2000; 275 (34): 26252 – 26258

Vitkovic L, Bockaert J, Jacque C, "Inflammatory" Cytokines: Neuromodulators in Normal Brain? J. Neurochem. 2000; 74: 457 – 471

Vyas A, Kim SK, Giacomini N, Boothroyd JC, Sapolsky RM, Behavioral changes induced by Toxoplasma infection of rodents are highly specific to aversion of cat odors, Proc Natl Acad Sci U S A. 2007; 104(15): 6442 - 6447

Wake H, Moorhouse AJ, Jinno S, Kohsaka S, Nabekura J, Resting microglia directly monitor the functional state of synapses in vivo and determine the fate of ischemic terminals, J Neurosci 2009; 29: 3974 – 3980

Webster JP, Prevalence and transmission of *Toxoplasma gondii* in wild brown rats, Rattus norvegicus. Parasitology 1994; 108: 407 – 411

Webster JP The effect of Toxoplasma gondii on animal behavior: playing cat and mouse, Schizophrenia Bulletin 2007; 33(3): 752 – 756

Wellmer A, Noeske C, Gerber J, Munzel U, Nau R, Spatial memory and learning deficits after experimental pneumococcal meningitis in mice, Neurosci Lett. 2000; 296(2-3): 137 - 40

Wilson JX, Young GB, Progress in clinical neurosciences: sepsisassociated encephalopathy: evolving concepts. Can J Neurol Sci 2003; 30: 98 –105

Wyss-Coray T, Inflammation in Alzheimer disease: driving force, bystander or beneficial response? Nat Med. 2006; 12(9): 1005–1015

Zhang Y, Liu L, Peng YL, Liu YZ, Wu TY, Shen XL, Zhou JR, Sun DY, Huang AJ, Wang X, Wang YX, Jiang CL, Involvement of inflammasome activation in lipopolysaccharide-induced mice depressive-like behaviors, CNS Neurosci Ther 2014; 20: 119 – 124

Ziv Y, Ron N, Butovsky O, Landa G, Sudai E, Greenberg N, Cohen H, Kipnis J, Schwart M, Immune cells contribute to the maintenance of neurogenesis and spatial learning abilities in adulthood, Nature Neuroscience 2006; 9: 268 – 275

Zubenko GS, Zubenko WN, McPherson S, Spoor E, Marin DB, Farlow MR, Smith GE, Geda YE, Cummings JL, Petersen RC, Sunderland T, A collaborative study of the emergence and clinical features of the major depressive syndrome of Alzheimer's disease, Am J Psychiatry. 2003; 160(5): 857 – 66

Zucker RS, Short-term synaptic plasticity. Annu Rev Neurosci 1989; 12: 13 – 31

Zucker RS, Regehr WG, Short-term synaptic plasticity, Annu Rev Physiol. 2002; 64: 355 - 405

6. LIST OF ABBREVIATIONS

Aβ	amyloid beta
AD	Alzheimer's disease
ACSF	artificial cerebrospinal fluid
AIF-1	allograft inflammatory factor 1
AMPA	α-amino-3-hydroxy-5-methyl-4-isoxazol propionic acid
ASC	apoptosis-associated-speck-like protein
ATP	adenosine triphosphate
APP	amyloid precursor protein
BBB	blood-brain barrier
BDNF	brain-derived neurotrophic factor
BSA	bovine serum albumine
CA	*cornu ammonis*
CamKII	Ca^{2+}/calmodulin-dependent protein kinase II
CC	cytokine with C-C structure
CD	cluster of differentiation
COX	cyclooxygenase
CNS	central nervous system
CREB	cyclic AMP-responsive element-binding protein
CX_3C	cytokine with CXXXC structure
DAMP	danger-associated molecular pattern
DAPI	4´,6-diamidino-2-phenylindole
DiI	1,1'-dioctadecyl-3,3,3'3'-tetramethylindocarbocyanine perchlorate
DNA	deoxyribonucleic acid
EC	entorhinal cortex
fEPSP	field excitatory post-synaptic potential
GABA	γ-aminobutyric acid
GFAP	glial fibrillar acidic protein
HMGB1	high-mobility group box 1 protein
IFN-γ	interferon-gamma
IBA-1	ionized calcium-binding adapter molecule 1
IL	interleukin
IL-1R	interleukin 1 receptor
IL-1RA	interleukin 1 receptor antagonist
IRAK	IL-1R-associated kinases
iNOS	inducible nitric oxide synthase
ISI	inter stimulus interval
LBP	lipopolysaccharide-binding protein
LPS	lipopolysaccharide
LTA	lipoteichoic acid

LTD	long-term depression
LTP	long-term potentiation
MAL	MyD88-adaptor-like protein
MAP	microtubule associated proteins
MAPK	mitogen-activated protein kinase
MD-2	lymphocyte antigen 96
MHC	major histocompatibility complex
MIP-1	macrophage inflammatory protein-1
MWM	Morris water maze
MyD88	myeloid differentiation primary response gene (88)
NF-κB	nuclear factor-kappa B
NLR	NOD like receptor
NLRP3	NOD-, LRR- and pyrin domain-containing 3
NMDA	N-methyl-D-aspartate
NO	nitric oxide
NSAID	non-steroidal anti-inflammatory drugs
NT-3	neurotrophin 3
$p75^{NTR}$	pan neurotrophin receptor 75
PAMP	pathogen associated molecular pattern
PBS	phosphate buffered saline
PCR	polymerase chain reaction
PGN	peptidoglycan
PKA	protein kinase A
PPF	paired pulse facilitation
PRR	pattern recognition receptors
PS1	presenilin 1
ROI	region of interest
RAGE	receptor for advanced glycation end-products
ROS	reactive oxygen species
RT	room temperature
TGF-β	transforming growth factor-beta
TIR	toll/interleukin receptor
TIRAP	TIR domain-containing adapter protein
TLR	toll-like receptor
TNF-α	tumor necrosis factor-alpha
TNF-R	tumor necrosis factor-receptor
TRAF	TNF receptor-associated factor
TRAM	TRIF-related adaptor molecule
TREM-2	triggering receptor expressed on myeloid cells 2
TRIF	TIR domain-containing adaptor protein inducing IFN-β
WT	wildtype

7. DANKSAGUNG

An dieser Stelle möchte ich allen Menschen danken, die mich während meiner Doktorarbeit begleitet und unterstützt haben:

Als erstes geht ein besonderer Dank an meinen Doktorvater Prof. Dr. Martin Korte für das große Interesse und die Förderung und für die einmalige Gelegenheit diese Doktorarbeit an der Schnittstelle der immunologischen und neurobiologischen Forschung anfertigen zu dürfen.

Prof. Dr. Reinhard Köster danke ich für die Übernahme des Koreferates und Prof. Dr. André Fleißner für die Leitung der Promotionskommission.

Des Weiteren danke ich Prof. Dr. Michael Heneka für die hilfreichen Ideen während unserer Kooperation in der Neuroinflammation.

Dr. Ildiko Rita Dunay und Dr. Alexandru Parlog möchte ich für die Kooperation im Bereich der Infektionen mit *Toxoplasma gondii* danken.

Mein weiterer Dank gilt Dr. Marta Zagrebelsky, Dr. Kristin Michaelsen-Preusse, Dr. Gayane Grigoryan und Dr. Qin Li für die experimentelle Unterstüzung.

Dr. Marta Zagrebelsky möchte ich zusätzlich ganz herzlich für die Korrekturen meiner zahlreichen Abstracts, Poster und für die Hilfe beim Schreiben dieser Dissertation danken.

Heike Kessler und Eva Saxinger danke ich von Herzen, dass sie mir die Genotypisierungen abgenommen haben.

Mein weiterer Dank gilt Dr. Martin Rothkegel und Tania Meßerschmidt. Ihr wisst, dass ich ohne euch niemals in der Neurobiologie gelandet wäre und ich freue mich, dass ihr immer noch jederzeit den 184er Spirit verbreitet!

Ebenso haben Franziska Scharkowski, Susann Ludewig, Dr. Ulrike Herrmann, Shirin Hosseini, Jan Klevemann, Dr. Stefanie Schweinhuber, Dr. Sabine Zessin und Cristina Iobbi für eine angenehme Laboratmosphäre und viel Spaß gesorgt.
Mein Dank gilt aber auch allen anderen Mitarbeitern der Arbeitsgruppe für die gute Laune und Unterstützung bei jeglichen Tätigkeiten.

Dr. Anita Remus und Nina Gödecke, ihr meine liebsten Elfenpalast-Mitbewohner, es war eine schöne Zeit mit euch! Ich danke euch für die wunderbare Unterstützung!

Den Fredes, Beyers, Lafferdern und Bayreuth-Mädels danke ich für die hervorragende Freizeitgestaltung während all der Jahre!

Einen ganz besonderen Dank hat meine wundervolle Familie verdient. Danke, dass ihr mich immer unterstützt habt!

Und zuletzt: Martin, jag älskar dig, älskar dig, älskar dig!